EnMAP Science Plan

Environmental Mapping and Analysis Program (EnMAP)

Chabrillat, S.; Guanter, L.; Kaufmann, H.; Foerster, S.; Beamish, A.; Brosinsky, A.; Wulf, H.; Asadzadeh, S.; Bochow, M.; Bohn N.; Boesche, N.; Bracher, A.; Brell, M.; Buddenbaum, H.; Cerra, D.; Fischer, S.; Hank, T.; Heiden, U.; Heim, B.; Heldens, W.; Hill, J.; Hollstein, A.; Hostert, P.; Krasemann, H.; LaPorta, L.; Leitão, P.J.; van der Linden, S.; Mauser, W.; Milewski, R.; Mottus, M.; Okujeni, A.; Oppelt, N.; Pinnel, N.; Roessner, S.; Röttgers, R.; Schneiderhan, T.; Schickling, A.; Soppa, M.; Staenz, K.; Segl, K.

Recommended citation:

Chabrillat, S; Guanter, L.; Kaufmann, H.; Foerster, S.; Beamish, A.; Brosinsky, A.; Wulf, H.; Asadzadeh, S.; Bochow, M.; Bohn N.; Boesche, N.; Bracher, A.; Brell, M.; Buddenbaum, Cerra, D.; H.; Fischer, S.; Hank, T.; Heiden, U.; Heim, B.; Heldens, W.; Hill, J.; Hollstein, A.; Hostert, P.; Krasemann, H.; LaPorta, L.; Leitão, P.J.; van der Linden, S.; Mauser, W.; Milewski, R.; Mottus, M.; Okujeni, A.; Oppelt, N.; Pinnel, N.; Roessner, S.; Röttgers, R.; Schneiderhan, T.; Schickling, A.; Soppa, M.; Staenz, K.; Segl, K. (2022) EnMAP Science Plan. EnMAP Technical Report, GFZ Data Services.

DOI: http://doi.org/10.48440/enmap.2022.001

Imprint

EnMAP Consortium

GFZ Data Services

Telegrafenberg
D-14473 Potsdam

Published in Potsdam, Germany
October 2022

http://doi.org/10.48440/enmap.2022.001

Scientific Principal Investigator

Sabine Chabrillat (GFZ German Research Centre for Geosciences, Leibniz University Hannover) supported by the EnMAP Science Advisory Group (EnSAG)

Funding

The core funding of the mission is provided by the German Space Agency at DLR with resources of the German Ministry for Economic Affairs and Climate Action and with contributions from the German Aerospace Center (DLR), OHB System AG and GFZ.

Supported by:

on the basis of a decision
by the German Bundestag

www.enmap.org

Science Plan authors

S. Chabrillat (1,2), L. Guanter (1,3), H. Kaufmann (1), S. Foerster (1), A. Beamish (1), A. Brosinsky (1), H. Wulf (1), S. Asadzadeh (1), M. Bochow (1), N. Bohn (1), N. Boesche (1), A. Bracher (4,5), M. Brell (1), H. Buddenbaum (6), D. Cerra (7), S. Fischer (8), T. Hank (9), U. Heiden (7), B. Heim (10), W. Heldens (7), J. Hill (6), A. Hollstein (1), P. Hostert (11), H. Krasemann (12), L. LaPorta (8), P.J. Leitão (11), S. van der Linden (11,13), W. Mauser (9), R. Milewski (1), M. Mottus (14), A. Okujeni (11), N. Oppelt (15), N. Pinnel (7), S. Roessner (1), R. Röttgers (12), A. Schickling (8), T. Schneiderhan (7), M. Soppa (4), K. Staenz (16), K. Segl (1)

Affiliation at the time of contribution to the Science Plan:
(1) Helmholtz Centre Potsdam, German Research Centre for Geosciences (GFZ)
(2) Leibniz University Hannover, Germany
(3) Universitat Politècnica de València, Spain
(4) Alfred Wegener Institute for Polar and Marine Research, Bremerhaven, Germany
(5) University Bremen, Germany
(6) University Trier, Germany
(7) German Aerospace Centre (DLR), Oberpfaffenhofen, Germany
(8) German Space Agency at DLR, Bonn, Germany

(9) Ludwig-Maximilian-Universität München (LMU), Germany
(10) Alfred Wegener Institute for Polar and Marine Research - Research Unit Potsdam (AWI), Germany
(11) Humboldt-Universität zu Berlin, Germany
(12) Helmholtz-Centre Hereon, Geesthacht, Germany
(13) University Greifswald, Germany
(14) VTT Technical Research Centre of Finland, Finland
(15) Kiel University, Germany
(16) University of Lethbridge, Canada

Contents

Preface

The scope of the Science Plan is to describe the scientific background, applications, and activities of the Environmental Mapping and Analysis Program (EnMAP) imaging spectroscopy mission. Primarily, this document addresses scientists and funding institutions, but it may also be of interest to environmental stakeholders and governmental agencies. It is designed to be a living document that will be updated throughout the entire mission lifetime.

Chapter 1 provides a brief overview of the principles and current state of imaging spectroscopy. This is followed by an introduction to the EnMAP mission, including its objectives and impact on international programs as well as major environmental and societal challenges. Chapter 2 describes the EnMAP system together with data products and access, calibration/validation, and synergies with other missions. Chapter 3 gives an overview of the major fields of application such as vegetation and forests, geology and soils, coastal and inland waters, cryosphere, urban areas, atmosphere and hazards. Finally, Chapter 4 outlines the scientific exploitation strategy, which includes the strategy for community building and training, preparatory flight campaigns and software developments.

A list of abbreviations is provided in the annex to this document and an extended glossary of terms and abbreviations is available on the EnMAP website.

1 Introduction

1.1 Principles of imaging spectroscopy

Surface materials such as vegetation, soil, and rock can be differentiated and characterized based on their so-called spectral signatures, i.e., diagnostic absorption and reflection characteristics over the electromagnetic spectrum. Because every material is formed by chemical bonds, their harmonics and overtones of vibrational electronic transitions result in characteristic spectral absorption features that can be detected in narrow wavelength intervals. Some of the most significant absorption features occur between wavelengths of 400 nm and 2500 nm, where reflected solar radiation dominates the natural electromagnetic spectrum (Figure 1). These absorption characteristics can vary in their spectral depth, width, and location and, therefore, serve as diagnostic indicators enabling characterization of vegetation condition (e.g., Knipling, 1970) detection of water constituents (Lee et al., 1999) or identification of mineral assemblages (e.g., Hunt and Salisbury, 1970).

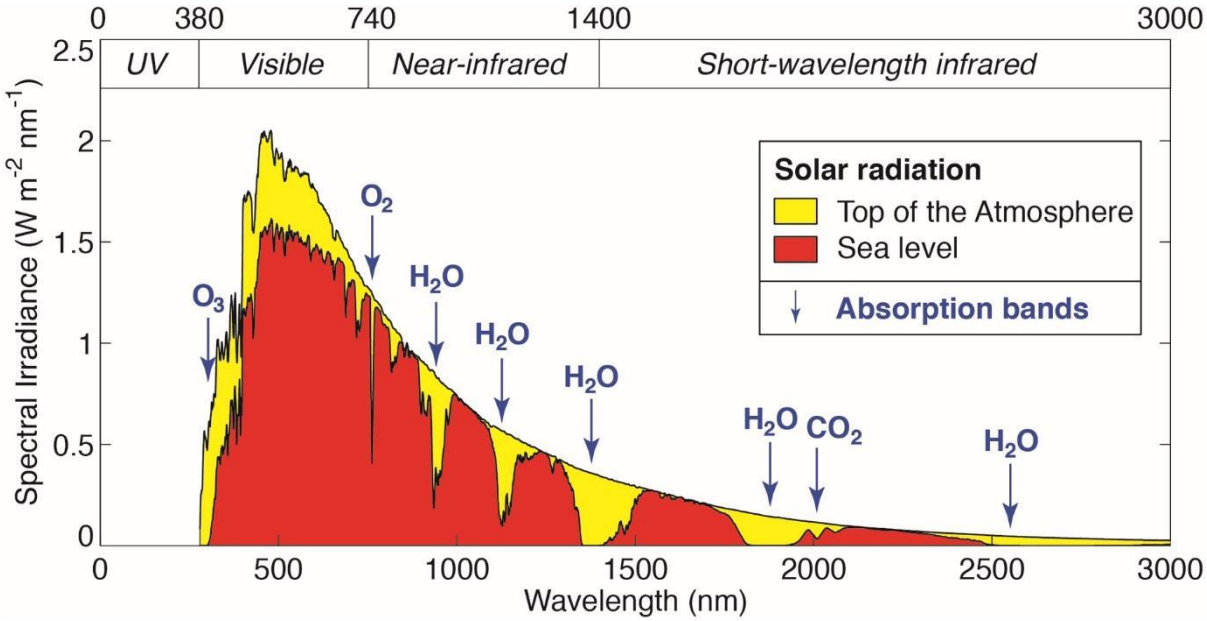

Fig. 1: Solar radiation spectrum of extraterrestrial radiation (Top of Atmosphere) and global radiation (Sea level, composed of incoming, diffuse, and reflected radiation) with major atmospheric absorption bands. Irradiance data are derived from the American Society for Testing and Materials (ASTMs) Terrestrial Reference Spectra (http://rredc.nrel.gov/solar/spectra/am1.5/).

Imaging spectroscopy, also known as hyperspectral imaging, is defined as a passive remote sensing technology that acquires simultaneous images in many spectrally contiguous, narrow bands so that for each pixel a reflectance spectrum can be derived (Goetz et al., 1985; Schaepman, 2007). Common biogeochemical applications of hyperspectral remote sensing include ecosystem processes, surface mineralogy, water quality, soil type and erosion, vegetation type and condition, canopy chemistry, and snow and ice properties, but it is also widely used in other disciplines such as medicine and manufacturing.

Ecosystem studies focus on the spectroscopic detection and identification of plant composition, phenology, and health, as well as invasive species to provide information about ecosystem conditions and environmental stress (Asner et al., 2008; Schmidtlein and Sassin, 2004; Ustin et al., 2004). In the

past, most research has been focused on the spectral properties of leaves and canopies, providing estimates of (forest) species, foliar chemistry, biomass and carbon (Goodenough et al., 2012). In general, the spectral characteristics of vegetation exhibit strong pigment absorptions in the visible (VIS: 400 nm to 700 nm) portion of the spectrum (Figure 2). The near infrared (NIR: 700 nm to 1400 nm) is marked by a steep increase of reflectance that is related to biomass, state and type of cellular arrangement, density, geometry and water content of the vegetation canopy. A shift of the "red edge" between 680 nm and 780 nm to shorter wavelengths is related to a decrease in chlorophyll, which in turn can be an indication of heavy metal, water or nutrient stress. Senescing leaves are also characterized by a decrease in chlorophyll, followed by losses of other pigments and leaf water content (Ustin et al., 2004). The biochemical content of leaves and canopies, including nitrogen-containing compounds and lignin, absorb radiation at fundamental stretching frequencies, generally in the NIR and shortwave-infrared (SWIR: 1400 nm to 2500 nm) regions. In general, stress and aging increase reflectance in the VIS and SWIR and decrease reflectance in the NIR (Ustin et al., 2004). Consequently, imaging spectroscopy is highly suitable to assess vegetation condition and to distinguish between vegetation species.

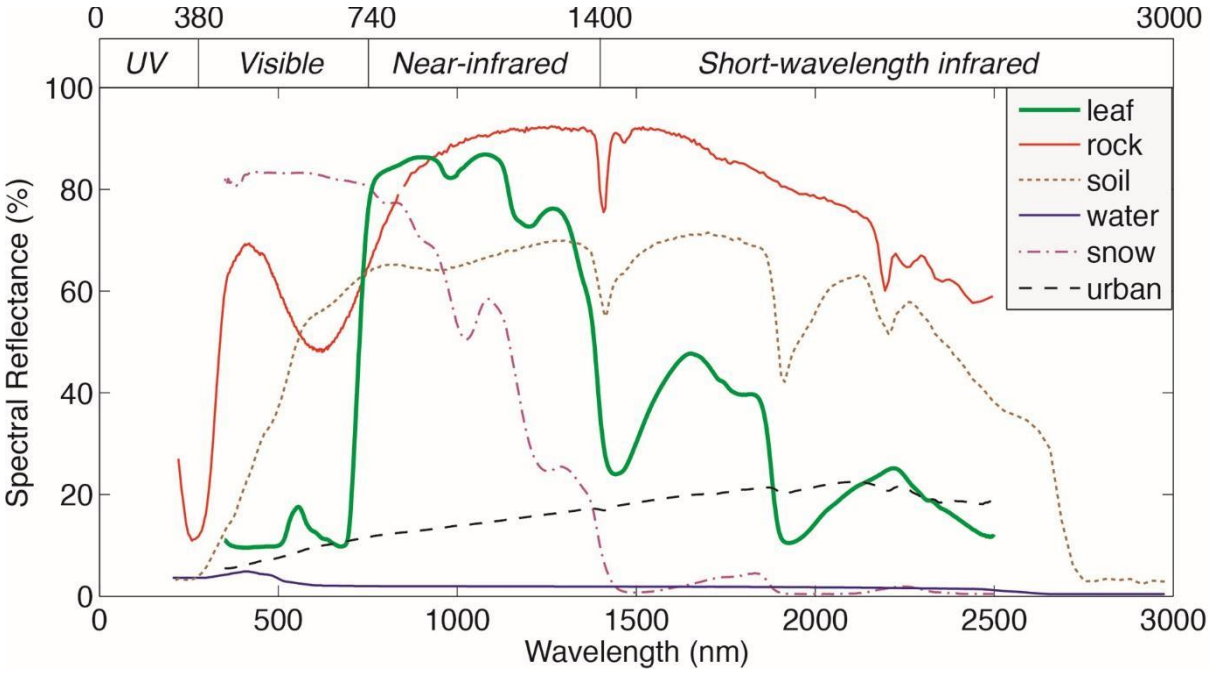

Fig. 2: Reflectance spectra of selected Earth's surface components. Reflectance data are derived from the USGS Digital Spectral Library (http://speclab.cr.usgs.gov/spectral.lib06/). The laboratory measurements represent samples of an oak leaf from Colorado (leaf), Aventurine quartz from India (rock), montmorillonite and illite from Virginia (soil), seawater from the Pacific Ocean (water), fresh snow from Colorado (snow), and black road asphalt from Colorado (urban).

For geological applications, imaging spectroscopy is used to map surface mineralogy and lithology as well as quantify rock and soil chemistry based on spectral absorption features. The spectral reflectance of minerals is dominant in the visible near-infrared (VNIR) wavelength range (400 nm to 1400 nm) due to the presence or absence of transition metal ions (e.g., Fe, Cr, Co, Ni) resulting in absorption features due to electronic processes. The presence of water, hydroxyl, carbonate, and sulfate determine absorption features in the SWIR region due to vibrational processes. These phyllosilicates, sorosilicates, inosilicates, oxides, hydroxides, sulfates and carbonates are widespread components of the Earth's surface. The absorption band depth, or the amount of light scattered and absorbed by a mineral is

dependent on grain or particle size (van der Meer et al., 2012). Based on the relative absorption depth, for example, kaolinite and organic carbon content can be derived with an accuracy of about 2% by weight (Krueger et al., 1998).

Soils are dynamic environmental components of extremely variable physical and chemical composition (Ben-Dor et al., 1999) and are essential for ecosystem functioning. Soils comprise a major sink for biospheric carbon and organic matter in the topsoil, the proportions of which provide a good indication of soil quality, erosion, and dominant physical processes (Ustin et al., 2004). Since the major constituents of soil minerals do not exhibit absorption features in the VNIR and SWIR range (Hunt, 1977), their spectral reflectance characteristics are mainly influenced by organic matter content, clay mineral composition, iron-oxide content, moisture content, salinity, texture and surface roughness. Typically, soils have broad, shallow absorption features at wavelengths between 400 nm and 2500 nm that are related to iron oxide and organic matter (Figure 2). In general, reflectance decreases with increasing organic matter and/or soil moisture content. Increases in particle size also cause a decrease in overall reflectance. Even small amounts of iron oxides can alter VNIR spectral reflectance significantly, causing broad absorption features particularly around 400 nm, 700 nm and 870 nm (Ben-Dor et al., 1999). In contrast, several clay minerals (e.g., montmorillonite, kaolinite, illite, smectite) and carbonates display distinctive narrow-band absorption features in the SWIR range between 2000 nm and 2500 nm (Ustin et al., 2004). Studies on soil properties and imaging spectroscopy have focused on soil degradation, genesis and formation, contamination, classification and mapping, as well as on soil water content and swelling soils (Ben-Dor et al., 2009).

Imaging spectroscopy has been widely used to investigate oceans, coastal and inland waters, which are characterized by an overall high absorption of radiant energy compared to land surfaces (Figure 2). Sunlight that reaches the water and penetrates is attenuated by water molecules and other optically active substances that absorb and scatter light. The type and concentration of these substances determine the spectrum and intensity of light in the water. A fraction of this light is scattered out of the water, interacting once again with the atmosphere and travels back to the satellite sensor. This backscattered signal can be used to measure the optical constituents of water, such as pigments (e.g., chlorophyll), a wide range of phytoplanktonic species, dissolved organic matters, and suspended non-algal particles (e.g., minerogenic sediments). Aquatic environments are a complex mixture of optically dissolved and particulate material. Coastal and inland waters have high optical variability; ranging from very clear and shallow to highly turbid or hypertrophic waters (Giardino et al., 2019).

Snow cover and its change of state dominate local to regional climate and hydrological regimes in mountainous and Polar Regions. Modeling snowmelt distribution and its impact can be facilitated by hyperspectral remote sensing through the retrieval of snow properties, such as snow-covered area, albedo, grain size, very near surface liquid water, and impurities (Dozier and Painter, 2004). Among natural materials at the Earth's surface, snow has a huge range of spectral reflectance values depending on its physical characteristics, primarily the grain size but also dust or soot content, organic substances such as algae, and liquid water (Dozier et al., 2009). Clean, deep snow is highly reflective in the VIS spectrum, whereas reflectance in the NIR and SWIR wavelengths shows a general decrease but varies considerably depending primarily on grain size (Figure 2).

Urban areas are characterized by a wide range of spectrally distinct surface materials, the spectral signatures of which are determined by chemical composition (Heiden et al., 2012). For example, roofing tiles and polyethylene exhibit pronounced absorption features and high-spectral variation, whereas other urban surfaces, such as concrete and asphalt, are characterized by low reflectance and low spectral variation. Spaceborne imaging spectroscopy data will offer new possibilities for mapping urban environments at improved accuracy and higher thematic detail, due to its high spectral information content (van der Linden et al., 2019a). Heldens et al., (2011) identified the following current major

topics regarding urban applications: urban development and planning, urban growth assessment, risk and vulnerability assessment, and urban climate.

EnMAP has the capability to detect individual absorption features in the spectra of many solid, liquid, and gaseous materials. Actual detection depends on the instrument's spectral coverage, spectral resolution, signal-to-noise ratio, the abundance of the material, and the strength of the material's absorption features in the measured wavelength region. The molecular spectral absorption and scattering properties of materials form the basis for the identification and determination of the abundance of surface and atmospheric constituents. Accordingly, research and development efforts within the EnMAP mission employ these fundamental spectral characteristics as a basis for the extraction of information from spaceborne hyperspectral data.

1.2 Current scenario in imaging spectroscopy and EnMAP

More than three decades of effort have been devoted to the development of instruments capable of acquiring contiguous spectra in different wavelength regions, facilitating precise and quantitative analysis of terrestrial and aquatic ecosystems. These imaging spectrometers have primarily been flown on aircrafts for experimental and commercial purposes, e.g., AIS, (Vane et al., 1983), FLI and CASI (Gower et al., 1992), AVIRIS (Green et al., 1998; Vane et al., 1993), GER/DAIS (Collins and Chang, 1990), SFSI (Neville and Powell, 1992), Hydice (Rickard et al., 1993), MIVIS (Bianchi et al., 1994), HyMap (Cocks et al., 1998), APEX (Itten et al., 2008; Schaepman et al., 2015, 2004), AVIS (Oppelt and Mauser, 2007), AISA (www.spectralcameras.com/aisa), HySpex (www.hyspex.no), and Hyperspec (www.headwallphotonics.com) (Figure 3). However, data acquisition from an aircraft platform cannot provide a synoptic view of large areas and repeated acquisitions are costly. For a more complete overview of airborne imaging spectroscopy sensors and their history refer to Schaepman et al., (2009).

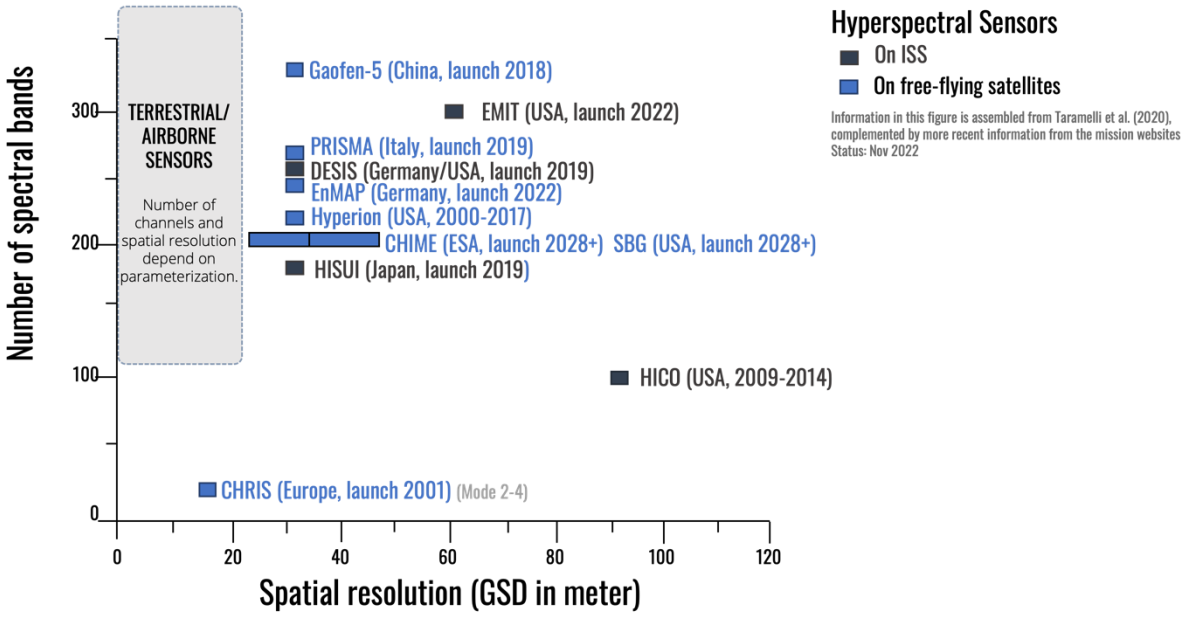

Fig. 3: Overview of the spectral and spatial resolution of airborne sensors and spaceborne hyperspectral missions.

Until recently, most operational optical satellite sensors have been multispectral instruments acquiring discrete bands in the VNIR and in some cases the SWIR and thermal infrared (TIR) regions of the spectrum (e.g., Landsat, ASTER). Panchromatic sensors only provide spatial information, while

multispectral instruments such as Sentinel 2, Landsat, SPOT, IRS, CBERS, ASTER, and ALI augment the spatial data with qualitative information about the surface materials. With the successful launches of the Chinese Gaofen-5 in 2018, the Italian Space Agency's (ASI) PRISMA satellite in 2019 (PRecursore IperSpettrale della Missione Operative; Pignatti et al., 2013) and the German Space Agency's (DLR) EnMAP in 2022 the availability of spaceborne hyperspectral data has greatly increased in recent years.

In addition to these satellites, several imaging spectrometers have recently been installed on the International Space Station (ISS) including DESIS (DLR), HISUI (JAXA, Iwasaki et al., 2011) and EMIT (NASA). Past missions that also contribute to available spaceborne hyperspectral data include NASA's Hyperion (2000 - 2017; Pearlman et al., 2003; Ungar et al., 2003), NASA's HICO (2009 - 2015; Corson et al., 2008; Lucke et al., 2011), and European Space Agency's (ESA) CHRIS (since 2001; Barnsley et al., 2004) (Figure 3). Considering that Hyperion and CHRIS were designed for a 1-year lifetime, they have provided exceptional results. However, CHRIS and HICO were limited to the VNIR region, while Hyperion was characterized by a low signal-to-noise ratio. Both these factors limit feature detection capabilities. Therefore, past spaceborne sensors provide only limited information on biochemical and geochemical parameters, which are required for detailed environmental studies. Future, next generation imaging spectroscopy missions include ESA's CHIME mission (Copernicus Hyperspectral Imaging Mission; Nieke and Rast, 2018), NASA's SBG missions (Surface Biology and Geology) and PACE (Plankton, Aerosol, Cloud, ocean Ecosystem), and Centre National d'Études Spatiales's HYPXIM (Michel et al., 2011).

EnMAP is a German hyperspectral satellite mission that aims to monitor and characterize the Earth's environment on a global scale. EnMAP serves to measure and model key dynamic processes of the Earth's ecosystems by extracting geochemical, biochemical and biophysical parameters to provide information on the status and evolution of various terrestrial and aquatic ecosystems. An overview of the EnMAP mission is provided in Guanter et al., (2015). EnMAP provides unique data needed to address major environmental issues related to human activity and climate change. The mission's main objective is to study and decipher coupled environmental processes and to assist and promote the sustainable management of the Earth's resources. Despite being a primarily scientific mission, EnMAP has a clear potential to evolve towards an operational service.

The satellite mission is managed by the German Space Agency at DLR Bonn with core funding from the Federal Ministry of Economic Affairs and Climate Action. The German Centre for Geosciences (GFZ) in Potsdam is responsible for the scientific management of the mission and is supported by a Science Advisory Group (EnSAG). OHB SE in Bremen and Oberpfaffenhofen was responsible for developing the EnMAP instrument and building the associated satellite platform. The ground segment is operated by DLR. Specifically the satellite operation is managed by the German Space Operations Center and data processing and provision is done by the German Remote Sensing Data Center and the DLR Remote Sensing Technology Institute.

1.3 EnMAP mission objectives

The main scientific goal of the hyperspectral EnMAP mission is to study environmental changes, investigate ecosystem responses to human activities and monitor the management of natural resources. By measuring diagnostic parameters of environmental change, ecosystem stability, and sustainable resource use, the EnMAP mission aims to provide critical information to improve our understanding and management of the Earth System.

The primary mission objectives are to:

- provide high-quality, calibrated hyperspectral data for advanced remote sensing analyses;
- foster and develop novel methodologies that improve the accuracy of currently available remote sensing-derived information and provide advanced science-driven information products;
- obtain diagnostic geochemical, biochemical and biophysical variables that describe the status and dynamics of various ecosystems to improve our understanding of complex environmental processes;
- provide information products that can serve as input for ecosystem models;
- contribute significantly to environmental research studies, particularly in the fields of ecosystem functioning, natural resource management, natural hazards and Earth system modeling; and
- develop new concepts and techniques for data extraction and fusion to achieve synergies with other sensors.

EnMAP significantly increases the availability of hyperspectral data. To understand and fully exploit the information provided by EnMAP, novel techniques need to be developed that utilize its regional coverage on a global scale. EnMAP data provide a unique opportunity to adapt and extrapolate existing hyperspectral data analysis approaches derived from laboratory, field, and airborne measurements. Integration of these data in regional ecosystem models will complement, enhance, and expand on local case study findings. Improved regional scale science on the state and change of ecosystems is a prerequisite for improved global ecosystem models. Such upscaling studies require a consolidation and generalization of the derived ecosystem parameters and synergistic analyses with other spaceborne imagery like ESA's Copernicus satellites. Due to the 30° across track off-nadir pointing capability, EnMAP is suited for repeat acquisitions of multiple key target sites with a maximum revisit time of four days. This allows EnMAP to repeatedly observe a globally distributed network of key target sites during its five years of mission operation.

1.4 Overarching research themes for EnMAP

The repeat observations of EnMAP in combination with an advanced spectral range and resolution will provide new insights into many interrelated fields of environmental science and will open new horizons in ecosystem research as well as resource and disaster management. EnMAP will make significant contributions to the following scientific questions:

Climate Change Impact and Interventions

- How does climate change affect the functioning, composition and phenology of terrestrial and aquatic ecosystems?
- What interventions can effectively combat climate change and how can their implementation be monitored?

Land Cover Changes and Surface Processes

- What is the spatial distribution and extent of land degradation and land use/land cover change?
- What processes drive land degradation and how efficient are interventions?
- How does land degradation and land use/land cover change impact food security and environmental sustainability?

Biodiversity and Ecosystem Processes

- How do ecosystems change in their composition, spatial distribution and health?

- To what extent does ecosystem change affect the loss of biodiversity and the migration of species?
- How successful are measures to achieve ecosystem stability and to combat biodiversity loss?

Water Availability and Quality

- What areas are affected by water scarcity and poor water quality?
- How do climate change and human activities reinforce water scarcity and water quality problems?

Natural Resources

- How can natural resources, such as mineral deposits, soils, energy sources and ground water sources, be explored and managed in a sustainable way?
- What impact does industry, mining and agriculture have on natural resources?
- What is the degree and extent of environmental damage from natural resource extraction and to what extent is the damage being restored?

Hazard and Risk Assessment

- What regions are most vulnerable to natural and man-made hazards?
- In the case of a natural or man-made disaster, what areas are most affected?

1.5 Impact on international programs

The products and information generated from EnMAP data are of substantial interest for the scientific community, European and international organizations, and the general public. First and foremost, researchers need EnMAP data to improve their understanding of Earth surface processes and reduce uncertainties in associated ecosystem models. Scientific requirements for terrestrial and aquatic observations have long been articulated by the International Geosphere-Biosphere Program (IGBP), the Future Earth Coasts (FEC), the International Human Dimensions Program (IHDP), DIVERSITAS, the World Climate Research Program (WCRP), the Global Land Project (GLP), the Global Biodiversity Information Facility (GBIF), the Global Environment Outlook (GEO), the UN Agenda for Sustainable Development defining 17 Sustainable Development Goals (SDGs), the Committee on Earth Observation Satellites (CEOS) and others. The major new “Future Earth” alliance on Earth system research for global sustainability integrates and consolidates international expertise in environmental and social science under one umbrella and forms a programmatic and societal justification for Earth observation research and development. This is underlined by the welcoming of Future Earth as a participating organization in the Group on Earth Observations (GEO) in 2015. GEO aims at building the Global Earth Observation System of Systems (GEOSS) that will link global Earth observation resources contributed by organizations and countries within GEO across multiple Societal Benefit Areas (SBAs) to facilitate access to the data for better informed decision-making. The SBAs include biodiversity and ecosystem sustainability, disaster resilience, energy and mineral resources management, food security and sustainable agriculture, infrastructure and transportation management, public health surveillance, sustainable urban development, and water resources management (GEO, 2015).

Key international stakeholders with an interest in the scientific results of the EnMAP mission, include organizations that make up the United Nations System (e.g., UNEP, FAO, UNESCO and WMO) as well as global observing systems, such as the Global Climate Observing Systems (GCOS), Global Ocean Observing System (GOOS) and Global Terrestrial Observing System (GTOS). Furthermore, EnMAP data will be a valuable source of information needed for multilateral environmental

agreements, such as REDD+, UNFCCC, UNCCD, and CBD, as well as for key international entities, such as the Intergovernmental Panel on Climate Change (IPCC), the Intergovernmental Platform on Biodiversity & Ecosystem Services (IPBES) and the International Union for Conservation of Nature (IUCN). EnMAP data have already been requested by UNEP to contribute to their International Methane Emissions Observatory (IMEO). Within IMEO, EnMAP data will enable the detection of methane point sources from fossil fuel activities, which will be used to guide mitigation efforts (see Section 3.6).

At the European Union level, the European Green Deal will greatly benefit from the detail of EnMAP data to monitor Earth surface processes and resources to meet its ambitious goals. In addition, several Commission directories (e.g., DG VI - Agriculture, DG VIII - Development, DG XI - Environment, DG XII - Transport, and DG XVI - Regional policy) require continuous remotely sensed surface observations so government agencies can set, monitor, and enforce their policy agendas. For example, specified biological, hydromorphological and physico-chemical parameters of water bodies must be monitored on a regular basis according to the EU Water Framework Directive (EU WFD). The EU WFD is working towards integrated watershed management for the European continent. The EU is also working towards the sustainable extraction of raw materials from exploration to post mine closure that align with defined Sustainable Development Goals (SDG). In addition, national and local authorities will need increasingly detailed information for implementing measures to combat desertification and plan alternative land use. The European Soil Protection Directive requires detailed mapping of topsoil properties to monitor the carbon cycle and soil health, soil erosion and degradation, as well as soil fertilization and agricultural practices (i.e., conservation agriculture and carbon farming). In view of these developments, EnMAP data products (e.g., soil condition, vegetation cover, change detection maps, degradation index maps) will be beneficial for decision makers. In particular, the European Copernicus program provides users with reliable and up-to-date information through a set of services related to environmental and security issues (European Commission, 2015)

2 EnMAP system and data products

2.1 Technical parameters and observational requirements

The EnMAP satellite carries a push-broom type hyperspectral imager, that records reflected solar radiation from the Earth surface between 420 nm to 2450 nm in 246 contiguous bands. At the nominal start of the mission 224 of the 246 are provided as Bottom of Atmosphere (BOA) reflectance data product (L2A). The mean bandwidth is 6.5 nm the VNIR range and 10 nm in the SWIR range. Accurate radiometric and spectral responses are ensured by a reference signal-to-noise ratio (SNR) of ≥ 400:1 in the VNIR and ≥170:1 in the SWIR (based on an albedo of 30% and a solar zenith angle of 30°), a radiometric calibration accuracy of better than 5%, and a spectral calibration uncertainty of 0.5 nm in the VNIR and SWIR.

The sensor is characterized by a ground sampling distance of 30 m (nadir at sea level) and provides a swath width of 30 km. EnMAP can record strip lengths between 30 km and 1000 km (subject to potential conflicts in the acquisition plan) with a capacity of 5000 km per day. The nominal target revisit time of 27 days can be reduced to 4 days by use of an across-track off-nadir pointing capability of ±30°. EnMAP has a sun-synchronous orbit (653 km altitude at 48°N, 97.96° inclination) with a local equatorial crossing time of 11:00 ± 00:18 hr. The satellite was successfully launched on April 1st, 2022, onboard a SpaceX Falcon 9 rocket from Cape Canaveral, Florida and has a designed lifetime of five years. A summary of the main mission and instrument specifications is given in Table 1. Further descriptions can be found in Guanter et al., (2015) and Kaufmann et al., (2015).

Table 1: EnMAP mission and instrument specifications at the start of the nominal phase.

Hyperspectral instrument	
Imaging principle	Push-broom-prism
Spectral range	VNIR: 420 nm - 1000 nm SWIR: 900 nm - 2450 nm
Mean spectral sampling distance	VNIR: 6.5 nm SWIR: 10 nm
Spectral oversampling	1.2
SNR at reference radiance	VNIR: > 400:1 at 495 nm (nadir looking, 30° solar zenith angle) SWIR: > 170:1 at 2200 nm (0.3 earth albedo)
Spectral calibration accuracy	VNIR: 0.5 nm SWIR: 1.0 nm
Spectral stability	0.5 nm
Radiometric calibration accuracy	< 5 %
Radiometric stability	< 2.5 %
Radiometric resolution	14-bit, dual gain in VNIR
Sensitivity to polarization	< 5 %
Spectral smile/keystone effect	maximum < 15 % / < 25 % of a pixel (< 10 % / < 10 % for majority of pixels)
Co-registration VNIR-SWIR	< 30-40 % of a pixel (expected to reach <20%)
Mission	
Ground sampling distance	30 m

Swath width	30 km
Swath length	up to 1000 km/orbit and 5000 km/day
Coverage	Global in near-nadir mode (VZA ≤5°)
Orbit	Sun-synchronous,11:00 +/- 00:18 local time descending node
Target revisit time	27 days (4 days with 30°across track pointing)
Pointing accuracy (knowledge)	500 m (100 m) at sea level

2.2 Data products and access

The following EnMAP data products are delivered to the user community: Product Level 1B, 1C, and 2A. The raw data and subsequent Level 0 products are not available to the user community (Figure 4). This section provides a short definition of these products. A more detailed description of the data products can be found in Guanter et al., (2015) and on the mission website.

The Level 1B (L1B) product represents top-of-atmosphere radiance. The L1B processor corrects the hyperspectral image for known effects, e.g., radiometric non-uniformities, and converts the system corrected data to physical at-sensor radiance values based on the up-to-date radiometric calibration values. The L1B product is also annotated with auxiliary information for further processing, e.g., defective pixels mask and data quality. At the start of the nominal phase, the data cubes for the two spectrometers are independent, as they have not yet been co-registered.

The Level 1C product represents spectral smile corrected and geocoded top-of-atmosphere radiance. This product is derived from the Level 1B product, which is subsequently geometrically corrected (orthorectified) and re-sampled to a specified grid. Smile is corrected by applying a simplified atmospheric correction, spectral resampling, and back transformation. The Level 1C processor creates orthoimages by direct geo-referencing, utilizing an adequate digital elevation model. The extraction of ground-control-points from existing reference images using image matching techniques serve to improve the line-of-sight vector and, therefore, to increase the geometric accuracy of the orthoimages. The Level 1C processor orthorectifies image tiles from the VNIR and SWIR instrument independently. The co-registration error is 0.3–0.4 pixels and is expected to reach less than 0.2 pixels. Further updates of the L1B and L1C processor are expected soon, which will further improve data quality with respect to striping artifacts and detector co-registration.

Finally, the Level 2A processor will convert the Level 1C products to surface reflectance separately for land and water applications. The atmospheric correction involves generation of sun glint maps for water surfaces by specular reflection identification, haze and cirrus detection (and correction), aerosol optical thickness and columnar water vapor estimation, and retrieval of surface reflectance after adjacency and terrain correction. It is anticipated that most applications will use the Level 2A products ($L2A_{land}$, $L2A_{water}$ or $L2A_{combined}$) for further analyses. Thanks to this operational approach, the end user will be provided with CEOS Analysis Ready Data for Land (CARD4L) compliant data products (Bachmann et al., 2021) including rich metadata and quality information, which can be readily integrated into analysis workflows and combined with data from other sensors.

The EnMAP website (www.enmap.org) is the entry point for all users interested in the EnMAP mission, its objectives, status, data products and processing chains. Additionally, the website provides the requirements and conditions for the EnMAP data access and ongoing scientific program activities. Access to EnMAP data is provided using two different order options: 1) the user can request acquisitions through the EnMAP Instrument Planning portal (EIP; https://planning.enmap.org/). The EIP links to a set of functions for registered users that will support the international user community. This portal includes the Proposal Portal for proposal submission by all scientific users responding to an Announcement of Opportunity (AO) and the Observation Request Portal providing planning support of

observation requests and submission of future orders. 2) Data from the archive catalog can be ordered using the EOWEB® GeoPortal. All archived data have ISO (International Organization for Standardization) metadata sets and can be visualized using CSW (Catalogue Service for the Web) and WMS (Web Mapping Service) protocols standardized by the OGC (Open Geospatial Consortium). Due to the multiple processing options, each product is generated specifically for the order and delivered using SFTP (secure file transfer protocol).

Acquisition requests should be submitted at least 24 hours before the scheduled acquisition to ensure the uplink. The final scheduling depends on factors such as available data storage, cloud probabilities (e.g., historical and predicted cloud coverage) and, if requested by the user, sun glint probability (this is relevant for water products only). L0 products will be in the archive within 24 h after completion of the downlink. L2A products will be processed and delivered within a maximum of 6 days for acquisition orders and 10 days for catalog orders. The user can choose the image formats BSQ, BIL BIP, JPEG2000 and GeoTIFF, where the last two are compressed. The metadata is in Extensible Markup Language (XML) format and the product is accompanied by a PDF report.

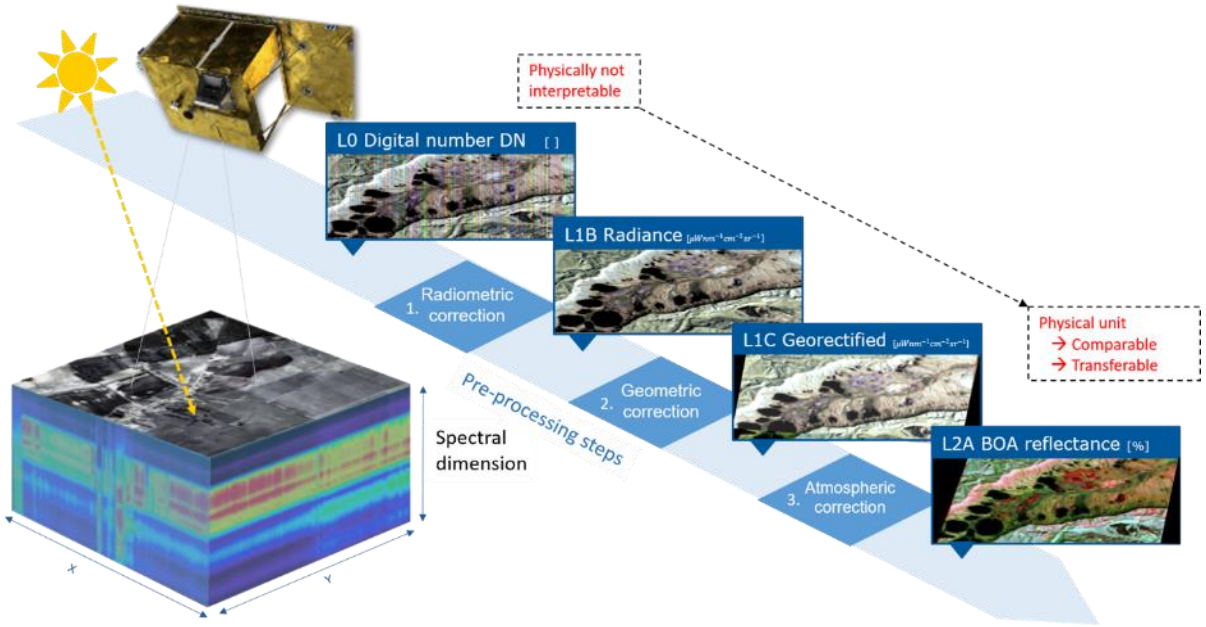

Fig. 4: The EnMAP data processing chain from the raw data to the geometrically and atmospherically corrected Level 2A product (reproduced from (Guanter et al., 2015)

EnMAP is based on an open data policy and every user is in principle entitled to request acquisitions and download data, however there are different user categories to set acquisition priorities. After registration through the EIP, users are assigned roles before obtaining access to the data. Management of available satellite resources requires prioritization of observation requests. The purpose of assigning roles is to assign priorities to observation requests. The scientific category-1 user (Cat-1) has high priority and must submit a research proposal, which will undergo a technical evaluation. Category-2 users (Cat-2) are commercial users and will be able to acquire new data without a proposal but will be granted a lower priority. The priorities for data requests in decreasing order are: 1) internal (high priority, e.g. calibration); 2) emergency Cat-2 (e.g. international charter on space and major disasters); 3) scientific Cat-1 (high priority, science proposal); 4) scientific Cat-1 (standard priority, science proposal); 5) non-emergency Cat-2 (e.g. commercial users); and 6) internal (low priority, e.g. background mission to fill up or extend requests). Requests of the first two priorities are scheduled

regardless of their success concerning cloud probabilities or quota. Requests of the last two priorities are advised to take the revisit times into account when planning the acquisition time period in order to increase the probability that the scheduling meets their requirements.

The EnMAP website (www.enmap.org) is the central entry point for all users interested in the EnMAP mission, its objectives, status, data products and processing chains. Additionally, this platform informs about the conditions and requirements for the EnMAP data access and the ongoing scientific program and activities.

2.3 Sensor calibration and product validation

To ensure high quality EnMAP data, a well-characterized primary sensor, on-board calibration facilities, and ongoing vicarious calibration measurements are prerequisites throughout the entire mission lifetime. The derived official data products also require independent validation using *in situ*/field measurements and scene/image processing techniques.

The pre-flight sensor characterization was performed in the laboratory for the individual subsystems and the complete end-to-end sensor system. It includes spectral, radiometric, and geometric calibrations. The band centers, bandwidths, and spectral response profiles for each band of each pixel in the detector array have been derived by spectral measurement. The radiometric measurements encompass the detector array responsivity, linearity, uniformity, noise characterization, straylight, optics transmittance and characterization of the diffusor as well as calibration of reference spheres against standards to properly characterize instrument performance. The geometric measures include the total field-of-view, the view angle for each pixel and each band, and the modulation transfer function. After launch, in-flight calibration was carried out using on-board calibration devices including 1) the solar full aperture diffuser for the absolute radiometric calibration using the sun as the known reference, 2) a main sphere for the relative radiometric calibration, 3) a small sphere for spectral characterization, 4) focal plane assembly LEDs for non-linearity calibration and 5) a shutter for dark current calibration. Additionally, residual signals caused by thermal emissions from the shutter mechanism are regularly determined by looking into deep space. Vicarious calibration experiments on demand complement the measurements. As the imaging spectrometer and the on-board calibration instrumentation age, there will be a growing need for periodic in-flight, vicarious and on-board calibrations.

The quality of the official EnMAP data products is crucial for the usability and value of the data and the mission's success. Therefore, the radiometric, spectral, reflectivity, geometric, and general uniformities of the three official EnMAP data products (L1B, L1C, and L2A) are validated intensively during the commissioning phase and the operational mission period. The external product validation activities are performed by the GFZ and EnSAG with support *in situ* end user validation teams. Validation activities are independent of the calibration and data quality control activities done by the Ground Segment (GS) at DLR Earth Observation Center (EOC) and German Space Observation Center (GSOC). The validation procedures and scenarios are described in the EnMAP Product Validation Plan (PVP).

In situ and scene-based validation scenarios and algorithms derive characteristic error estimates for the final EnMAP Products (Brell et al., 2022, 2021):

- L1B validation: absolute and relative radiometric uncertainty, spatially coherent artefacts (striping and dead pixel), signal-to-noise ratio (SNR), spectral parameters (e.g., SRF and smile), and spatial parameters (keystone and modulation transfer function).
- L1C validation: geometric performance (absolute and relative spatial mis-registrations), detector co-registration and band-to-band co-registration.

- L2A validation: reflectance uncertainty and aerosol and water vapor contents.

The *in situ*-based validations rely on *in situ* measurements from globally covered validation sites. Experienced international partners, extensive science-oriented field- and airborne campaigns, and selected core sites support the validation efforts with valuable *in situ* reference measurements. Established CAL/VAL sites and networks (e.g., CEOS, RadCalNet, AERONET, and HYPERNETS) supplement the respective validation scenarios. For stability- and cross-validation scenarios, Pseudo Invariant Calibration Sites (PICS) and data from other missions (e.g., PRISMA, EMIT, DESIS, Sentinel-2) are used.

For scene-based validation scenarios, such as, e.g., striping, keystone, smile (Guanter et al., 2006), and absolute and relative spatial misregistration (Scheffler et al., 2017), suitable data products/images are sufficient. These validations are performed regularly with state-of-the-art image processing and specifically designed validation algorithms.

Based on these comprehensive validation efforts, detailed information on the spatial, spectral and radiometric performance of the instrument is derived. Potential error sources can be traced back to the instrument and processing chain levels and can be incorporated into calibration and processing activities. All these combined calibration and validation efforts guarantee a high EnMAP data quality for the end-users.

2.4 Synergies of EnMAP with other Earth observation missions

While EnMAP was conceived as a stand-alone mission with scientific objectives driven by the user community, yet valuable synergies exist between EnMAP and optical and radar imagery. Synergy potential exists between EnMAP and Copernicus's Sentinel missions (Berger et al., 2012). The Sentinels provide high quality data with global coverage in the optical and microwave domain in both high and medium spatial resolution. These missions serve the Copernicus program by providing continuous and global Earth observation from space on an operational basis.

Sentinel-2 provides multispectral imagery in high spatial (10 m – 60 m) resolution and a moderate temporal (<5 days) and spectral (13 bands) resolution (Drusch et al., 2012). The global coverage of Sentinel-2 in a comparable spatial resolution to that of EnMAP (30 m) holds the synergistic potential to expand the advanced spectral regional information of EnMAP to a global scale. Sentinel-3 and similar medium-spatial-resolution optical missions operating concurrently with EnMAP, provide global data coverage in an almost daily temporal resolution (Donlon et al., 2012). Synergies between EnMAP and these missions include more frequent ecosystem observations allowing the characterization of surface processes with high temporal variations.

In addition to optical sensors, Synthetic Aperture Radar (SAR) missions also provide complementary information to EnMAP data. For example, Sentinel-1 operationally provides C-band SAR-data of the Earth's surface with spatial resolutions of 10 m – 20 m (Torres et al., 2012). This spatial resolution facilitates analysis and monitoring of physical parameters, such as surface roughness and soil moisture, which complements the biogeochemical focus of EnMAP data. Furthermore, digital elevation model (DEM) data derived from TerraSAR-X or Tandem-X using InSAR techniques can be used for data correction purposes, such as the removal of geometric distortion effects in mountainous terrain (Kokaly et al., 2013a).

The high spectral resolution of EnMAP can be combined with the current and future panchromatic and multispectral satellite systems like IKONOS, QuickBird, WorldView series, RapidEye, and Pleiades, which are characterized by a high to very high spatial resolution. Such sensors offer additional options to improve object recognition, product validation, and temporal coverage. For example, the high

temporal and spatial resolution data provided by RapidEye (one day revisit time, 6.5 m ground sampling distance) can be combined with EnMAP to augment temporal coverage, which is suitable to monitor disturbance or infestations in agricultural crops and forests.

For the development and utilization of data synergies, a thorough understanding of small-scale interactions between irradiation and complex 3D surface objects is required. Airborne data, especially in-flight fusion of hyperspectral and LiDAR data, provides expanded data dimensionality (X, Y, Z, λ) and very high spectral and spatial information to deepen the understanding of such processes (Asner et al., 2012; Brell et al., 2018, 2017). These data can serve as a small-scale link between EnMAP and other Earth observation missions. Especially the comparability and the transferability of derived surface parameters to larger scales can be refined and evaluated based on such airborne data.

3 Main application fields for EnMAP

Accurate, quantitative information on the state and evolution of terrestrial and aquatic ecosystems is needed to support resource management, conservation strategies, restoration measures, and ecosystem services. Hyperspectral image analysis can support a wide range of environmental applications from the assessment of vegetation status over mineral assemblages to water constituents and environmental hazards. EnSAG identified some of the most challenging environmental issues to which EnMAP can contribute (see section 1.4). Interdisciplinary approaches are required to address these issues as they are interconnected by multiple processes and interactions (Figure 5). Fluxes of energy, water, carbon and sediment affect multiple spheres through complex feedback mechanisms that can be directly and indirectly assessed with imaging spectroscopy. This chapter provides an overview of current areas of research and potential contributions of EnMAP data to the study of vegetation, geology and soils, coastal and inland waters, cryosphere, urban areas, atmosphere and hazards.

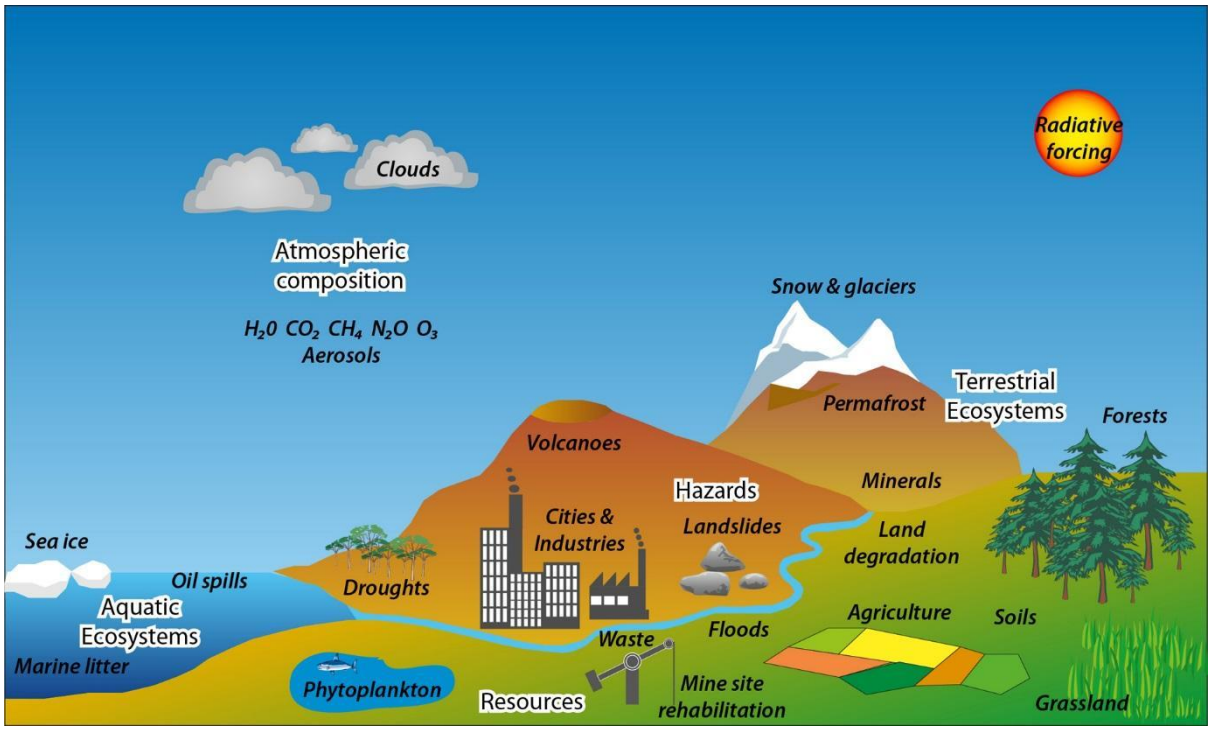

Fig. 5: Major research themes and associated application areas for imaging spectroscopy.

3.1 Vegetation

3.1.1 Natural ecosystems and ecological gradients

Natural or pristine ecosystems, defined as ecosystems largely untouched by human land use, unmanaged ecosystems or protected areas, are rare (Kareiva et al., 2007). Global environmental change impacts even the most remote areas of our planet. Characterizing and monitoring natural or close to natural vegetation in these ecosystems is essential to support sustainable human-environment systems and to deepen our understanding of indirect global impacts from local to global scales.

Unlike managed ecosystems, natural ecosystems are characterized by high heterogeneity, often with multiple ecological gradients and gradual transitions between different ecosystem types and conditions. Effective monitoring and characterization of natural ecosystems requires meso- to macro-scale data that is consistent and reproducible through space and time. This information can only be obtained by means of remote sensing (DeFries et al., 2005). EnMAP data will address these requirements by providing highly detailed spectral information at a 30 m spatial scale with regular revisit intervals (Asner et al., 2005; Leitão et al., 2015).

The application of *in situ* and airborne imaging spectroscopy data to derive taxonomic, biophysical, biochemical and phenological properties of heterogeneous vegetated surfaces has been ongoing for decades (Gamon et al., 2019; Thenkabail and Lyon, 2016; Verrelst et al., 2019, 2015). More recently, simulated and real satellite imaging spectroscopy data have been applied to questions of vegetation change and monitoring at a range of spatial scales providing new insights into vegetation traits and ecosystem functioning (Zhang et al., 2021). Vegetation remote sensing has recently undergone a paradigm shift to focus on quantifying and monitoring plant functional traits rather than biophysical parameters as they are increasingly recognized as crucial to understanding and predicting ecosystem adaptation to global change (Rocha et al., 2019; Van Cleemput et al., 2019; Zhang et al., 2021). Satellite hyperspectral remote sensing is key to describing the spatial and temporal variability of plant functional traits at scales relevant for comprehensive monitoring as well as Earth system and ecosystem modeling (Rogers et al., 2017; Zhang et al., 2021).

Derivation of vegetation properties is achieved through accurate measurements of photosynthetic pigments and the cellular structure of individual plants and plant canopies captured by spectral reflectance across narrow wavelengths. These data are then used in a variety of retrieval methods falling broadly into three categories of physical, statistical, and hybrid modeling (Verrelst et al., 2019, 2015). Physical-based leaf and canopy radiative transfer models developed in agricultural settings are being used with greater frequency to address questions of ecosystem functioning in natural ecosystems (see Ali et al., 2016; Feilhauer et al., 2017; Kattenborn et al., 2017; Kennedy et al., 2020). Using RTMs in natural ecosystems requires complex model calibration due to the heterogeneous nature of vegetation structure and canopies. Schiefer et al., (2021) highlighted the sensitivity of trait retrieval by inverse RTMs to plant phenology highlighting the difficulty in producing accurate and transferable results in natural ecosystems. Advances in statistical and machine learning provide a set of methods that can couple qualitative and quantitative analyses without being affected by collinearity effects in contiguous datasets. Developments from machine learning such as self-learning decision trees, partial least square regressions, sparse ordination methods, Gaussian processes or support/import vector machines (Breiman, 2001; Helland, 1990; Vapnik, 1998; Witten et al., 2009; Zhu and Hastie, 2002) used independently or in combination with physical models have high potential in making best use of the extended information in EnMAP data.

Beyond the use of generic algorithms for empirical modeling approaches, the development of new multi-band indices and thematic, non-linear transformations is needed. These developments must be robust and transferable. However, in most cases a biome-specific calibration procedure will be required and will be a key aspect of future algorithm development.

The parameters derived from these various retrieval methods are then used as proxies for a variety of vegetation properties including taxonomic variables such as floristic or species composition (Britz et al., 2022; Feilhauer et al., 2021), plant functional type (Lavorel et al., 2011; Ustin and Gamon, 2010; Van Cleemput et al., 2021), and invasive species mapping (Kopeć et al., 2019; Skowronek et al., 2017; Somers and Asner, 2013) biophysical variables such as leaf area index (LAI, Lee et al., 2004; Xie et al., 2021), leaf mass per area (Féret et al., 2019), and canopy equivalent water thickness (Wocher et al., 2018); and biochemical variables such as relative chlorophyll content (Jiang et al., 2022) and canopy

nitrogen and phosphorous content (Watt et al., 2020). The advancements in plant trait retrieval methods have also facilitated advancements in multi-scale biodiversity monitoring (Lausch et al., 2016). Traits retrieved from imaging spectroscopy can be powerful indicators of aboveground plant biodiversity (Gholizadeh et al., 2020; Seeley and Asner, 2021). Satellite hyperspectral data like EnMAP are recognized as a key tool in deriving priority Essential Biodiversity Variables (EBV; (Pereira et al., 2013; Skidmore et al., 2021, 2015), thereby contributing to the Aichi Targets set by the Convention on Biological Diversity (Petrou et al., 2015).

Additional vegetation properties including photosynthetic activity (Braun et al., 2017; Smith et al., 2002), aboveground biomass (Cho et al., 2007; Halme et al., 2019; Mutanga and Skidmore, 2004), carbon and water fluxes (Fuentes et al., 2006), ecosystem structure (Asner et al., 2005), and successional stage (Oldeland et al., 2010) have also been successfully retrieved from *in situ* and airborne imaging spectroscopy data. Given the sensitivity of hyperspectral data to pigments, these data are well suited for identifying and monitoring phases of plant phenology (Dronova and Taddeo, 2022). Phenological studies using air and spaceborne imaging spectroscopy have successfully identified invasive species, unique flower pigments, chemical traces of flowering events, as well as differentiating between flowers and other plant parts (Landmann et al., 2015; Rizaludin Mahmud et al., 2020; Zhang et al., 2019). These data are fundamental in improving carbon emission monitoring and accounting (Numata et al., 2011; Nurda et al., 2020) and necessary to achieve goals set out by initiatives such as The European Green Deal: Commission on Sustainable Carbon Cycles and REDD (UN Collaborative Initiative on Reducing Emissions from Deforestation and Forest Degradation

In preparation for the operational phase of EnMAP, many studies using simulated EnMAP spectra and imagery have demonstrated the utility of spaceborne hyperspectral remote sensing in monitoring and understanding natural ecosystems. Simulated EnMAP data have been successfully applied to classify plant species and assemblages in a wide variety of natural, non-forested ecosystems including wetlands (Gasela et al., 2022), shrublands (Suess et al., 2015), wildland-urban interface (Jänicke et al., 2020; Okujeni et al., 2021), subalpine and alpine ecosystems (Jędrych et al., 2017; Marcinkowska-Ochtyra et al., 2017), and Arctic tundra (Beamish et al., 2017). Retrieval of LAI (Locherer et al., 2015b), aboveground biomass (Cooper et al., 2021), as well as chlorophyll content and maximum carboxylation rate (Pacheco-Labrador et al., 2020). Though EnMAP will provide high spectral resolution data and systematic coverage, the relatively coarse spatial resolution does present challenges to some applications in heterogeneous natural ecosystems. This is particularly true in ecosystems where sub pixel heterogeneity cannot be spectrally resolved.

EnMAP imagery will provide extremely useful data at regional scales for monitoring natural ecosystems and their services, by facilitating quantification of biophysical and biochemical gradients, and heterogeneous species composition and pixel fractional cover.

The following main scientific tasks are related to vegetation applications:

- Retrieval of biochemical and biophysical variables as input for ecosystem and species habitat models to improve understanding of ecosystem and ecological processes;
- Assessment of spatial patterns of ecosystems and biodiversity from local to global scales in the context of nature conservation legislation, such as the European Special Areas of Conservation (Habitats Directive) within the Natura 2000 Network;
- Mapping and quantification of species traits, which can relate to ecological processes, ecosystem functioning and provided ecosystem services;
- Assessment of the state of biodiversity and ecosystems, as well as the services they provide, such as the above-ground carbon sequestration potential, to contribute to international initiatives, such as

the regional and global assessments being done by the Intergovernmental Platform on Biodiversity and Ecosystem Services (IPBES) and the European Green Deal Commission on Sustainable Carbon Cycles;

- Monitoring of natural or quasi-natural vegetation areas (such as protected areas, naturalized, un-used or extensively used areas) to understand causes and driving forces of changes; for example, in the context of land abandonment, forest disturbance or land degradation processes in order to combat biodiversity loss and promote ecosystem stability (e.g., REDD);
- Retrieval of Essential Biodiversity Variables (EBV) relating to species populations, species traits, community structure, ecosystem structure and ecosystem function, thereby contributing to international targets such as the Aichi targets set by the Convention on Biological Diversity (CBD);
- Quantification of spatial and temporal ecosystem transitions, such as vegetation succession, habitat heterogeneity, plant or animal community transitions, and assessment of potential feedback mechanisms; and
- Investigation of the effect of climate change and other anthropogenic and non-anthropogenic forces on global vegetation gradients.

3.1.2 Forests

Worldwide, forests provide timber and non-timber products as well as numerous environmental goods and services. These include conservation of biological diversity and climatic regulation, which are crucial for local livelihoods (FAO, 2010). Forests and forested ecosystems are rapidly degrading under increasing global change pressure (Peng et al., 2011) and the expansion of human population and economies (Hansen et al., 2008). Deforestation and the loss of carbon and biodiversity associated with conversion of forests to agricultural land, legal and illegal timber harvesting, drought stress, biotic stress, and recurrent wildfires are some of the most important processes affecting forested landscapes (Anderegg et al., 2013; Bond et al., 2010; Ciais et al., 2005; Huang et al., 2019; Schuldt et al., 2020).

Forest management challenges are multiscale and intricately linked to society's needs to preserve forest integrity while also benefiting from forest products. Sustainable forest management must combine economic interests with ecological concerns. In this context, remote sensing data can serve both economically oriented assessments and management needs as well as studies of ecological processes and functioning (Franklin, 2001). Applications of remote sensing data to sustainable forest management are generally presented in four categories that include 1) classification of forest cover type (i.e., tree species), 2) estimation of forest structure and available resources (i.e., timber volume, height, age, crown closure), 3) forest change detection and 4) forest modelling. For each category, measurable indicators are needed to quantify the effects of management activities and natural phenomena on the sustainability of forest resources. Current research is directed at quantitatively relating remotely sensed spectral information to ground-based assessments of structural and physiological aspects of forest condition.

EnMAP data will facilitate the efficient characterization of the spatial distribution of forest ecosystems and support inventories of forest resources. Such inventories are typically comprised of quantitative attributes related to forest species, health, and functioning, including estimates of chlorophyll, nitrogen, lignin and canopy water content (Asner et al., 2011; Goodenough et al., 2003; Matson et al., 1994; Schlerf et al., 2010, 2005). Quantifying species-specific canopy biochemistry using imaging spectroscopy is well established to map forest species and ecosystems (Goodenough et al., 2003; Martin et al., 1998). The fusion of hyperspectral data with other remote sensing data sources like SAR or LiDAR offers additional perspectives to estimate forest structure, forest type, biomass, timber volume,

tree heights, stem densities, and age classes (Anderson et al., 2008; Buddenbaum et al., 2013; Dalponte et al., 2008; Huang et al., 2010). It is also possible to estimate above-ground carbon by combining hyperspectral imagery with geographic information, *in situ* measurements, and physiological models (Le Maire et al., 2005), as well as texture and object information (Blaschke, 2010; Buddenbaum et al., 2005; Van der Linden, 2007). The high spectral resolution of EnMAP data is expected to improve estimates of forest structure and condition and therefore above-ground carbon stocks.

Like other biomes, hyperspectral data of forests will facilitate the quantification of essential biodiversity variables (Skidmore et al., 2021). Sustainable forest management, as prescribed in the New EU Forest Strategy for 2030 (European Commission, 2021) aims to increase the climate effects of forests (e.g., by increasing the carbon stocks and sinks in forests) while preserving biodiversity loss. Imaging spectroscopy with a spatial resolution comparable to that of EnMAP allows the quantification of beta diversity, i.e., variation in plant species composition (Schweiger et al., 2018). The scale of diversity which can be directly mapped depends on the ratio of pixel to plant size: airborne hyperspectral data is capable of separating overstory species (e.g., Laurin et al., 2016; Schäfer et al., 2016). It is therefore possible that EnMAP can detect relatively homogeneous patches of a single species in semi-managed landscapes, but its applicability to different forest biomes needs further investigation. Information on biodiversity and especially on the spatial distribution of forest stands with a larger diversity value will be essential in future forest management and protection.

Imaging spectroscopy-derived structural and biochemical properties serve as required inputs to initialize, calibrate, and validate regional and global models of carbon exchange, evapotranspiration and nutrient cycling (Tenhunen et al., 1998). The availability of EnMAP data will provide new insights into regional scale models which in turn can assist management decisions to mitigate the effects of climate change on a regional scale. A final property that has received increased attention in the last decade is sun-induced chlorophyll fluorescence (SIF). SIF is closely linked to photosynthetic activity and can be measured using imaging spectroscopy (Guanter et al., 2014; Meroni et al., 2009; Rascher et al., 2009; Wang et al., 2022). However, the spectral resolution of the sensor used to derive SIF is critical for reliable measurements (Damm et al., 2014). Therefore, it remains to be seen if the spectral band design of EnMAP will allow for estimates of vegetation fluorescence; this will be important with respect to defining instrument requirements for future spaceborne systems.

Spaceborne hyperspectral imagery has the potential to improve assessments of reforestation, afforestation, and deforestation rates at regional scales (Clark et al., 2011; Goodenough et al., 1998). These measures are essential for documenting changes in forests over time and are urgently required for the implementation of the Agreement of the Paris Summit on Climate Change (December 2015). Previous studies on forest ecosystems emphasize the utility of imaging spectroscopy to provide detailed and accurate retrievals of relevant vegetation properties (Ollinger and Smith, 2005; Schaepman et al., 2004). The most important vegetation properties for assessing forest health, biochemistry and overall ecosystem functioning are leaf chlorophyll and nitrogen content, the fractions of photosynthetically absorbed radiation (fAPAR), canopy water content, annual maximum leaf mass per area (LMA), and annual maximum leaf area (LAI) (e.g., (Lausch et al., 2017; le Maire et al., 2008; Meiforth et al., 2020). An important requirement for the successful retrieval of some of these properties is that leaf-level signals are compensated for in canopy-scale measurements (Knyazikhin et al., 2013; Malenovský et al., 2019).

The quantification and monitoring of additional forest-related phenomena such as wildfires and disturbance will also benefit from EnMAP data. The enhanced potential of imaging spectrometers to identify drought and moisture levels of critical fuel will provide important perspectives for wildfire management (Koetz et al., 2008; Kötz et al., 2004; Veraverbeke et al., 2018, 2014). Additionally, spaceborne imaging spectrometers have the potential to identify insect attacks at early stages when the

effects on forest reflectance are subtle and cannot be detected with conventional multispectral sensors (Abdullah et al., 2019; Fassnacht et al., 2012; Niemann et al., 2015; Wulder et al., 2009).

Given the complexity of hyperspectral data analysis, advanced methods have been developed to support the analysis of EnMAP data (Goodenough et al., 2012, 2007). Forest leaf and canopy reflectance models require the integration of forest structure, clumping, shadowing and understory effects. Reflectance models ranging from simple approaches like INFORM (Atzberger, 2000) or 4-scale (Chen and Leblanc, 1997) to more complex geometric-optical radiative transfer models like FRT (Kuusk and Nilson, 2002) or ray tracing models like FLIGHT (Gerard and North, 1997) have been developed and validated in order to analyze the complex hyperspectral signal of forests (Förster et al., 2010). Despite some successful attempts (Combal et al., 2003; Kötz et al., 2004; Schlerf and Atzberger, 2006; White et al., 2000), the inversion of these models is still a challenge and a pressing research issue for the future.

EnMAP will enable derivation of spectral indices that will serve as bio-indicators of forest health. Through repetitive sampling of selected forest condition test sites, EnMAP will add the phenological history to the full spectral sampling data to yield effective bio-indicators of forest condition. EnMAP will provide a capability to compare observations of spectral properties of forests in many different countries. This is essential to develop a consistent tool for monitoring the carbon state of the world's forests and their response to climate change. Frequent and broad coverage will increase our understanding of the links between pigments, canopy chemistry, stress, and forest type. For forest inventory programs, hyperspectral data from EnMAP will provide an important sampling system to ensure precise measurements of indicators for a sustainable development.

Accordingly, the following main scientific tasks are considered important concerning forest applications:

- Mapping of forest species distributions using hyperspectral, fused and multitemporal datasets, exploring the potential of advanced classification algorithms, texture and object information, and linkages to geographic databases, etc.;
- Estimation of forest biomass, above-ground carbon, and productivity;
- Detection of biodiversity hotspots and essential biodiversity variables for forest management and protection planning;
- Assimilation of biochemical and structural forest parameters into process models;
- Enhancement and development of invertible vegetation canopy reflectance models for the extraction of forest parameters, and forest mensuration, health, and risk assessment;
- Investigation of the viability of phenological signatures through indicators of canopy pigments and chemistry with regard to ecophysiological processes;
- Development of improved indicators of forest condition and health;
- Development of forest monitoring procedures, including multi-temporal and multi-sensor data, for the detection of changes in forest quality and canopy cover; and
- Creation of advanced expert systems to improve the efficiency of hyperspectral information extraction within the forestry context.

3.1.3 Agricultural lands

Limited bioproductive land coupled with progressing land degradation, rising population, increasingly meat-prone diets and a growing demand for biofuels cause substantial land use conflicts between food, fiber and energy production. The additional pressure of on-going climate change and increasing extreme

meteorological events also threatens ecosystem services like biodiversity. To protect natural ecosystems while meeting the growing demand for agricultural commodities global land productivity must be substantially increased (Mauser et al., 2015). Global studies highlight that large appropriation of land resources leads to low efficiencies in land management (e.g., water use; Haberl et al., 2007; Kijne et al., 2009). The challenge of sustainably meeting global agricultural demands involves a wide range of land management aspects, including selecting suitable crops and cultivars, monitoring and improving water productivity, promotion of organic farming, fertilizer optimization and plant protection, soil conservation, and efficient irrigation systems. Recently, the role of agricultural soils as long-term carbon sinks to mitigate the negative climate-related effects of agricultural activities has been intensely discussed. Known as "Carbon Farming" practices such as working in crop residues and cultivating intermediate crops aim to enrich soil organic carbon in agricultural soils (Mattila et al., 2022a). Due to spatial variability in climate, soils, and topography, as well as societal aspects like culture, education, technology, and markets, agricultural management critically relies on spatial data to support management decisions. Modern farming practices naturally incorporate the identification, analysis, and management of spatial and temporal heterogeneity and variability to optimize profitability, sustainability, and environmental protection (Mauser et al., 2015).

More than 20 years ago Moran et al., (1997) identified key areas where remote sensing could provide spatial information relevant for agricultural management. These areas included mapping crop yield and biomass status as well as monitoring seasonally and spatially heterogeneous soil and crop characteristics. Since this early assessment, our understanding of farming-related land management has progressed to detailed site-specific management to support sustainable production and increased productivity. Sustainable agricultural management includes early detection of plant disease, water and nutrient stress, monitoring agriculture intensification and evaluation of changing land viability due to climate-induced shifts in cultivation belts (Franke et al., 2022; Zabel et al., 2014). The implementation of these land management practices has led to a new demand for more complex and integrated spatial information around the globe. For example, land evaluation requires data to evaluate site and plant specific yield gaps (i.e., the differences between potential and actual harvested yields), fertilizer use intensity, as well as determination of seeding dates and detection of phenological phenomena.

Hyperspectral data like that provided by EnMAP delivers more detailed agricultural information compared to multispectral data and can better support farming management decisions (Hank et al., 2019). Multispectral data are commonly used to derive agriculturally relevant information through statistical regression analyses between ground-based measurements of biophysical variables and simple spectral indices. Hyperspectral data enable the application of more complex approaches that fully exploit the continuous spectral information provided by imaging spectrometers. One important approach making use of the continuous spectral information are invertible leaf and canopy radiative transfer models (RTM). RTMs infer biochemical/biophysical parameters from continuous canopy spectral reflectance and have been successfully applied to field crops and grasslands (Berger et al., 2018a, 2018b; Danner et al., 2019; Jacquemoud et al., 2009). Combined with machine learning algorithms, an improved physical understanding of interactions between electromagnetic radiation and matter is made accessible with high computational efficiency. These computational advancements are crucial for large regional hyperspectral datasets recorded by spaceborne systems like EnMAP. The recent synergies between physically-based and machine learning approaches are referred to as hybrid retrieval and show great promise in agricultural applications (Berger et al. 2021a).

Variables that control productivity and health of crops and can be estimated using hyperspectral data and RTM inversion:

- Leaf area index (LAI) describing the size of the producing layer and the surface that is available for exchange processes between the Earth's surface and the atmosphere (Locherer et al., 2015a; Weiss et al., 2001);
- Absorbed photosynthetically active radiation (APAR) providing the amount of absorbed energy potentially usable for production (Weiss et al., 2010);
- Chlorophyll content as the chemical agent for photosynthesis, which is dependent on the crop nitrogen status (Danner et al., 2017; Haboudane et al., 2002; Oppelt and Mauser, 2003);
- Water content as an indicator for crop water status and crop maturity (Hank et al., 2010; Wocher et al., 2018);
- Plant density as an indicator of disease sensitivity (Larsolle and Hamid Muhammed, 2007); and
- Plant pigments, such as carotenoids and anthocyanins, as indicators of adaptation of the canopy to varying light conditions or other stressors (Blackburn, 2007; Gamon et al., 2015; Wocher et al., 2020).

The development of new canopy reflectance models such as PROSPECT-PRO, where the absorption caused by proteins and carbon-based constituents can explicitly be discerned (Féret et al., 2021), have led to new variables of interest, which can be retrieved from hyperspectral data:

- Canopy nitrogen content, which is key to monitoring the nitrogen use efficiency, i.e., the relation between nitrogen fertilizer input and nitrogen content achieved in the harvested parts of the canopy, and the yield quality of crops, which for example for cereals directly depends on the protein content of the grains (Berger et al., 2020; Verrelst et al., 2021)
- Non-photosynthetic vegetation (NPV) or carbon stored in crop biomass, which is important to assess the impact of agricultural management on the carbon cycle (Berger et al., 2018b; Pepe et al., 2020).

Although not supported in all cases by physical absorption features, statistical retrieval approaches using hyperspectral data have recently shown promising results for detailed canopy constituents such as:

- Micro- and macronutrients, e.g., Kalium, Potassium, Nitrogen, Sulphur, Calcium, Ferrum, Magnesium, Zinc, which all depend on agricultural management and determine the nutritional value of crop production (Belgiu et al., 2021).
- Different biotic and abiotic stressors, which strongly influence vegetation development and where hyperspectral methods may successfully contribute to plant stressor discrimination (Berger et al., 2022; Lassalle, 2021).

Assimilation of plant properties into agro-ecological models allows for an explicit simulation of crop growth, development, and yield using spatially heterogeneous hyperspectral data. Model-based assimilation approaches provide site-specific information on key farming variables, such as biomass, plant height, crop yield, nitrogen or phosphorus deficit and/or uptake, which are not directly observable with remote sensing. Time series of remotely sensed crop variables account for spatiotemporal heterogeneity in agricultural production models, which then can be used to explore the suitability of different management options (Hank et al., 2012; Huang et al., 2019). Vegetation properties such as LAI, phenology, seeding and harvesting dates or soil moisture can also be derived from multispectral, thermal or microwave sensor time series. Ultra-high spectral resolution systems allow for the monitoring of SIF, which can be used as a proxy for photosynthetic efficiency (Guanter et al., 2014; Rascher et al., 2015).

Dynamic vegetation models that assimilate spatially heterogeneous hyperspectral data simulate plant growth based on eco-physiological processes and feedbacks during photosynthesis and respiration. The most realistic representation of vegetation dynamics in regional agro-ecological models as well as regional to global ecosystem and Earth system models is based on a combination of dynamic vegetation models, agricultural management models, and canopy models. Together they simulate the distribution of assimilates among the plant constituents (i.e., roots, stem, leaves, grains) to represent complex canopy layers (e.g., LPJ-mL (Bondeau et al., 2007), PROMET (Hank, 2008), DSSAT(Hoogenboom et al., 2019)). Studies have shown that data assimilation approaches are viable and provide good results (Hank et al., 2015; Machwitz et al., 2014). Nevertheless, further research and development is needed to improve models, in particular process representation and accuracy. To reach an operational stage of such coupled model systems, various data assimilation methods should be tested under a broad range of farming conditions, especially in regions with low-efficiency farming systems. Testing should also include different crops (e.g., cassava, sorghum, groundnut) and energy plants (e.g., sugar cane, oil palm, jatropha), different stresses (e.g., water, fertilizer, temperature), irrigated agriculture, and mixed silvi-agricultural systems.

For all remote sensing applications investigating managed farmlands, continuous monitoring of temporal dynamics is crucial. EnMAP will be one of the first imaging spectrometers to provide high-quality multi-temporal hyperspectral imagery from space and, together with contemporary missions such as PRISMA, CHIME and SBG, will contribute to enhanced process understanding. Based on the knowledge already gained in numerous studies with airborne sensors, EnMAP will offer hyperspectral data in a suitable spatial and temporal resolution to approach the next major scientific steps, leading away from regression analysis and towards mechanistic process representation.

Accordingly, the following major scientific tasks are of importance for agricultural applications:

- Development and improvement of accurate, robust and reliable biophysical variable retrieval methods based on inversion of improved canopy RTMs using imaging spectroscopy data and being computationally supported by machine learning algorithms (crop type, LAI, APAR, chlorophyll content, plant water content, canopy geometrical structure);
- Development and improvement of methods for the quantitative mapping of soil variables, also taking the spectral signal of green and senescent vegetation into account, that will allow for tracing the gradual enrichment of soil organic carbon as part of soil melioration processes;
- Development and improvement of approaches to derive complex canopy variables, e.g., canopy nitrogen/protein content, crop phenology, management intensity, yield gaps, non-photosynthetic plant tissue and crop residues, from hyperspectral remote sensing data in conjunction with ancillary remotely sensed data;
- Development of operational methods for biomass, yield mass and yield quality estimation and forecasting based on hyperspectral remote sensing and ancillary data in combination with complex process models;
- Mapping of crop species distribution using time series of hyperspectral information;
- Distinguishing of crop stressors like nitrogen or other micro- and macronutrients deficiency, crop disease, insect infestation, water stress, and chlorosis; and
- Development and improvement of approaches to assimilate remote sensing derived spatial distributions of vegetation and soil variables into dynamic agro-ecological models, which can serve as a basis for integrated information-driven agricultural management systems

3.2 Geology and soils

Imaging spectroscopy is an effective tool to detect, monitor, and manage key abiotic natural resources including minerals, soils, and fossil fuels, which are largely non-renewable. Current research in hyperspectral remote sensing focuses on the assessment of mineral deposits (Bedini, 2017; Peyghambari and Zhang, 2021), the detection of oil spills (Lammoglia and Filho, 2011; Yang et al., 2020), the derivation of soil properties (Ben-Dor et al., 2009; Chabrillat et al., 2019; Ge et al., 2011; Lu et al., 2020), and the evaluation and monitoring of soil quality (e.g., water and carbon storage, acidification and erosion) (Schmid et al., 2016; Stevens et al., 2013).

3.2.1 Geology and exploration

Minerals, or more specifically ore minerals, contain economically valuable elements (mainly metals), which are essential to modern industry and, therefore, the development of society. The constantly changing demand of ores and the criticality to the producing industry causes perennial re-evaluations of existing occurrences, deposits and mines, and the global detection and validation of new deposits. Among geophysical and geochemical field surveys, hyperspectral remote sensing surveys are increasingly applied to exploration investigations. The basic principle of hyperspectral remote sensing for mineral detection is the mathematical description and statistical analysis of material characteristic signals in the spectral ranges of the visible and infrared wavelength range (Clark et al., 2003; Hunt, 1977; van der Meer, 2004; van der Meer et al., 2012). These characteristic signals (absorption bands) are physically based on electronic transitions in the d- or f-orbitals of the elements (e.g., transitions into the valence band for Fe and crystal field transitions for rare earth elements), or vibrational motions and their overtones in the molecular bonds (e.g., Fe-OH and Mg-OH in amphiboles, Al-OH in clay minerals, CO3 in calcium carbonates) (Dieke and Crosswhite, 1963; Hunt, 1977; Swayze et al., 2014).

The EnMAP hyperspectral satellite has the potential to identify, characterize, and map many VNIR–SWIR active minerals on the Earth's surface provided that the mineral occurrences are large enough to be resolved at 30 m and vegetation cover does not exceed 30% of the pixel area. The detectable minerals can be grouped into the following classes (Hunt and Ashley, 1979):

- Phyllosilicates (di-, and tri-octahedral): clay minerals comprising the kaolinite group of minerals (kaolinite, halloysite, dickite, nacrite, etc.), smectites (montmorillonite, nontronite, saponite, and hectorite), and illite, talc, pyrophyllite, mica group (muscovite, phengite, biotite, vermiculite), chlorite (Fe-, and Mg-rich species), and serpentine group (antigorite, chrysotile, and lizardite).
- Sorosilicates: epidote and clinozoisite.
- Nesosilicates: olivine and topaz.
- Syclosilicates: tourmaline (schorl, dravite).
- Tectosilicate: opal, scapolite, zeolite
- Inosilicates: tremolite series (tremolite, actinolite, hornblende, riebeckite) and pyroxene group (diopsite).
- Carbonates: calcite, dolomite, siderite, magnesite, and ankerite.
- Sulphates: gypsum, anhydrite, alunite, jarosite, copiapite, schwertmannite
- Oxides & hydroxides: hematite, maghemite, chromite, goethite, lepidocrocite, ferrihydrite, diaspore, gibbsite, brucite
- Ammonium-bearing minerals: buddingtonite (ammonium feldspar), a–illite, etc.

EnMAP hyperspectral data are expected to be widely used for mineral and resource exploration. The mineral systems that could be studied in this way include porphyry copper (±Au–Mo) (Graham et al., 2018), low-, and high-sulfidation epithermal gold (Bedini, 2009; Portela et al., 2018; Swayze et al., 2014; Thomas and Walter, 2002), Carlin-type gold (Rockwell and Hofstra, 2008), Archean Lode gold (Bierwirth et al., 2002), volcanogenic massive sulfide (VMS) deposits (Cudahy, 2016; Van Ruitenbeek et al., 2012), iron oxide-copper-gold (IOCG) (Laukamp et al., 2011), calcic and magnesium skarns and polymetallic deposits (Rowan and Mars, 2003; Wan et al., 2021), sediment-hosted Pb-Zn mineralization (Budkewitsch et al., 2000; Yang et al., 2018), uranium mineralization (Salles et al., 2017), carbonatites and associated REE and niobium (Nb) deposits (Bedini, 2009), kimberlites (Kruse and Boardman, 2000), as well as lithium resources (Cardoso-Fernandes et al., 2020), iron ore deposits (Cudahy, 2016), bauxites (Kusuma et al., 2012), and many industrial minerals (King et al., 2012).

In the volcanic environment, EnMAP data could be used for lithologic mapping and characterization of different rock units including felsic (Rivard et al., 2009), mafic (Harris et al., 2005), ultramafic rocks (Rogge et al., 2014; Rowan et al., 2004), ophiolite sequences (Roy et al., 2009), peridotites (Launeau et al., 2002), and mapping and monitoring of volcanoes and their resulting debris (Kereszturi et al., 2018). Over metamorphic rocks, EnMAP data could be useful to study metamorphism (T-P path) and map the zonation associated with metamorphic minerals (Kozak et al., 2004).

In sedimentary terrain, EnMAP could be used for facies mapping and stratigraphic classification (Dadon et al., 2012), characterization of post-depositional history in a sedimentary basin, mapping of red-bed bleaching (Bowen et al., 2007), differentiation between different carbonate phases (Keeling et al., 1998), dolomitization discrimination (McCormick et al., 2021; Windeler and Lyon, 1991), gypsum quantification (Milewski et al., 2019) and identification of micro seepage-prone zones in a sedimentary basin (Asadzadeh and de Souza Filho, 2017). In playa and evaporative lakes, hyperspectral data could be applied to differentiate between evaporate minerals in the environment (Crowley, 1993; Kodikara et al., 2012). Eventually, the imaging spectroscopic data could be useful for regolith mapping in highly weathered terrains (Agustin, 2017) and for determining the mineralogical variations of aeolian deposits (dunes) in desert environments (Hubbard et al., 2018).

Four key products could be directly extracted from EnMAP spectral reflectance data including mineral classification, mineral abundance (i.e., areal fractional cover of mineral within each pixel), mineral compositional variations (e.g., the degree of Tschermak substitution in white micas), and finally mineral crystallinity (e.g., kaolinite crystallinity) (Asadzadeh and de Souza Filho, 2017). The spectroscopic contents of the image, however, could be statistically correlated to a rich variety of other geological-geochemical variables.

Classification maps derived from hyperspectral data are useful for the identification and characterization of alteration mineral assemblages, visualization of zonation patterns around mineral deposits as well as for lithology mapping. Abundance maps provide semi-quantitative information about the proportion of minerals present in each pixel and scene, which can be indicative of ore grades (e.g., in the case of monoaminergic deposits). Composition maps can indicate physiochemical conditions (temperature, pressure, redox, pH, and chemical activities) of the mineralized/metasomatized/altered systems and provide a vector toward the orebodies (Cudahy et al., 2008). It is also useful for demonstrating the large footprints of a mineral system. Composition maps can also be deployed to infer paleo-fluid pathways and fluid-rock reaction zones in outcropping lithology (Cudahy, 2016). Crystallinity maps (e.g., for kaolinite) can indicate mineral quality and origin and the degree of bedrock weathering. Other information extractable from EnMAP data products could be oxidation-reduction fronts, paleo-erosion and paleo-surface levels, and pH of mining sites (more on this in section 3.7).

In many aspects, EnMAP data can complement high-spatial and/or high-temporal resolution multispectral data for mapping and monitoring purposes and improve the resource exploration processes.

The following main scientific tasks are related to geological exploration:

- Development of versatile algorithms for the identification and mapping of listed minerals under complex mixing conditions;
- Analysis of the capability of hyperspectral data for the detection of rare earth minerals based on different globally distributed sites;
- Development of new algorithms and models for non-linear, weighted unmixing and mineral quantification approaches; and
- Analysis of the capability of EnMAP data in new fronts in geology and mineral exploration including (but not limited to) lithium and rare earth element resources.
- Investigation of the effects of mineral-induced stress on the spectral signature of dense vegetation canopies to establish a link between vegetation stress and specific minerals.
- Spectral unmixing and removal of the effect of vegetation on spectral signatures of minerals.

3.2.2 Digital soil mapping

Soil is a fundamental and irreplaceable natural resource, which is largely non-renewable. Soils are complex dynamic systems, which are formed and developed through the combined effects of climate and biotic activities, modified by topography. Soil development can be either progressive or regressive with time, and a modification of the chemical, physical, and mineralogical properties of soil surfaces can take place at variable time scales from event-based to seasonal. Soil provides a multitude of land-based ecosystem goods and services supporting and regulating life on the planet. It carries out several key environmental functions that are essential for human subsistence, such as food, fiber and timber production, water storage and redistribution, pollutant filtering and carbon storage. In the last years, the role of soils as long-term carbon sinks and land management practices of so called “carbon farming” have gotten much attention (e.g., on the EU level) to tackle climate change, bringing benefits in terms of carbon sequestration, storage and other co-benefits. Understanding the response of soils to external drivers (global environmental changes, management) to assist in decision making at all scales requires precise spatially referenced soil data and maps. However, conventional soil surveys are scarce, expensive, time intensive and often not comparable (harmonized), which precludes a meaningful assessment of the state of soil resources at large scales. As an alternative, laboratory soil spectroscopy has proven to be a fast, cost-effective, non-destructive, and repeatable analytical technique that can be used to monitor the state of soils (Chabrillat et al., 2019; Nocita et al., 2015). From airborne platforms, hyperspectral remote sensing of soil can quantify key topsoil properties (organic carbon, texture, mineralogy) over a broad gradient of soils. In particular, the amount of organic matter and iron content, particle size distribution, clay mineralogy, water content, soil contamination, cation exchange capacity and calcium carbonate content, can be determined with imaging spectroscopy (e.g., Ben-Dor et al., 2009; Chabrillat et al., 2019; Stevens et al., 2013). Due to the complexity of soil as a mixture of organic and inorganic compounds and expressed in VNIR reflectance properties, simple band assignment techniques or spectral matching, such as those done in the field of geology, are rarely used. Instead, multivariate calibration (i.e., statistical) approaches, which allow full quantification of the soil properties based on field data for local calibration, are preferred. In recent years, digital soil mapping has been driven by novel artificial intelligence (AI) algorithms for the prediction of soil properties from spectral data. AI and more concrete the machine (ML) and deep learning (DL) algorithms lie at the core

of soil spectroscopy regression analyses (Angelopoulou et al., 2019; Gholizadeh et al., 2018), since they achieve unprecedented levels of performance when learning to solve increasingly complex computational tasks, especially using hyperspectral data. Furthermore, localized learning approaches have been shown to yield better results compared to global approaches, as spectrally and/or spatially neighboring samples tend to produce concentrated clusters with limited spectral variation (Ramirez-Lopez et al., 2013; Tziolas et al., 2019; Ward et al., 2020).

Hyperspectral data provided by EnMAP has considerable potential to characterize the pedosphere by identifying soil properties, their changes over time, and relationships between soil degradation and canopy spectroscopy (Milewski et al., 2022). Digital soil mapping toolboxes that include automatic identification and semi-quantification of key soil properties, such as organic carbon, water content, clay, iron, carbonates mineral content, are already available at a global scale (Chabrillat et al., 2011). For the full quantification of soil properties, EnMAP simulations (Chabrillat et al., 2014; Milewski et al., 2019; Steinberg et al., 2016) and recent PRISMA data (Mzid et al., 2022) facilitated the generation of soil maps in specific test sites where ground-reference data were available. In view of limited arable land area and rising population, the emerging field of precision farming is receiving increased attention and the soil science community is facing a growing need for regional, continental, and worldwide digital soil databases to monitor the status of the soil. Supported by imaging spectroscopy, soil conditions can be better assessed allowing farmers to better evaluate critical needs such as irrigation, nutrient supply, and cultivation to gain increased agricultural yields (Demattê et al., 2000; Wesemael, 2022). Nonetheless, advances are still necessary to fully develop hyperspectral products that can support, in a credible manner, digital mapping and monitoring of soils (Wulf et al., 2015). To exploit the full potential of spaceborne imaging spectroscopy for soil mapping, challenges have been identified, e.g., linked to limitations in reference data availability (specifically global standardized soil spectral library databases) and in methodological approaches and tools adequate to process spectral data into practical soil model solutions that are globally applicable (e.g., Ben-Dor et al., 2019; Chabrillat et al., 2019). In this context, extensive efforts are currently being made to establish regional, national, continent-wide, and global soil spectral libraries.

A number of recent case studies emphasize leveraging open source, regional to continental soil spectral libraries such as the European LUCAS SSL (Orgiazzi et al., 2018) to exploit upcoming hyperspectral remote sensing data (e.g., EnMAP data) by using state of the art machine learning and deep learning techniques to model soil properties with high accuracies (Tziolas et al., 2020; Ward et al., 2020). New developments to harmonize global soil spectral databases that should be acquired following common standards and procedures so that they can be merged with other soil spectral libraries (Ben Dor et al., 2015; Chabrillat et al., 2019; Francos and Ben-Dor, 2022). A further ongoing challenge of digital soil monitoring efforts are soil surface conditions that disturb the spectral signal at the spatial resolution of the sensor such as soil moisture, roughness, and mixing with residual photosynthetic active, as well as none-active vegetation that also can be dynamic over time (Chabrillat et al., 2019; Van Wesemael et al., 2021). For some disturbance effects, new physical-based and empirical modelling approach have been proposed to correct the impacts on soil property mapping, e.g., Diek et al., (2019) and Dupiau et al., (2022) for soil moisture, Kuester et al., (2017) and Li et al., (2017) for modelling of partial vegetation cover. However, the applicability of these methods to spaceborne hyperspectral imagery is not yet completely resolved. Experience in this domain from multispectral satellites (e.g., Rogge et al., 2018) might help to develop such strategies for hyperspectral satellite data (Chabrillat et al., 2019).

The following main scientific tasks are related to digital soil mapping:

- Retrieval of soil properties, such as organic matter and iron content, particle size distribution, clay mineralogy, water content, soil contamination, cation exchange capacity and calcium carbonate content to analyze status and changes of soils;

- Improvement of methodologies and algorithms for the extraction of key soil parameters based on remote sensing spectral signal with emphasis on prediction accuracy and influence of spatial scale;
- Quantitative estimation of the influence of surface parameters in bare and semi-bare areas (such as water content, vegetation cover, surface roughness) on the spectral signature of soils and on the retrieval of soil properties;
- Analysis of the contribution of global soil databases to calibrate the remote sensing-based soil condition indices against reference samples; and
- Monitoring of the state of soils and development of spatio-temporal maps of soil properties.

3.3 Coastal and inland waters

Coastal and inland water bodies are vital for recreation, food supply, commerce and human health, and they also support habitats for a large floral and faunal diversity. For decades, coastal and inland aquatic ecosystems have experienced pressure from increasing social and economic activities as well as climate change. As sinks for pollutants, coastal and freshwater ecosystems are among the most sensitive indicators of environmental impacts related to human activities (UNEP, 2012). For example, increasing eutrophication and pollution of coastal and inland water bodies caused by fluvially transported substances is a major global ecological problem. Substances such as phosphate and nitrogen compounds that cause eutrophication are derived from intensified agricultural and industrial activities. Monitoring and managing the water quality of coastal and inland habitats is necessary as they are vital to urbanization, tourism, transportation, industry, fish farming and drinking water supply. According to the EU Water Framework Directive, specified biological, hydro-morphological and physico-chemical parameters of water bodies have to be monitored on a regular basis to assess water quality. Water quality assessment is relevant for freshwater security and the ever-increasing aquaculture-influenced coastal and inland water bodies. Water quality assessment is also crucial for monitoring and managing endangered ecosystems, such as coral reefs, seagrass meadows and mangrove forests (Bell et al., 2008; Van Langevelde and Prins, 2007).

A major advantage of hyperspectral data for monitoring coastal and shallow freshwater bodies is the ability to spectrally unmix optical constituents in the water column and the sea floor or lake bottom (Carder et al., 1993; Goetz, 2011). The advanced spectral resolution of EnMAP in the VIS, NIR, and SWIR spectrum will allow the assessment of phytoplankton pigments, suspended matter, dissolved organic matter, dissolved organic carbon concentration, and water transparency. Moreover, phytoplankton taxonomy can be identified, which can indicate the occurrence of harmful algal blooms (Bracher et al., 2009). Chlorophyll-a concentration is widely used as an indicator of algal biomass that depends on nitrogen and phosphate availability in water bodies (Kamarainen et al., 2009; R.E. and J., 1996). Water transparency is a widely used indicator of the trophic state, which is influenced by the abundance of organic and inorganic suspended particulate and dissolved matter (Kirk, 1994). Researchers have developed algorithms using imaging spectroscopy data to quantify various parameters, including chlorophyll-a, humic substances, suspended matter, yellow substances, and water transparency (Dinter et al., 2015; Giardino et al., 2007; Kallio et al., 2001; Oelker et al., 2022; Schiller and Doerffer, 1999; Thiemann and Kaufmann, 2002, 2000). EnMAP can make use of these standards for detailed observations of coastal zones and inland waters, while sensors such as MODIS, VIIRS, and the recent OLCI as part of ESA's Sentinels are designed for ocean applications with frequent observations at coarser spatial resolutions. Algorithms for coastal and inland water constituents with different phytoplankton, particulate and dissolved matter composition will be adapted and improved for EnMAP to provide water quality data at a higher spatial resolution (Bracher et al., 2021; Gege, 2021).

EnMAP data will provide frequent information on the type and status of seafloor substrates for optically shallow waters. Water column correction approaches using hyperspectral data allow the identification of bottom vegetation types and, if regularly monitored, the observation of sedimentation dynamics, as well as short- and long-term changes in species distribution and structure (Vahtmäe, 2011). Quantitative analyses of coastal benthic communities can provide information on net primary production (Dierssen et al., 2010) and many benthic species act as environmental indicators. Therefore, their consistent monitoring provides information of the state of coastal marine environments and evidence for environmental changes (Phinn et al., 2005; Vahtmäe et al., 2006). In this context, the fusion of EnMAP data and satellite data with a high spatial resolution (e.g., Worldview, GeoEye) offers the potential to pinpoint heterogeneously distributed benthic vegetation and sediment patches. The fusion with high spatial resolution data also offers the potential to monitor frequently invasive benthic and emergent species (Albright and Ode, 2010; Forrest et al., 2012). Monitoring benthic vegetation can also support integrated coastal zone management to monitor species (e.g., Ulva, Laminaria, seagrasses) that are grown for human consumption or for aquaculture (Anderson et al., 2007; Radiarta et al., 2011). Coastal ecosystems are highly productive and store large amounts of carbon (Cole et al., 2007; Pidgeon, 2009). The distribution and dynamics of organic carbon in vegetation, in combination with dissolved organic matter, are important for understanding regional and global carbon cycles. In this context, the EnMAP data provide efficient means to characterize the role of coastal and inland water bodies in carbon uptake and release.

Coastal and freshwater ecosystem management involves modelling and monitoring, which require reliable information and robust analytical techniques. Conventional mapping methods are logistically constrained, and airborne campaigns are cost intensive and often limited to a few acquisitions. The EnMAP satellite will enable consistent quantitative monitoring of the water-related environmental parameters mentioned above. The combination of hyperspectral data with ecological or hydrological models, geographic information systems and *in situ* measurements allows the development of advanced integrated management plans for coastal zones and catchments characterized by inland water bodies, wetlands, or reservoirs (Radiarta et al., 2011; Yang, 2009). The fusion of hyperspectral data with thermal infrared data offers additional perspectives to the analysis of the trophic state of coastal or freshwater ecosystems. A combination of EnMAP derived bathymetry with SAR, LiDAR or Laserscan data can be useful to derive underwater topography and morpho-dynamics of shallow water areas (Pleskachevsky et al., 2011).

3.3.1 Coral Reefs

Coral reefs are spatially heterogeneous mosaics of coral, algae and sand. They occupy between 250,000 km² and 600,000 km² (Hochberg, 2011) corresponding to about 5 % – 15 % of shallow sea areas (0 m – 30 m depth) globally. Coral reefs host a diversity of organisms whose complex dynamics are affected by a vast range of interconnected processes. In addition to their ecological value, they also provide significant economic value, supporting fisheries, aquaculture, tourism and recreation (Andréfouët et al., 2005). Thriving in a narrow range of conditions, they are very sensitive to environmental changes and react quickly to new stressors, making them one of the most threatened coastal ecosystems in the world and a unique indicator of global change (e.g., Andréfouët et al., 2007). A decline in reef status is represented by a shift from coral- to algal-dominated community structures and accompanied by a general decrease in biodiversity. However, current reef surveys usually cover only small regions, leaving vast areas of the world's coral reefs unsurveyed (Hochberg, 2011). Remote sensing is one technique with a high potential for quantifying reef community status at large scales.

Beginning in the 2970s, remote sensing approaches used Landsat, SPOT HRV and ASTER data for the detection of reefs and reef geomorphology (Hochberg, 2011). The development of airborne imaging

spectrometers in the 1990s provided new opportunities for the identification and mapping of reef communities. While multispectral data can discrimination three to six classes of coral reefs (Caras et al., 2017; Mumby et al., 2004), an increased number of and narrower bands may allow more than 10 habitat types to be discriminated (Hedley, 2013). More recent developments include spectral unmixing, "wavelength feature" approaches and radiative transfer model inversion methods that require hyperspectral data (Hedley, 2013). Change detection analyses still depend on multispectral imagery due to limitations in multi-temporal hyperspectral data availability. The most ambitious objectives, such as the discrimination of live coral versus dead coral and/or macroalgae, quantification of live coral cover, or the detection of coral bleaching events, are not yet routinely achieved (Hedley, 2013).

In summary, coral reef remote sensing is a very dynamic field and upcoming sensors like EnMAP, are expected to have a major impact in the near future by providing data at new spatial scales and temporal frequency. Not only will the high-spectral resolution of EnMAP will allow for identification of the three basic reef bottom-types with high accuracy, spectral unmixing to discriminate sub-pixel composition, or modelling of light absorption and water optical properties, it will enable regional mapping of benthic community structure and long-term monitoring of reef status, increasing the understanding of the large-scale oceanographic and ecological processes that affect reef health (Hochberg, 2011).

Accordingly, the following main scientific tasks are related to coastal and inland water body applications:

- Improvement of the identification of different substances by their spectral characteristics, such as improved chlorophyll quantification, the differentiation between ecological important phytoplankton groups, and dissolved organic compounds;
- Enhancement of the identification of different fractions of suspended mineral and organic particles;
- Monitoring of the spatio-temporal dynamics and structure of optical shallow sea/lake bottom substrate (vegetation and sediment);
- Monitoring of the distribution patterns of invasive submersed and emergent algae;
- Monitoring of the variety of algal species/genera in space and time as a bio-indicator of coastal and freshwater ecology;
- Monitoring and taxonomic identification of (potentially toxic) algal and phytoplankton blooms in eutrophicated coastal and inland waters;
- Estimation of processes, such as primary production in inland and coastal waters and suspended matter transport and its impact on coastal ecosystems;
- Monitoring of the distribution of sediments in tidal flats, wetlands, coral reefs and mangrove forests; and
- Monitoring of coastal erosion and changes in coastal morphology.

3.4 Cryosphere

Components of the modern cryosphere include snow, freshwater ice, sea ice, glaciers, ice caps, ice sheets, and permanently frozen ground (permafrost) and depend on a consistently cold mean state. Given that the greatest magnitude of warming is occurring in high-latitude and high-altitude regions, the modern cryosphere is particularly vulnerable to global change (IPCC, 2022). Rapid warming of the cryosphere also induces a range of complex feedback mechanisms resulting in cascading climatic, geomorphological, hydrological, and ecological changes (i.e., Post et al., 2009; Prevéy et al., 2017;

Wrona et al., 2016). These changes in turn can influence global carbon budgets and energy balance, biodiversity, infrastructure and socially and culturally important activities (see AMAP, https://www.amap.no/). Monitoring the state and changes of the cryosphere is hampered by a scarcity of *in situ* observations due to challenging logistics associated with the remote and complex terrain. Satellite observations represent a key tool to track and quantify changes to the cryosphere. Despite the environmental limitations of optical remote sensing in the Polar Regions (i.e., months of polar night, persistent cloud cover, and year-round low solar incidence angles), air and spaceborne hyperspectral data offer unique information on biogeochemical and -physical surface properties providing new insight into important input and enabling from data in space and time to derive terrestrial and aquatic energy, water, sediment, and carbon fluxes.

3.4.1 Permafrost and Vegetation

Permafrost is a sub-surface thermal phenomenon which cannot be directly observed by optical remote sensing. However, spectral indicators derived from optical remote sensing can be used to infer the state of permafrost by quantifying and monitoring various permafrost related features and processes. These processes and features can be broadly divided into five categories of atmospheric, hydrological, land surface, thermal, and subsurface (Philipp et al., 2021). To effectively monitor the state and vulnerability of permafrost ecosystems, detailed remote sensing data at regional to biome scales with regular temporal frequency is necessary. Though there are many limitations associated with optical remote sensing in the Polar regions, EnMAP will provide data at a spectral and spatial resolution to northern latitudes that is currently not available (PRISMA has a latitudinal limit of 70°N).

The application of hyperspectral data in permafrost environments has increased significantly in recent years with greater availability and accessibility of field, drone-based and airborne sensors. For applications in heterogeneous permafrost environments, the high spectral resolution provided by hyperspectral data can capture the spatial variation in vegetation composition, structure and microtopography which in turn influence subsurface thermal regimes and related permafrost features and processes (Zhang et al., 2021). The identification and quantification of permafrost features and processes have most commonly been achieved using multispectral indices including NDVI. These include features and processes caused by rapidly thawing permafrost, drainage of lake basins, patterned ground and pingo development, frost heave, and ground subsidence after fire (Fraser et al., 2012; Jorgenson et al., 2015; Jorgenson and Grosse, 2016; Nitze et al., 2017; Rudy et al., 2013). Hyperspectral remote sensing has shown to be effective in capturing the high degree of spatial heterogeneity of seasonal active layer thickness (ALT) using modelling techniques (Zhang et al., 2021, 2020) as well as vegetation-active layer relationships (Anderson et al., 2019). Quantifying ALT is key to broadening our understanding of the influence of disturbance, hydrology and changing temperature regimes on permafrost. High spatial resolution airborne hyperspectral imagery has also been used to effectively identify and monitor methane hotspots across Arctic permafrost environments (Elder et al., 2020). Spaceborne imagers such as EnMAP with its high latitudinal limit and 30 m resolution will contribute greatly to better understanding methane and other carbon emissions in the Arctic (Miner et al., 2022)

As with other vegetated surfaces, spectral indices have been used extensively to map and monitor vegetation status and change in permafrost environments (Beamish et al., 2020; Laidler and Treitz, 2003; Stow et al., 2004). Time series analyses of NDVI and other vegetation indices using legacy multispectral platforms such as Landsat, AVHRR and MODIS are one of the most common applications of optical remote sensing in tundra landscapes (Beamish et al., 2020). These studies provide invaluable insight into the complex, non-linear changes in tundra productivity and growth in response to climate change (Bhatt et al., 2013; Myers-Smith et al., 2020). Multispectral remote sensing has also been used

to track a wide variety of vegetation phenomena including shrub expansion (Myers-Smith et al., 2011; Wookey et al., 2009) as well as vegetation disturbance and recovery from permafrost disturbance (Fraser et al., 2014; Walker et al., 2009), tundra fires (Jones et al., 2013), winter warming (Bokhorst et al., 2012), herbivory (Conkin and Alisauskas, 2017), and anthropogenic activities (Forbes et al., 2001). The derivation of taxonomical, biophysical, biochemical and phenological properties of Arctic vegetation has increased significantly with the rise in freely available remote sensing data (Beamish et al., 2020). Vegetation properties including biomass (Liu and Treitz, 2018; Raynolds et al., 2012), species composition (Macander et al., 2017), LAI (Williams et al., 2008), phenology (Zeng et al., 2013), and productivity (Shaver et al., 2013).

The last decade has seen a great increase in the application of *in situ* and airborne imaging spectroscopy studies of vegetation in Arctic permafrost environments. Hyperspectral remote sensing data is recognized as a key tool to quantifying and monitoring heterogeneous Arctic vegetation properties and change. Buchhorn et al., (2013a) and Buchhorn et al., (2013b) provided a detailed examination of the spectro-directional reflectance properties in high-latitude tundra permafrost landscapes under changing illumination conditions, demonstrating that vegetation communities can be spectrally distinguished. Further studies have demonstrated the utility of ground-based imaging spectroscopy and simple narrowband indices to differentiate plant functional types (PFTs; Beamish et al., 2017; Bratsch et al., 2016; Huemmrich et al., 2013) and to quantify photosynthetic pigment content (Beamish et al., 2018; Zagajewski et al., 2018) and biomass (Bratsch et al., 2017). Kennedy et al., (2021) applied the first physical-based inverse radiative transfer models and non-parametric modelling to *in situ* imaging spectroscopy data to estimate chlorophyll content and plant area index with moderate success. Taxonomic, biophysical and biochemical are important indicators of plant biodiversity, health and activity. Data from EnMAP will provide the first biome scale estimates of key vegetation properties in Arctic tundra landscapes.

- Monitoring of the spatio-temporal dynamics of permafrost disturbances and ALT
- Retrieval of surface thermal properties in permafrost landscapes
- Identification of vegetation succession in disturbed permafrost landscapes
- Retrieval of plant biophysical and biochemical plant properties in permafrost landscapes

3.4.2 Snow & Ice

Characterization of snow-covered areas and inland ice is critical for understanding the Earth's hydrology, climatology, and ecology. This is because of the significant effect of snow-covered areas on the energy balance at the land-atmosphere boundary and their importance as fresh water sources (Tedesco et al., 2016). However, detailed ground-based measurements of snow and inland ice properties are scarce due to the remoteness, challenging and often dangerous logistics. Satellite-based imaging spectroscopy can be used to retrieve key inland snow and ice parameters. Distributed snow-surface energy-balance models need the following spatially distributed parameters that can potentially be provided by spaceborne hyperspectral remote sensing data: snow-covered area, snow albedo, grain size, snow water equivalent, liquid water content, and concentration of light-absorbing particles (LAPs), such as dust, soot, or algae (Dozier et al., 2009). Accurate measurements of these physical snow properties are also prerequisites to derive distributed hydrological models to quantify timing and magnitude of snowmelt runoff and its source areas.

Snow albedo and snowmelt are directly linked to the growth of grain size (Warren and Wiscombe, 1980). Snow reflectance decreases dramatically, especially in the NIR range, as the snow grains evolve after deposition. Liquid water inclusions of melting snow yield albedo reductions because liquid water in snow causes the grains to form clusters (Dozier et al., 2009). Repeated hyperspectral measurements

of snow enable us to quantify the evolution of albedo by accounting for various effects like grain size and LAPs.

LAPs, including dust, soot, and algae, degrade snow reflectance significantly, especially in the VIS spectrum, by absorbing incoming radiation and at longer wavelength by increases in grain size through local microscale metamorphism (Di Mauro et al., 2020; Dozier et al., 2009; Flanner et al., 2007; Skiles et al., 2018). For example, an experiment that compared hyperspectral data to field-measured impurities showed good agreement between measured dust concentrations and snow reflectance (Tanikawa et al., 2002). The extensive glacial debris cover, which characterizes most mountain glaciers, can be spectrally analyzed to decipher the origin and to improve glacial mapping as well as our understanding of glacial ablation and kinematics (Casey et al., 2012).

Organic materials in snow and ice have more distinctive spectral features than inorganic LAPs (Takeuchi, 2002). Snow and glacier algae (e.g., *Chlamydomonas nivalis*, *Mesotaenium berggrenii*, or *Ancylonema nordenskioldii*) may be abundant on top of the snow and inland ice causing albedo to decrease. Their accumulation on the snow and ice surface appears in distinctive colors, such as green, red, brown, or purple, caused by pigment absorption which can be detected using multispectral satellite data (Gray et al., 2020; Takeuchi et al., 2006; Wang et al., 2020). However, deriving their concentration requires high-resolution imaging spectroscopy data that can resolve distinct carotenoid and chlorophyll absorption features (Painter et al., 2001). Bohn et al., (2021) recently presented an approach to simultaneously estimate atmosphere and surface constituents over glacier ice, including retrieval of grain size, liquid water content, and algae concentration. They validated algae mass mixing ratio, estimated from airborne AVIRIS-NG data, with one of the rare *in situ* samples and presented promising low residuals, which highlights the potential of hyperspectral measurements from space to both map and quantify organic cells and pigments in snow and ice.

Because varying grain sizes and liquid water content as well as ablation of biological and inorganic LAPs translate into variability of spectral reflectance, multiple snow endmembers are necessary to characterize snow. Spectral mixture analysis can accurately represent the spatial distribution of snow (Nolin et al., 1993). Painter et al., (2003) improved subpixel snow mapping by allowing the spectrum of the snow endmember to vary to match the spectral shape of the pixel's snow reflectance. The authors used hyperspectral airborne AVIRIS data to estimate both subpixel snow cover and grain size over a wide range of snow conditions in the Sierra Nevada. Rosenthal and Dozier, (1996) developed linear spectral mixture analysis for subpixel snow-covered area from Landsat. Although only based on multispectral data, they were able to map patchy snow cover several times during a season. This Landsat spectral mixing model was also used to map snow on glaciers. For example, Klein and Isacks, (1999) applied the spectral mixture analysis to identify the ablation and accumulation zones and the transient snowline on several tropical glaciers.

Quantifying sea ice properties is of great importance because sea ice albedo is among the most crucial parameters that governs climate processes. In the context of the changing Arctic climate, the spatial distribution of sea ice melt and the length of the melt season is required to predict the role of sea ice cover in the radiative balance. Melt ponds change the radiative balance in the Arctic because they drastically reduce the ice albedo and increase the flux of absorbed energy, speeding up the melting process (positive feedback mechanism). Snow accumulation on the sea ice is one of the most critical variables in determining ice permeability and melt pond development (Eicken et al., 2004).

Sediment-laden sea ice, or 'dirty sea ice', is a common phenomenon in the Arctic. Sea-ice sediments mainly consist of terrigenous sediments with clay minerals, quartz and feldspars (Nuernberg et al., 1994). Due to surface melt, sediments accumulate at the surface of multi-year sea ice in concentrated layers of mud several millimeters thick. The quantification of sediment transport by sea ice presents a considerable challenge due to the patchy distribution of sediments and the overall difficulty in obtaining

data on the areal distribution and suspended particulate matter concentrations. Published quantitative estimates of sea-ice transported sediment loads differ significantly (Eicken et al., 2005). Lisitzin (2002) postulated that 10 to 50% of the total Arctic sea-ice area is covered by dirty sea ice.

To assess changes in the Arctic energy budget, sea ice reflective properties, such as pure ice or 'dirty ice', snow, and melt pond coverage on sea ice must be quantified. These products can serve as inputs for Global Climate Models, hydrological models, and estimates of sediment flux on sea-ice. In addition to these applications, knowledge of the spectral properties of sea ice surface, such as the melt pond fraction, is useful for maritime navigation. Therefore, hyperspectral remote sensing potentially provides the different sea-ice albedo types, extracts melt pond fractions, maps the extent of particle-laden sea ice, and assesses its particulate loading. Perovich et al., (2007) refer to direct measurements of the anisotropic reflectance factor for snow covered, bare, and ponded sea ice. Huck et al., (2007) built a radiative transfer model for sea ice coupled with an optical model for particulates included in sea ice to model different sea ice surfaces of variable sediment load. They distinguish between different degrees of sediment loading and the melt pond fraction. Istomina et al., (2015) developed an algorithm to retrieve the melt pond fraction and different sea ice types from MERIS data and validated it against aerial, shipborne and *in situ* data. The developed algorithm is based on a newly developed optical model of sea ice reflection, accounting also for the bi-directional reflection from the ice/snow surface (Zege et al., 2015). This is particularly important for Polar Regions where the SZA is high. The results show the best correlation for land-fast and multiyear ice of high ice concentrations. The presented melt pond fraction and sea ice albedo retrieval needs various spectral bands in the VIS and NIR regions of the spectrum (Istomina et al., 2015; Zege et al., 2015). Bohn et al., (2022) demonstrated the potential of spaceborne imaging spectroscopy to characterize Arctic melt ponds using PRISMA data. Their approach proved valid in quantifying different water surface brightness, distinguishing turbid and clear water as well as identifying potential ice cover. Furthermore, even weak chlorophyll absorption by algae deposited on the melt pond surface could be resolved.

Future snow and ice research will benefit from a synergistic data collection that combines fine spectral (EnMAP) and spatial resolution with sensors with a broad swath and daily coverage of the whole Earth (MODIS, Sentinel 3, VIIRS). Initial results from combining Sentinel 3 and PRISMA data show promising potential to develop comprehensive time series of biogeophysical snow and ice properties (Bohn et al., 2022). Envisioned applications include regular tests of medium-spatial resolution data with EnMAP and data fusion to improve mapping and monitoring of sea-ice types, snow cover on inland ice and sea ice, ice algae, sediment and dust on ice, melt pond fraction and evolution on inland ice and sea ice. In this context, the Greenland Ice Sheet should be a focal area of interest, since recent climate research confirms that it is the largest single contributor to global sea level rise (Bamber et al., 2018). EnMAP can contribute to an improved understanding of melt processes, which is essential to evaluate the associated impacts on climate change (Bohn et al., 2022, 2021; Stibal et al., 2017).

The following main scientific tasks are related to snow and ice:

- Development and improvement of new hyperspectral approaches to retrieve snow properties (e.g., albedo, grain size and near-surface liquid water, biological and inorganic LAPs) and spatial snow cover distribution;
- Exploration of synergies to multispectral sensors with varying spatial scales to improve snow mapping in forests and adapt to angular variability;
- Determination of the spatial and temporal variability of ponded ice spectral reflectance properties as a key parameter in determining the large-scale sea-ice albedo; and

- Determination of snow accumulation, melt pond areal fraction, and sediment load on sea ice to overcome problems associated with the significant spatial inhomogeneity observed and the fact that it occurs in largely inaccessible parts of the world's oceans.

3.5 Urban areas

The world is currently experiencing rapid urbanization and an increase in the number of megacities, particularly in developing countries. According to the United Nations Development Program, urban population growth will continue over the next decades, though at decreasing growth rates (UN, 2022). The process of urbanization always results in changes in land use and cover and causes serious problems, such as environmental pollution, destruction of ecosystems, and waste disposal. Urban areas are responsible for 75 % of the global CO2 emissions (UNEP, 2022). Reduction in vegetation cover due to urban expansion may result in desertification (Cherlet et al., 2018) and affect the quality of nearby surface water (Jordan et al., 2014). In addition to these climatic changes, urbanization impacts socioeconomic processes increasing per capita demand for energy, goods and services (Meyerson et al., 2007). Land conversions, introduced by urban consumption patterns, have regional effects on the biophysical system that may lead to global consequences (Sanchez-Rodriguez et al., 2005). Thus, there is a critical need to map urban land cover composition and monitor urban growth.

Remote sensing techniques are widely used to study urban environments. Although the use of airborne hyperspectral images has proven to be a valuable data source for urban hydrological, climatic and environmental studies (Franke et al., 2009; Heiden et al., 2012; Okujeni et al., 2013), spaceborne hyperspectral applications are comparably scarce (Cavalli et al., 2008; Weng et al., 2008; Xu and Gong, 2007). This can be explained by the spectral and structural complexity of urban areas (Small, 2003, 2001; van der Linden and Hostert, 2009) and the limited availability of repeat hyperspectral data acquisitions covering urban areas globally (Roberts et al., 2012). EnMAP hyperspectral data opens new opportunities to describe and monitor land cover composition in urban areas and along urban-suburban gradients assisting in the understanding of the dynamics of global urbanization (Heldens et al., 2011).

Land cover classification schemes for urban areas are generally influenced by the scope of related studies (Heiden et al., 2007; Herold et al., 2004; van der Linden et al., 2019b). The advantage of EnMAP compared to multispectral sensors is the detailed spectral resolution of the data combined with a high signal-to-noise ratio. Given the 30 m ground sampling distance of EnMAP, urban mapping requires novel strategies to retrieve new compositional information about the urban surface. Information on urban surface materials is key to understanding climatic and hydrological processes in urban areas (Heldens et al., 2019). In a first proof-of-concept study, specific material compositions for typical densely built neighborhoods, industrial areas, commercial areas and residential districts have been detected based on simulated EnMAP data (Jilge et al., 2015). However, research questions remain about the robustness (Ji et al., 2022) and the transferability (Ji et al., 2021) of gradient analysis used initially for studies in natural environments (Feilhauer et al., 2011; Schmidtlein and Sassin, 2004).

The spectral decomposition of land-cover composition at the sub-pixel level is another promising strategy to better characterize urban surfaces. Techniques such as spectral unmixing or regression modelling designed to deal with the spectral diversity and variability of urban surfaces have been successfully implemented using airborne data (Franke et al., 2009; Okujeni et al., 2013; Priem and Canters, 2016; Roberts et al., 2012; Roessner et al., 2001). New developments are needed to enable the use of spaceborne EnMAP data as input for such techniques. This would enable mapping of surface materials for various cities providing complementary information for existing surveys such as Local Climate Zone (LCZ) mapping, a concept especially developed for climate studies in urban areas (Stewart and Oke, 2012)

For both qualitative and quantitative analyses of urban areas, the development of reference spectral libraries is essential (Bieniarz et al., 2014; Heiden et al., 2012; Heldens et al., 2011; Herold et al., 2004; Jilge et al., 2015). There is a need to develop techniques to handle the spectral inter- and intra-class variability of urban surfaces. Up-and-coming methods such as spectral library pruning (Degerickx et al., 2017; Dennison and Roberts, 2003; Priem et al., 2021) and normalization of spectral indices (Ji et al. 2022b) have shown the value of spectral libraries for urban studies. The greatest challenge to this research is the need for extensive collaboration between international research groups (Canters et al., 2021; Hueni et al., 2009; Rasaiah et al., 2011). Additional research on the spatial transfer of models to accurately map multiple urban areas is also needed (Canters et al., 2021; Okujeni et al., 2018).

One essential application regarding urban planning is reliable mapping of imperviousness. This is a critical parameter as it can lead to flooding in heavily urbanized areas lacking permeable surfaces (Konrad, 2016). Within this context, approaches that combine qualitative and quantitative analyses appear most suited to make full use of the additional information from EnMAP. This additional spectral information will make approaches based on the V-I-S concept (vegetation - impervious surface - soil, (Lu and Weng, 2006; Ridd, 1995; Wu and Murray, 2003) more reliable and help to expand such models by differentiating built-up and non-built-up areas. The analysis of 18 m airborne and 30 m simulated spaceborne hyperspectral data indicates the potential for EnMAP to improve and expand V-I-S mapping compared to broadly available multispectral Landsat data (Okujeni et al., 2015a; Wetherley et al., 2018, 2017).

Reliable surface material indicators are needed for urban climate studies and other approaches that require knowledge on the biophysical properties of urban land cover. Remote sensing data is used more and more to study the urban climate at meso and macro scales. Especially physical properties of urban areas, such as reflection, absorption, emissivity, specific heat capacity, but also height and spatial arrangement of urban objects, are needed to parameterize climate models (De Foy et al., 2006; Jin et al., 2007; Yang, 2000). Spaceborne hyperspectral EnMAP data will have the potential to provide this information (Okujeni et al., 2015b) on an operational basis. However, suitable concepts are needed to derive urban ecological indicators (Behling et al., 2015) and to integrate the surface information into urban climate models and methodological gaps currently exist for spatial upscaling techniques preserving spectral information content (Dian et al., 2021). Overall, the synergistic use of hyperspectral, thermal, and optical data with advanced data analysis techniques may result in enhanced socioeconomic and environmental indicators to model urban dynamics and their social and environmental consequences.

Accordingly, main scientific tasks related to urban areas include:

- Mapping and monitoring of urbanization and its dynamics with high spectral detail worldwide;
- Development of comprehensive urban spectral libraries for universal urban land-cover mapping based on EnMAP data;
- Development and improvement of classification algorithms to quantify urban land cover, including classes that are spectrally ambiguous in multispectral data;
- Investigation of new concepts for information extraction based on spectral mixtures;
- Application and extension of the V-I-S concept to produce biophysical surface maps with respect to the needs of urban environmental process models, e.g., on urban climate and hydrology; and
- Mapping of the abundance of hazardous materials such as asbestos, e.g., in the context of risk analyses.

3.6 Atmosphere

Though EnMAP is not specifically designed for atmospheric research, variables that describe atmospheric conditions and atmospheric constituents can be retrieved from EnMAP data. EnMAP is well suited to retrieve concentrations of gases with absorption features in the NIR and SWIR regions of the spectrum like methane, carbon dioxide, and water vapor, whose detection and quantification are key to climate change mitigation efforts. The reduction of methane emissions from the fossil fuel industry is considered the most effective way to slow global warming in the next decades. Methane emissions from fossil fuel activities typically occur as plumes from point sources such as wells, compressor stations, storage tanks, flares, and mining vents. Imaging spectrometers that include the SWIR, offer an appropriate spectral and spatial configuration to map methane plumes. Methane mapping using imaging spectrometers started at the airborne scale with AVIRIS data (e.g., Duren et al., 2019; Frankenberg et al., 2016; Thorpe et al., 2017), but recent rapid developments have extended it to the satellite scale. The first maps of methane plumes with spaceborne imaging spectrometers were derived from EO-1/Hyperion during the Aliso Canyon massive methane blowout (Thompson et al., 2016). Later, a theoretical assessment of the potential of next generation satellite imaging spectrometers for methane mapping, with an emphasis on EnMAP, was presented by Cusworth et al., (2019). Currently, the Italian PRISMA mission is the main source of spaceborne imaging spectroscopy data for methane mapping. PRISMA data are being used to detect methane emissions from oil and gas extraction and coal mining activities all over the world (Guanter et al., 2021). The Chinese GF-05 AHSI and ZY1-AHSI imaging spectroscopy missions have also shown potential for methane mapping (Irakulis-Loitxate et al., 2021), but in general data are not accessible for scientists outside of China. The availability of EnMAP data increases our ability to detect methane emissions from point sources globally. EnMAP will likely join PRISMA as part of the International Methane Emissions Observatory (IMEO) being developed by the United Nations Environment Program (see Section 1.5).

The application of imaging spectroscopy to detect carbon dioxide emissions is less developed, but there are studies showing the feasibility of carbon dioxide mapping from both AVIRIS (Thorpe et al., 2017) and PRISMA (Cusworth et al., 2021). PRISMA data were used to detect and quantify carbon dioxide emissions from four coal-fired power plants around the world. Considering the similar spectral and spatial sampling of PRISMA and EnMAP, it is expected that carbon dioxide mapping will also be possible with EnMAP.

Finally, atmospheric water vapor is important for many environmental applications because it constitutes one of the most effective greenhouse gases in the atmosphere. It shows a high-spatial and temporal variability, depending on meteorological conditions and land use. Information on the regional distribution of atmospheric water vapor may facilitate the analysis of SAR data, because the radar signal transit time depends on atmospheric conditions. A few algorithms for the retrieval of columnar water vapor content from hyperspectral remote sensing data have already been developed (e.g., Barducci et al., 2004).

In addition to greenhouse gases, EnMAP can also contribute to the monitoring of atmospheric constituents such as mineral dust and particulate matter clouds originating from sandstorm areas or biomass-burning. The mineral composition of transported dust is essential to better understand climate forcing, mineralogy of dust sources, aerosol optical properties, and mineral deposition to the surface. Furthermore, the differentiation of spectral signals from the ground and from mineral dust may allow separating atmospheric influences from the actual ground signal by determining their mineral composition. Chudnovsky et al., (2009) showed that the absorption signature of suspended dust could be decoupled from scattering, allowing detection of key minerals. This work would benefit from

collaboration with the EMIT imaging spectroscopy mission, designed to measure the mineral composition of the Earth's arid land dust source regions.

Finally, Thompson et al., (2018) used long-term imaging spectroscopy data from the Hyperion mission to produce a global survey of cloud thermodynamic phase (distribution of ice, liquid, and mixed phase clouds). EnMAP could also be used to continue this line of research.

Accordingly, scientific tasks related to atmospheric applications include:

- Development of a retrieval algorithms for the retrieval of methane concentration enhancements from EnMAP observations;
- Estimation of figures on the detection limit and total accuracy of EnMAP methane retrievals;
- Development of a retrieval algorithms for the retrieval of carbon dioxide concentration enhancements from EnMAP observations;
- Estimation of figures on the detection limit and total accuracy of EnMAP carbon dioxide retrievals;
- Development and improvement of algorithms to retrieve columnar water vapor based on hyperspectral data;
- Development and improvement of algorithms to characterize mineral dust, and particulate matter clouds; and
- Development and improvement of algorithms to separate cloud thermodynamic phases.

3.7 Hazards and Risks

EnMAP data will improve identification and monitoring of both natural and man-made hazards as well as vulnerability and risk. Overall, the main benefit of hyperspectral data lies in their potential for a more detailed, material-oriented characterization of factors contributing to hazards.

3.7.1 Landslides

In mountainous areas, landslides of various forms and composition impose a constant threat to local communities and infrastructure. Remote sensing has long been used to improve landslide inventories (Guzzetti et al., 2012) and hazard assessments (Guzzetti et al., 2005) and improve characterization of driving factors (Behling et al., 2016, 2014; Metternicht et al., 2005; Scaioni et al., 2014). Hyperspectral remote sensing can further improve the characterization of the driving factors of landslides and other hazards. This includes a better characterization of lithological conditions and improved identification of inhomogeneities within landslide-prone slopes, which indicate increased potential for the onset of slope failures. Hyperspectral data also improve characterization of landslide deposits including their revegetation over time. A better characterization of active, unstable slopes like debris-covered areas, fractured/disjointed rock walls, landslide accumulation borders and individual structural features and landforms, such as major faults and fractures, trenches, elongated depressions, and counter slope scarps can be accomplished with hyperspectral data (Borgogno Mondino et al., 2009). So far, the application of hyperspectral data to landslides has been limited due to data availability. In Ye et al., (2019) EO-1/Hyperion data were used to investigate the potential of hyperspectral data for automated post-failure landslide detection representing only one of the many potential future applications for hyperspectral data in the diverse field of landslide research.

3.7.2 Swelling soils

Expansive clays and clay-shales cause costly damages world-wide every year. The reported instances of heaving indicate that the problem of expansive soils is widespread across the five continents, mostly confined to semi-arid regions of the world (Chen, 1988). Soil spectroscopy has been shown to be a useful tool for evaluating the expansive potential of soils (e.g., Goetz et al., 2001). Hyperspectral remote sensing, with its potential for direct identification of constituent minerals in soils, can facilitate detection and mapping of expansive clays in different locations and at different spatial scales (e.g., Chabrillat et al., 2002; Kariuki et al., 2004). Accurate identification and spatial distribution of heaving soils will provide practical help to manage this global hazard.

3.7.3 Floods

Many riverine and coastal areas in the world are threatened by flooding caused by rainstorms, snowmelt, cyclones, tidal waves or dam-failures. A major challenge related to flood monitoring is the timely detection and the broad regional extent. Consequently, satellite remote sensing has been extensively used since the 1970s to detect and monitor floods allowing for a more rapid emergency response, assessment of damaged areas, and study of water quality changes (Ip et al., 2006). Though the temporal resolution of EnMAP may not facilitate information relevant to emergency response, spaceborne hyperspectral remote sensing has proven to be particularly suited to estimating soil contamination in floodplains (e.g., Goetze et al., 2010).

3.7.4 Droughts

Droughts can have a substantial impact on the ecosystems and agriculture of the affected areas. Large-scale agricultural losses resulting from drought can have local to global socioeconomic implications in the form of income loss and increasing commodity prices (Simelton et al., 2012; Ubilava, 2012). In general, drought periods lead to an increased fire susceptibility and tree mortality, and carbon uptake decreases significantly (Asner et al., 2000; Nepstad et al., 1999; Williamson et al., 2000). Spaceborne imaging spectroscopy has high potential for applications of climate–vegetation interactions by detecting the state of vegetation at regional scales (Asner et al., 2004). Such ecosystem studies may yield an increased accuracy of ecological models and could result in drought-prevention measures for agricultural areas.

3.7.5 Volcanoes

In concert with seismic and geodetic measurements, hyperspectral information on volcanic debris flows, pyroclastic materials, and gas emissions are fundamental to the understanding of eruptive systems (Crowley et al., 2003; Tralli et al., 2005). Hyperspectral information may provide valuable insights into volcanic activity (Cipar et al., 2011; Gabrieli et al., 2019), processes (Kereszturi et al., 2020, 2018), and properties (Schaefer et al., 2021). The increase in regional and globally available hyperspectral data is promising for applications in volcanology including material mapping which can influence volcanic stability and in turn provide relevant information for disaster management strategies.

3.7.6 Land degradation and soil erosion

Deterioration in soil and plant cover has adversely affected nearly 70 % of the world's dry lands, which cover approximately one third of the continental surface of the Earth. These facts led to the ratification, of the UN Convention to Combat Desertification by almost 200 nations (UNCCD, 1994), which emphasizes the need to monitor and assess land degradation processes worldwide. Combating desertification requires accurate and up-to-date knowledge of land-degradation status and the magnitude of the potential hazard. It is widely agreed that accelerated erosion is one of the most

important sources of land degradation that, together with the destruction of vegetation cover and structure, contributes to further land degradation and desertification (Pickup, 1989).

EnMAP data can assess the degree of land degradation by retrieving important variables that control susceptibility to soil erosion, such as soil compaction, surface roughness, infiltration rate, and soil moisture (Haubrock et al., 2005, 2008). Due to distinct topsoil characteristics, soils previously affected by erosion can be spectrally distinguished from intact soils (Demattê et al., 2000), and soil erosion and deposition stages can be mapped with hyperspectral remote sensing (Schmid et al., 2016). Another manifestation of soil degradation is increased salinity, which is commonly caused by rising water tables induced by land clearing or irrigation. In this case, imaging spectroscopy proves to be an effective tool for inferring the degree of soil salinity as indicated by the shape of the hydroxyl absorption feature at 2200 nm and by the presence of indicator minerals such as gypsum or smectite (Taylor, 2004; Tucker et al., 2001). Further applications to investigate land degradation based on hyperspectral imagery include the analysis of spatial patterns and temporal dynamics of desertification (Asner and Heidebrecht, 2005) as well as the identification and mapping of dry senescent vegetation cover in arid areas (Chabrillat, 2006). Overall, EnMAP will create assist agricultural land use practices to combat land degradation and soil erosion processes.

3.7.7 Oil spills

Crude oil exhibits several diagnostic absorption features within the VNIR to SWIR spectrum. The most prominent are a triplet between 1700 and 1770 nm and a doublet between 2290 and 2360 nm, which are retrievable with EnMAP data (Lammoglia and Filho, 2011). Imaging spectroscopy has been routinely employed to detect and quantify the occurrence of petroleum in the environment arising from natural oil seeps (typically emanating from petroleum accumulation) and anthropogenic spills resulting from accidents (and illegal discharge) during the extraction, transportation, storage, and utilization by modern society. In the offshore (marine) environment, the detection of oil spills is dominated by SAR technology, but the identification of oil type and thickness of oil spills imaging spectroscopic data is needed (Leifer et al., 2012). In the terrestrial (onshore) environment the detection and characterization of petroleum relies on remote sensing data provided by either multispectral (Asadzadeh et al., 2022b) or hyperspectral instruments (Kokaly et al., 2013b). The arrival of EnMAP with a high signal-to-noise ratio is expected to open a new era of petroleum remote sensing. This includes direct detection and characterization of petroleum on-, and offshore, assessment of impacted ecosystems by oil spills, analysis of the health conditions of plants in petroleum-affected areas, and finally monitoring of the effectiveness of mitigation programs (Asadzadeh et al., 2022a).

3.7.8 Marine litter

The pollution of marine and coastal environments with plastic marine litter has been identified as a long-term hazard for ecosystems (Galgani et al., 2010; UNEP, 2009). Continually increasing disposal and low degradation rates of plastics (on the order of centuries) results in ever-increasing litter accumulation. Marine litter causes harm by entanglement of and ingestion by marine organisms (e.g., fishes, seabirds) (Gregory, 2009). Because persistent toxic substances, such as organochlorines (e.g., PCB, DDE, DDT) accumulate at high concentrations on the surface of plastics (e.g., Mato et al., 2001; Ogata et al., 2009), the ingestion of plastics by marine organisms represents the entry point of those substances into the food chain (e.g., Bjorndal et al., 1994; Boerger et al., 2010; Eriksson and Burton, 2003; Graham and Thompson, 2009). However, whether there is enrichment or depletion within the food chain is subject to on-going research (Zarfl et al., 2011). Despite a basic understanding of principle sources and sinks of plastic pollution, a detailed assessment of their quantities and transport pathways is still lacking (Conesa, 2022; Zarfl et al., 2011). The monitoring marine litter has been listed as a

mandatory task in the Marine Strategy Framework Directive (MSFD-indicator 10.1.3). At the EU and global level, guidelines have been compiled for monitoring best practices (Cheshire, 2009; JRC, 2013). Given that imaging spectroscopy can identify marine plastics (e.g., Kuriyama et al., 2002; Thompson et al., 2004), EnMAP has the potential to contribute to the localization of major pollution sources, sinks and pathways of marine litter. A potential application to localize marine litter is related to natural hazards like tsunamis and floods that transport large amounts of artificial materials into the marine environment. A major challenge in such a scenario is the timely acquisition and analysis of remote sensing images, which requires rapid tasking and the development of efficient image processing chains for a near-real-time support to reduce dispersion and enable the removal of marine litter.

3.7.9 Illegal waste dumping

The steadily growing problem of illegal waste dumping is a prioritized field in the European Commission's Communication on "EU actions to improve environmental compliance and governance", which explicitly suggests the use of satellite data as a potential solution (European Commission, 2018). It is estimated that illegal dumping costs the EU member states €72-90 billion in clean-up costs and lost revenues each year (Purdy, 2018) and poses considerable health and environmental risks.

Unmanaged or illegal dump sites can vary in size and shape, originate from different sources (e.g., construction waste, household waste, e-waste) and consist of different materials (e.g., plastic, car tires, metal, bricks, concrete). They range from small dump sites found along roads or rivers to mountains of plastic waste such as those found in Southeast Asia and Africa. The variability in the characteristics of illegal dumping sites, as well as their spectral similarity to construction sites and sand, clay, and gravel extraction sites represents a challenge to automated detection by remote sensing.

Recent demonstration projects on illegal waste detection by satellite data are limited and mostly based on single acquisitions of very high spatial resolution commercial imagery. The open data from the Copernicus Sentinel missions as well as PRISMA and EnMAP offer new opportunities for regular, global detection of illegal waste to a wide community of users such as environmental agencies worldwide, especially in developing countries. Imaging spectroscopy and chemometrics have the potential to identify the material composition of illegal waste to operationalize automatic classification and provide information on the hazard classification and necessary protection and disposal measures prior to an on-site inspection.

3.7.10 Industrial and mine waste and environmental rehabilitation

The extraction of natural resources is frequently associated with environmental degradation due to the dispersion of potentially toxic substances. Numerous abandoned mines (e.g., open pit coal, copper and gold mines) have left an environmental legacy of acidic drainage and toxic metals in downstream watersheds with adverse effects on human and ecosystem health (Swayze et al., 2000). Acid mine drainage is typically derived from an enhanced sulfide hydro-oxidation process related to an increased effective surface of the crushed/milled rocks during the mining process. Sulfuric acid can enter the food chain through contaminated soils and water, which can ultimately result in the collapse of wetlands (McCarthy et al., 2007) and the decline of ecosystem health in general (Wepener et al., 2011). Technical accidents or illegal dumping can release toxic industrial waste and contaminate the surrounding environment (Mattila et al., 2022b; Minh et al., 2003; Okoronkwo et al., 2009; Wong et al., 2007). Imaging spectroscopy can effectively identify contaminants and determine the sources and impacts on the water cycle and vegetation health (Clark et al., 2003; Kemper and Sommer, 2004) Today, many countries are strengthening legislation to enforce environmental protection and to implement rehabilitation measures (MMSD, 2002).

Hyperspectral remote sensing can be used to track the shape and wavelength minimum of key pH-sensitive secondary iron oxides and sulfate minerals (e.g., jarosite, copiapite, schwertmannite, ferrihydrite, and goethite) in the tailing environment. This enables pH mapping of areas affected by acid mine drainage (Ong et al., 2003b; Swayze et al., 2000; Zabcic et al., 2014), thus accelerating site clean-up and reducing the associated costs (EPA, 1998)This technology can be used to predict the potential sources of acid mine drainage discharge as well as the acid neutralization capacity of geologic materials including carbonate minerals in the environment. In a similar manner, the hydrochemical parameters of mining lakes can be monitored using imaging spectroscopic data (Gläßer et al., 2011). Minerals of environmental concern such as asbestos, which occur naturally in ultramafic rocks and/or arise from anthropogenic sources can be detected using EnMAP data (Swayze et al., 2009). The spectroscopic content of the data can predict heavy metal content and map chemical wastes and residues around active and abandoned mining sites (Choe et al., 2009; Kasmaeeyazdi et al., 2021; Mars and Crowley, 2003; Pfitzner et al., 2018). Imaging spectroscopy can also quantitatively measure dust derived from mining activities in neighboring areas (Ong et al., 2003a). From an economic perspective, mine wastes contain large quantities of high value metals, which can be assessed using imaging spectroscopic data (Gascueña, 2020). EnMAP has the potential to become an efficient operational tool to map and monitor both the geoenvironmental of waste materials as well as the progress made in the rehabilitation of affected sites during the life cycle of a mine.

The following main scientific tasks are related to hazards and risks:

- Monitoring of tectonic, lithological and soil parameters for better characterization of factors predisposing landslide formation to improve hazard assessments;
- Detection and mapping of swelling soils occurrences to assess swelling potential and to improve hazard assessment and application of adequate countermeasures;
- Detection and monitoring of flood occurrences to assess flood risks, damaged areas, and water quality;
- Monitoring of the state of vegetation during drought periods to improve the accuracy of ecological models and to develop drought-preventive measures for agricultural areas;
- Investigation of volcanic systems with regard to their crater types, lava flow types and volcanic deposits to improve risk assessment and evacuation measures;
- Monitoring land degradation processes (erosion and deposition) by providing regular maps of vegetation distribution and characteristics (considering highly variable background substrates) and soil status, such as organic matter (TOC), CaCO3, iron content, infiltration rate, salinity, and physical crusting development;
- Identification and quantification of various soil contaminants through their specific spectral signatures or indicators (e.g., bio-indicators based on eco-toxicological effects on vegetation) linked to change in chemical composition of the polluted soil;
- The detection limit of oil at the spatial resolution of EnMAP;
- A better understanding of the complex spectral behavior of petroleum in mixture with water in maritime and soil of different mineralogical and physical properties on land surfaces;
- A robust technique for identification of oil-type under variable background conditions;
- Identification of sources, sinks and pathways of marine litter during large-scale plastics discharge events;
- Monitoring of mining sites for their sustainable management; and

- Monitoring and quantification of the distribution of toxic materials in waste dumping sites and assess the degree of environmental contamination and the success of remediation strategies.

4 Scientific exploitation strategy

In the preparatory phase of the EnMAP mission, a considerable effort was dedicated to developing tools for data processing, to inform and train users of EnMAP data and to foster an expert user community to ensure full exploitation of the information content of EnMAP data (Foerster et al., 2016). Following the successful launch of EnMAP in April 2022, scientific mission and user support continues. This chapter provides a brief overview of the various activities.

4.1 Information and training

The primary source of information about the EnMAP mission is available on the mission website (www.enmap.org). A mailing list was also established to disseminate EnMAP-specific news and announcements. As of October 2022, the list has more than 250 subscribers from research institutes and universities, public authorities and companies. More information on the mailing list and a contact form can be found at https://www.enmap.org/contact/. Key documents of the EnMAP mission, targeting the scientific community and general public are listed in Table 2.

Table 2: Key documents of the EnMAP mission. Documents are regularly updated throughout the mission.

EnMAP Science Plan	PI, EnSAG	Scientists, funding agencies, stakeholders and public authorities	English	EnMAP mission overview, scientific potential and exploitation strategy	www.enmap.org (2022)
EnMAP flyer	PI, EnSAG	General public	English/ German	Brief information about mission, objectives and application fields	www.enmap.org (2022)
EnMAP booklet	PI, EnSAG	General public	English/ German	Illustrated overview about the mission and its main application fields	www.enmap.org (2022)
EnMAP Algorithms Theoretical Baseline Documents (ATBDs)	Ground segment	Users of EnMAP data	English	Detailed information on algorithms and databases used by the ground segment for data processing for L1B, L1C, L2A land, L2A water	www.enmap.org
EnMAP Portals User Manual	Ground segment	Users of EnMAP data	English	Information about the proposal and observation request flow and data access	www.enmap.org
The EnMAP Spaceborne Imaging Spectroscopy	PI, EnSAG	Users of EnMAP data	English	Overall mission overview. Reference publication when citing the mission.	Guanter et al. (2015)

Mission for Earth Observation					
Environmental Mapping and Analysis Program – A German Hyperspectral Mission	PI, OHB, EnSAG	Users of EnMAP data	English	Detailed technical description	Kaufmann et al. (2016)
Special Issue: Exploring the Earth System with Imaging Spectroscopy in Surveys in Geophysics	EnMAP science team, ESA and cooperation partners	Science community interested in imaging spectroscopy	English	Collection of papers on the state of the art of imaging spectroscopy	Editors: Foerster, Guanter, Lopez, Moreno, Rast, Schaepman (2019)

EnMAP workshops and training schools are organized as part of the EnMAP science program (see list of past and upcoming events at https://www.enmap.org/events_education/). EnMAP user workshops and organized conference sessions are held regularly to inform about the progress of the mission, present and discuss EnMAP-related research, and to raise awareness of the mission. During the operational phase of the mission, a bi-annual EnMAP user workshop will be held, alternating with the EARSeL imaging spectroscopy workshop. EnMAP training schools have been organized by the EnMAP science team since 2010, with lectures, hands-on training as well as lab and field visits. In 2019, the first EnMAP-Box workshop took place addressing PhD students and postdoctoral researchers interested in applying and developing EnMAP-Box algorithms.

4.2 HYPERedu online learning initiative

With the successful launch of EnMAP there is an increasing interest in hyperspectral data analyses. However, hyperspectral analyses require extensive training and educational resources on imaging spectroscopy are scarce, especially online learning platforms. To address this need, HYPERedu was developed in 2019 as part of the EnMAP science program.

HYPERedu is an online learning initiative for hyperspectral remote sensing. It provides online learning resources on principles, methods and applications of imaging spectroscopy at a master's level addressing students as well as professionals in research, business and public institutions. The resources include annotated slide collections and hands-on tutorials (based on the EnMAP-Box software) that are continuously updated and expanded and increasingly used in training courses as well as university teaching (Fig. 6).

Within HYPERedu a series of MOOCs (Massive Open Online Courses) are also being developed. A first MOOC on the basics of imaging spectroscopy titled "Beyond the Visible: Introduction to Hyperspectral Remote Sensing" was successfully launched in November 2021. It teaches the principles of imaging spectroscopy, sensor technologies and data acquisition techniques as well as data sources and software using state-of-the-art eLearning approaches. The course is structured in three thematic lessons and offers interactive activities such as interactive graphics, quizzes and expert-led, hands-on training exercises. It is designed to be completed in five to eight hours at the participants own pace. After successful completion, participants receive a certificate. This basic course is complemented by several shorter follow-up MOOCs from 2022 onwards that focus on specific hyperspectral data application fields such as agriculture, soil and geology and urban environments.

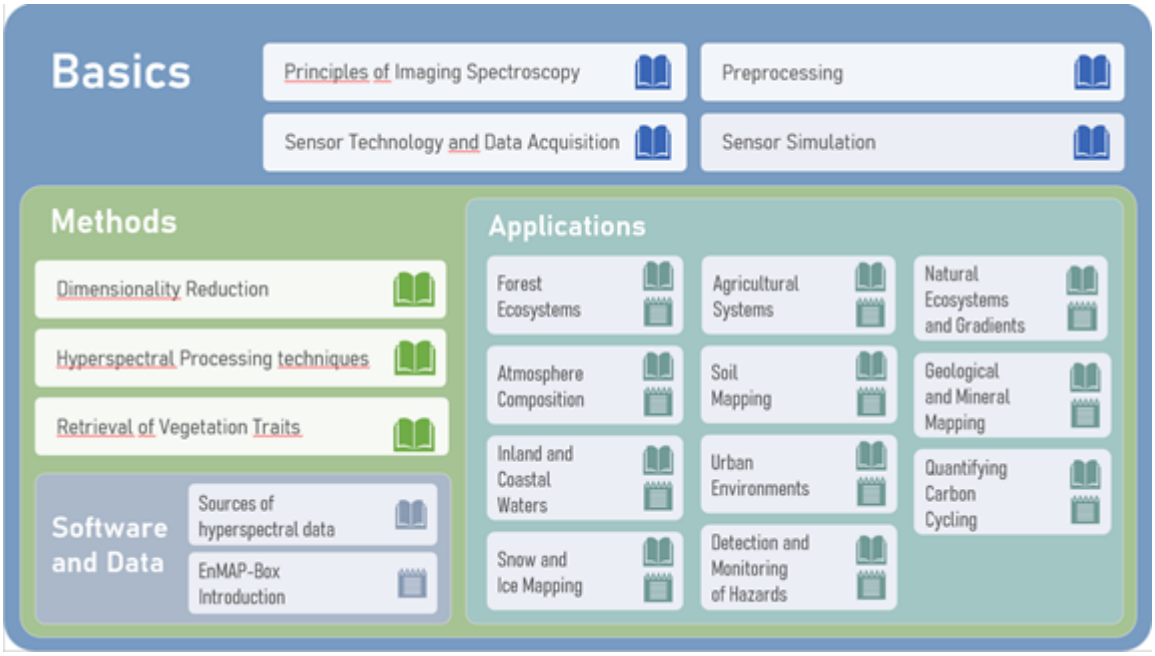

Fig. 6: HYPERedu learning resources overview

All resources and courses are hosted on the EO-College platform (https://eo-college.org/) and provided free of charge under a CC-BY license, except where otherwise noted. EO-College is a learning hub for online courses, open educational resources and discussion forums in the field of Earth Observation and funded by the German EO program of the DLR Space Agency.

Even though HYPERedu was initiated as part of the EnMAP science program, it is regarded as an initiative by and for the entire hyperspectral community: An increasing number of groups are already contributing to the development of HYPERedu and all resources are provided free of charge for use in training courses, university teaching or individual learning to increase the number of users employing hyperspectral data in the future.

4.3 EnMAP-Box

Full exploitation of the spectral information content of EnMAP data requires state-of-the-art image processing approaches for all users and application fields. The EnMAP-Box was developed targeting both novices as well as experienced users and offers basic processing and visualization functionality as well as advanced approaches for image analysis. The open-source code can easily be expanded and modifies for individual applications. This facilitates the exchange and centralized distribution of the latest developments within the EnMAP user community. From the very beginning, the conceptual development of the EnMAP-Box was driven by the following objectives:

- User-friendliness: achieved by an intuitive graphical user interface (GUI) (Fig. 7), focusing on the handling and visualization of data with high-spectral dimension, GUI-based application of machine learning algorithms or advanced methods such as RTM, common and flexible file formats, basic tools optimized for imaging spectroscopy data and quantitative assessments;
- Comprehensiveness: the set of available tools and applications as well as interfaces to scripting languages make the constant switch between different software obsolete;

- Standardization: the implementation and use of applications is standardized to assist external developers and provide the users a common look-and-feel, which also constitutes a key component of user-friendliness; and
- Addressing external developers: availability of well-documented source code and an application programming interface (API).

Since 2017, the EnMAP-Box consists of a registered plugin for the free and open source QGIS. This way, it combines custom-made processing algorithms for imaging spectroscopy data analyses with full GIS functionality. Besides general approaches for imaging spectroscopy, the EnMAP-Box includes advanced applications for atmospheric pre-processing over land and water, processing suites for agricultural applications, for geological mapping and for soil analysis.

To integrate data from different sources, the EnMAP-Box offers custom import options for most hyperspectral and the most relevant multispectral sensors.

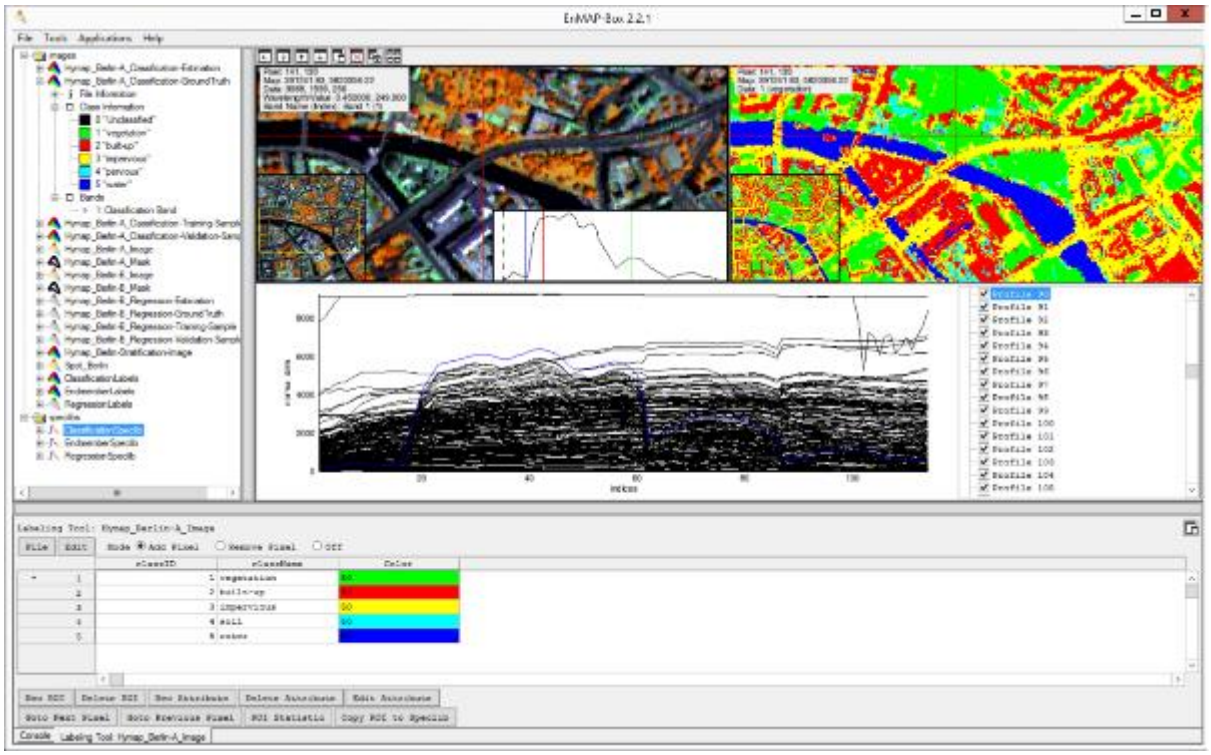

Fig. 7: Graphical user interface of the EnMAP-Box 3, showing simulated EnMAP data linked to map view with very high-resolution data and a vector layer, as well as the associated spectral library viewer.

4.4 EnMAP preparatory flight campaigns and *in situ* data

During the EnMAP scientific preparatory program, many hyperspectral airborne flight campaigns were carried out to support a wide range of scientific applications and algorithm development. Campaign data were used to evaluate the performance of variable retrieval, synergies with other sensors, development and testing of image processing algorithms and calibration/validation methods (Guanter et al., 2015). In addition, the datasets were input for EnMAP end-to-end scene simulations (see section 4.5).

At several test sites multi-seasonal acquisitions were acquired to support temporal analyses. Furthermore, acquisitions at different flight altitudes were obtained facilitating spatial scaling studies. For some campaigns, simultaneous data collection from other sensors (e.g., LiDAR) was conducted to enable multi-sensor studies. Most campaigns were accompanied by extensive ground sampling to

calibrate and validate the airborne data acquisitions. All datasets are freely available to the scientific community as DOI-referenced data publications under a Creative Commons License along with data reports (EnMAP Technical Reports), describing in detail how the data were acquired, and pre-processed and which ground truth and additional data are available. An overview of all available datasets is provided in the EnMAP campaign portal (https://www.enmap.org/data_tools/flights/). In addition to campaign data, several field guides developed within the mission's scientific preparatory program are available as EnMAP Technical Reports on the EnMAP website.

4.5 EnMAP end-to-end scene simulations

Preparatory activities involved the simulation of the entire image generation and processing chain using the EnMAP end-to-end scene simulator (EeteS; (Segl et al., 2012). EeteS is comprised of four main modules (atmospheric, spatial, spectral, and radiometric) to generate EnMAP-like raw data and is capable of simulating EnMAP-like data products using a L1B, L1C and L2A processor. These simulated data were important for the optimization of fundamental instrument configurations, allowing the effect of parameter changes to be tested using simulated benchmark datasets. In addition, these datasets supported the development and evaluation of data pre-processing algorithms as well as testing of new algorithms for the scientific exploitation of future EnMAP data. Tools for geometric alignment of EnMAP to co-existing Earth observation missions were developed that facilitated synergetic use with Sentinel-2 data. Sample datasets generated with EeteS were provided upon request to scientific users.

References

Abdullah, H., Skidmore, A.K., Darvishzadeh, R., Heurich, M., 2019. Timing of red-edge and shortwave infrared reflectance critical for early stress detection induced by bark beetle (Ips typographus, L.) attack. Int. J. Appl. Earth Obs. Geoinf. 82, 101900. https://doi.org/10.1016/J.JAG.2019.101900

Agustin, F., 2017. ASTER Mineral Classification for Regolith Mapping in Tick Hill Mount Isa, Northwest Queensland. Indones. J. Geosci. 4, 97–109. https://doi.org/10.17014/ijog.4.2.97-109

Albright, T.P., Ode, D.J., 2010. Monitoring the dynamics of an invasive emergent macrophyte community using operational remote sensing data. Hydrobiologia 661, 469–474–469–474.

Ali, A.M., Skidmore, A.K., Darvishzadeh, R., van Duren, I., Holzwarth, S., Mueller, J., 2016. Retrieval of forest leaf functional traits from HySpex imagery using radiative transfer models and continuous wavelet analysis. ISPRS J. Photogramm. Remote Sens. 122, 68–80. https://doi.org/10.1016/J.ISPRSJPRS.2016.09.015

Anderegg, W.R.L., Kane, J.M., Anderegg, L.D.L., 2013. Consequences of widespread tree mortality triggered by drought and temperature stress. Nat. Clim. Chang. 3, 30–36. https://doi.org/10.1038/nclimate1635

Anderson, J., Plourde, L., Martin, M., Braswell, B., Smith, M., Dubayah, R., Hofton, M., Blair, J., 2008. Integrating waveform lidar with hyperspectral imagery for inventory of a northern temperate forest. Remote Sens. Environ. 112, 1856–1870–1856–1870.

Anderson, J.E., Douglas, T.A., Barbato, R.A., Saari, S., Edwards, J.D., Jones, R.M., 2019. Linking vegetation cover and seasonal thaw depths in interior Alaska permafrost terrains using remote sensing. Remote Sens. Environ. 233, 111363. https://doi.org/10.1016/j.rse.2019.111363

Anderson, R.J., Rand, A., Rothman, M.D., Share, A., Bolton, J.J., 2007. Mapping and quantifying the South African kelp resource. African J. Mar. Sci. 29, 369–378–369–378.

Andréfouët, S., Hochberg, E.J., Chevillon, C., Muller-Karger, F.E., Brock, J.C., Hu, C., 2005. Multi-Scale Remote Sensing of Coral Reefs, in: Remote Sensing of Coastal Aquatic Environments. Springer-Verlag, Berlin/Heidelberg, pp. 297–315. https://doi.org/10.1007/1-4020-3100-9_13

Angelopoulou, T., Tziolas, N., Balafoutis, A., Zalidis, G., Bochtis, D., 2019. Remote Sensing Techniques for Soil Organic Carbon Estimation: A Review. Remote Sens. 11, 676. https://doi.org/10.3390/rs11060676

Asadzadeh, S., de Souza Filho, C.R., 2017. Spectral remote sensing for onshore seepage characterization: A critical overview. Earth-Science Rev. 168, 48–72. https://doi.org/10.1016/j.earscirev.2017.03.004

Asadzadeh, S., Oliveira, W.J. de, Souza Filho, C.R. de, 2022a. UAV-based remote sensing for the petroleum industry and environmental monitoring: State-of-the-art and perspectives. J. Pet. Sci. Eng. https://doi.org/10.1016/j.petrol.2021.109633

Asadzadeh, S., Plata Arango, I.R., de Souza Filho, C.R., 2022b. Mapping natural oil seeps in the Middle Magdalena Basin (Colombia) using WorldView-3 satellite data. Am. Assoc. Pet. Geol. Bull. 106, 783–801. https://doi.org/10.1306/09282120069

Asner, G., Elmore, A., Flinthughes, R., Warner, A., Vitousek, P., 2005. Ecosystem structure along bioclimatic gradients in Hawai\textquotesinglei from imaging spectroscopy. Remote Sens. Environ. 96, 497–508–497–508.

Asner, G.P., Heidebrecht, K.B., 2005. Desertification alters regional ecosystem-climate interactions. Glob. Chang. Biol. 11, 182–194. https://doi.org/https://doi.org/10.1111/j.1529-8817.2003.00880.x

Asner, G.P., Knapp, D.E., Boardman, J., Green, R.O., Kennedy-Bowdoin, T., Eastwood, M., Martin, R.E., Anderson, C., Field, C.B., 2012. Carnegie Airborne Observatory-2: Increasing science data dimensionality via high-fidelity multi-sensor fusion. Remote Sens. Environ. 124, 454–465.

https://doi.org/10.1016/j.rse.2012.06.012

Asner, G.P., Knapp, D.E., Ty, K.-B., Jones, M.O., Martin, R.E., Boardman, J.W., Hughes, F.R., 2008. Invasive species detection in Hawaiian rainforests using airborne imaging spectroscopy and {LiDAR} 112.

Asner, G.P., Martin, R.E., Knapp, D.E., Tupayachi, R., Anderson, C., Carranza, L., Martinez, P., Houcheime, M., Sinca, F., Weiss, P., 2011. Spectroscopy of canopy chemicals in humid tropical forests. Remote Sens. Environ. 115, 3587–3598. https://doi.org/10.1016/j.rse.2011.08.020

Asner, G.P., Nepstad, D., Cardinot, G., Ray, D., 2004. Drought stress and carbon uptake in an Amazon forest measured with spaceborne imaging spectroscopy. Proc. Natl. Acad. Siences United States Am. 101, 6039–6044.

Asner, G.P., Townsend, A.R., Braswell, B.H., 2000. Satellite observation of El Niño effects on Amazon Forest phenology and productivity. Geophys. Res. Lett. 27, 981–984–981–984.

Atzberger, C., 2000. Development of an invertible forest reflectance model The INFORM-Model. A Decad. trans-European Remote Sens. Coop. Proc. 20th EARSeL Symp. 39–44.

Bachmann, M., Alonso, K., Carmona, E., Gerasch, B., Habermeyer, M., Holzwarth, S., Krawczyk, H., Langheinrich, M., Marshall, D., Pato, M., Pinnel, N., de los Reyes, R., Schneider, M., Schwind, P., Storch, T., 2021. Analysis-Ready Data from Hyperspectral Sensors—The Design of the EnMAP CARD4L-SR Data Product. Remote Sens. 2021, Vol. 13, Page 4536 13, 4536. https://doi.org/10.3390/RS13224536

Bamber, J.L., Westaway, R.M., Marzeion, B., Wouters, B., 2018. The land ice contribution to sea level during the satellite era. Environ. Res. Lett. https://doi.org/10.1088/1748-9326/aac2f0

Barducci, A., Guzzi, D., Marcoionni, P., Pippi, I., 2004. Algorithm for the retrieval of columnar water vapor from hyperspectral remotely sensed data. Appl. Opt. 43, 5552–5563. https://doi.org/10.1364/AO.43.005552

Barnsley, M.J., Settle, J.J., Cutter, M.A., Lobb, D.R., Teston, F., 2004. The PROBA/CHRIS mission: a low-cost smallsat for hyperspectral multiangle observations of the Earth surface and atmosphere. IEEE Trans. Geosci. Remote Sens. 42, 1512–1520–1512–1520.

Beamish, A., Coops, N., Chabrillat, S., Heim, B., 2017. A Phenological Approach to Spectral Differentiation of Low-Arctic Tundra Vegetation Communities, North Slope, Alaska. Remote Sens. 9, 1200. https://doi.org/10.3390/rs9111200

Beamish, A., Raynolds, M.K., Epstein, H., Frost, G. V., Macander, M.J., Bergstedt, H., Bartsch, A., Kruse, S., Miles, V., Tanis, C.M., Heim, B., Fuchs, M., Chabrillat, S., Shevtsova, I., Verdonen, M., Wagner, J., 2020. Recent trends and remaining challenges for optical remote sensing of Arctic tundra vegetation: A review and outlook. Remote Sens. Environ. 246, 111872. https://doi.org/10.1016/j.rse.2020.111872

Beamish, A.L., Coops, N.C., Hermosilla, T., Chabrillat, S., Heim, B., 2018. Monitoring pigment-driven vegetation changes in a low-Arctic tundra ecosystem using digital cameras: Ecosphere 9, e02123. https://doi.org/10.1002/ecs2.2123

Bedini, E., 2017. The use of hyperspectral remote sensing for mineral exploration: a review. J. Hyperspectral Remote Sens. 7, 189. https://doi.org/10.29150/jhrs.v7.4.p189-211

Bedini, E., 2009. Mapping lithology of the Sarfartoq carbonatite complex, southern West Greenland, using HyMap imaging spectrometer data. Remote Sens. Environ. 113, 1208–1219. https://doi.org/10.1016/j.rse.2009.02.007

Behling, R., Bochow, M., Foerster, S., Roessner, S., Kaufmann, H., 2015. Automated GIS-based derivation of urban ecological indicators using hyperspectral remote sensing and height information. Ecol. Indic. 48, 218–234. https://doi.org/10.1016/j.ecolind.2014.08.003

Behling, R., Roessner, S., Golovko, D., Kleinschmit, B., 2016. Derivation of long-term spatiotemporal landslide activity—A multi-sensor time series approach. Remote Sens. Environ. 186, 88–104. https://doi.org/10.1016/j.rse.2016.07.017

Behling, R., Roessner, S., Kaufmann, H., Kleinschmit, B., 2014. Automated spatiotemporal landslide mapping over large areas using rapideye time series data. Remote Sens. 6, 8026–8055.

https://doi.org/10.3390/rs6098026

Belgiu, M., Marshall, M., Boschetti, M., Pepe, M., Stein, A., Lievens, C., 2021. HyNutri: Estimating the Nutritional Composition of Wheat from Multi-Temporal Prisma Data, in: 2021 IEEE International Geoscience and Remote Sensing Symposium IGARSS. IEEE, pp. 471–474. https://doi.org/10.1109/IGARSS47720.2021.9553614

Bell, S.S., Fonseca, M.S., Kenworthy, W.J., 2008. Dynamics of a subtropical seagrass landscape: Links between disturbance and mobile seed banks. Landsc. Ecol. 23, 67–74. https://doi.org/10.1007/S10980-007-9137-Z

Ben-Dor, E., Chabrillat, S., Demattê, J., 2019. Characterization of Soil Properties Using Reflectance Spectroscopy, in: Fundamentals, Sensor Systems, Spectral Libraries, and Data Mining for Vegetation. pp. 187–247.

Ben-Dor, E., Chabrillat, S., Demattê, J.A.M., Taylor, G.R., Hill, J., Whiting, M.L., Sommer, S., 2009. Using Imaging Spectroscopy to study soil properties. Remote Sens. Environ. 113, S38–S55. https://doi.org/10.1016/j.rse.2008.09.019

Ben-Dor, E., Irons, J.R., Epema, G.F., 1999. Soil reflectance, in: Rencz, A.N. (Ed.), Remote Sensing for the Earth Sciences: Manual of Remote Sensing 3/3. pp. 111–188.

Ben Dor, E., Ong, C., Lau, I.C., 2015. Reflectance measurements of soils in the laboratory: Standards and protocols. Geoderma 245–246, 112–124. https://doi.org/10.1016/j.geoderma.2015.01.002

Berger, K., Atzberger, C., Danner, M., D'Urso, G., Mauser, W., Vuolo, F., Hank, T., 2018a. Evaluation of the PROSAIL model capabilities for future hyperspectral model environments: A review study. Remote Sens. https://doi.org/10.3390/rs10010085

Berger, K., Atzberger, C., Danner, M., Wocher, M., Mauser, W., Hank, T., 2018b. Model-Based Optimization of Spectral Sampling for the Retrieval of Crop Variables with the PROSAIL Model. Remote Sens. 10, 2063. https://doi.org/10.3390/rs10122063

Berger, K., Machwitz, M., Kycko, M., Kefauver, S.C., Van Wittenberghe, S., Gerhards, M., Verrelst, J., Atzberger, C., van der Tol, C., Damm, A., Rascher, U., Herrmann, I., Paz, V.S., Fahrner, S., Pieruschka, R., Prikaziuk, E., Buchaillot, M.L., Halabuk, A., Celesti, M., Koren, G., Gormus, E.T., Rossini, M., Foerster, M., Siegmann, B., Abdelbaki, A., Tagliabue, G., Hank, T., Darvishzadeh, R., Aasen, H., Garcia, M., Pôças, I., Bandopadhyay, S., Sulis, M., Tomelleri, E., Rozenstein, O., Filchev, L., Stancile, G., Schlerf, M., 2022. Multi-sensor spectral synergies for crop stress detection and monitoring in the optical domain: A review. Remote Sens. Environ. 280, 113198. https://doi.org/10.1016/j.rse.2022.113198

Berger, K., Verrelst, J., Féret, J.B., Wang, Z., Wocher, M., Strathmann, M., Danner, M., Mauser, W., Hank, T., 2020. Crop nitrogen monitoring: Recent progress and principal developments in the context of imaging spectroscopy missions. Remote Sens. Environ. 242, 111758. https://doi.org/10.1016/J.RSE.2020.111758

Berger, M., Moreno, J., Johannessen, J.A., Levelt, P.F., Hanssen, R.F., 2012. ESAs sentinel missions in support of Earth system science. Remote Sens. Environ. 120, 84–90. https://doi.org/10.1016/j.rse.2011.07.023

Bhatt, U.S., Walker, D.A., Raynolds, M.K., Bieniek, P.A., Epstein, H.E., Comiso, J.C., Pinzon, J.E., Tucker, C.J., Polyakov, I. V., 2013. Recent declines in warming and vegetation greening trends over pan-arctic tundra. Remote Sens. 5, 4229–4254. https://doi.org/10.3390/rs5094229

Bianchi, R., Marino, C., Pignatti, S., 1994. Airborne hyperspectral remote sensing in Italy, Proceedings of the European symposium on Satellite Remote Sensing. Eur. Ser. pp.-pp. 26–30.

Bieniarz, J., Aguilera, E., Zhu, X.X., Muller, R., Heiden, U., Reinartz, P., 2014. Spectral-spatial joint sparsity unmixing of hyperspectral data using overcomplete dictionaries.

Bierwirth, P., Huston, D., Blewett, R., 2002. Hyperspectral Mapping of Mineral Assemblages Associated with Gold Mineralization in the Central Pilbara, Western Australia. Econ. Geol. 97, 819–826. https://doi.org/10.2113/GSECONGEO.97.4.819

Bjorndal, K.A., Bolten, A.B., Lagueux, C.J., 1994. Ingestion of Marine Debris by Juvenile Sea-Turtles in Coastal Florida Habitats. Mar. Pollut. Bull. 28, 154–158.

Blackburn, G.A., 2007. Wavelet decomposition of hyperspectral data: a novel approach to quantifying pigment concentrations in vegetation. Int. J. Remote Sens. 28, 2831–2855. https://doi.org/10.1080/01431160600928625

Blaschke, T., 2010. Object based image analysis for remote sensing. ISPRS J. Photogramm. Remote Sens. 65, 2–16. https://doi.org/https://doi.org/10.1016/j.isprsjprs.2009.06.004

Boerger, C.M., Lattin, G.L., Moore, S.L., Moore, C.J., 2010. Plastic ingestion by planktivorous fishes in the North Pacific Central Gyre. Mar. Pollut. Bull. 60, 2275–2278.

Bohn, N., Di Mauro, B., Colombo, R., Thompson, D.R., Susiluoto, J., Carmon, N., Turmon, M.J., Guanter, L., 2022. Glacier Ice Surface Properties in South-West Greenland Ice Sheet: First Estimates From PRISMA Imaging Spectroscopy Data. J. Geophys. Res. Biogeosciences 127, e2021JG006718. https://doi.org/10.1029/2021JG006718

Bohn, U.N., Di Mauro, B., Colombo, R., Guanter, L., Thompson, D., Susiluoto, J., Carmon, N., 2021. Glacier Ice Surface Properties from PRISMA hyperspectral Data: first Results for the Greenland Ice Sheet. AGUFM 2021, GC15B-0676.

Bokhorst, S., Bjerke, J.W., Tømmervik, H., Preece, C., Phoenix, G.K., 2012. Ecosystem response to climatic change: The importance of the cold season. Ambio 41, 246–255. https://doi.org/10.1007/s13280-012-0310-5

Bond, I., Chambwera, M., Jones, B., Chundama, M., Nhantumbo, I., 2010. Issues and Prospects for Pro-poor REDD in the Miombo Woodlands of Southern africa, in: REDD + in Dryland Forests. p. 83.

Bondeau, A., Smith, P.C., Zaehle, S., Schaphoff, S., Lucht, W., Cramer, W., Gerten, D., Lotze-campen, H., Müller, C., Reichstein, M., Smith, B., 2007. Modelling the role of agriculture for the 20th century global terrestrial carbon balance. Glob. Chang. Biol. 13, 679–706. https://doi.org/10.1111/j.1365-2486.2006.01305.x

Borgogno Mondino, E., Giardino, M., Perotti, L., 2009. A neural network method for analysis of hyperspectral imagery with application to the Cassas landslide (Susa Valley, NW-Italy). Geomorphology 110, 20–27. https://doi.org/10.1016/j.geomorph.2008.12.023

Bowen, B.B., Martini, B.A., Chan, M.A., Parry, W.T., 2007. Reflectance spectroscopic mapping of diagenetic heterogeneities and fluid-flow pathways in the Jurassic Navajo Sandstone. Am. Assoc. Pet. Geol. Bull. 91, 173–190. https://doi.org/10.1306/08220605175

Bracher, A., Soppa, M.A., Gege, P., Losa, S.N., Silva, B., Steinmetz, F., Dröscher, I., 2021. Extension of Atmospheric Correction Polymer To Hyperspectral Sensors: Application To Hico and First Results for Desis Data, in: International Geoscience and Remote Sensing Symposium (IGARSS). IEEE, pp. 1237–1240. https://doi.org/10.1109/IGARSS47720.2021.9553568

Bracher, A., Vountas, M., Dinter, T., Burrows, J.P., Röttgers, R., Peeken, I., 2009. Quantitative observation of cyanobacteria and diatoms from space using PhytoDOAS on SCIAMACHY data. Biogeosciences 6, 751–764. https://doi.org/10.5194/bg-6-751-2009

Bratsch, S.N., Epstein, H., Buchhorn, M., Walker, D., Landes, H., 2017. Relationships between hyperspectral data and components of vegetation biomass in Low Arctic tundra communities at Ivotuk, Alaska. Environ. Res. Lett. 12. https://doi.org/10.1088/1748-9326/aa572e

Bratsch, S.N., Epstein, H.E., Buchhorn, M., Walker, D.A., 2016. Differentiating among four Arctic tundra plant communities at Ivotuk, Alaska using field spectroscopy. Remote Sens. 8, 51. https://doi.org/10.3390/rs8010051

Braun, D., Damm, A., Paul-Limoges, E., Revill, A., Buchmann, N., Petchey, O.L., Hein, L., Schaepman, M.E., 2017. From instantaneous to continuous: Using imaging spectroscopy and in situ data to map two productivity-related ecosystem services. Ecol. Indic. 82, 409–419. https://doi.org/10.1016/j.ecolind.2017.06.045

Breiman, L., 2001. Random Forest. Mach. Learn. 45, 5–32–5–32.

Brell, M., Guanter, L., Segl, K., 2018. Pysically based data fusion between airborne LiDAR and hyperspectral data: Geometric and radiometric synergies. Int. Geosci. Remote Sens. Symp. 2018-July, 8865–8868. https://doi.org/10.1109/IGARSS.2018.8517682

Brell, M., Segl, K., Guanter, L., Bookhagen, B., 2017. Hyperspectral and Lidar Intensity Data Fusion: A Framework for the Rigorous Correction of Illumination, Anisotropic Effects, and Cross Calibration. IEEE Trans. Geosci. Remote Sens. 55, 2799–2810. https://doi.org/10.1109/TGRS.2017.2654516

Britz, R., Barta, N., Schaumberger, A., Klingler, A., Bauer, A., Pötsch, E.M., Gronauer, A., Motsch, V., 2022. Spectral-Based Classification of Plant Species Groups and Functional Plant Parts in Managed Permanent Grassland. Remote Sens. 14, 1154. https://doi.org/10.3390/rs14051154

Buchhorn, M., Petereit, R., Heim, B., 2013a. A Manual Transportable Instrument Platform for Ground-Based Spectro-Directional Observations (ManTIS) and the Resultant Hyperspectral Field Goniometer System. Sensors 2013, Vol. 13, Pages 16105-16128 13, 16105–16128–16105–16128.

Buchhorn, M., Walker, D., Heim, B., Raynolds, M.K., Epstein, H.E., Schwieder, M., 2013b. Ground-based hyperspectral characterization of Alaska tundra vegetation along environmental gradients. Remote Sens. 5, 3971–4005. https://doi.org/10.3390/rs5083971

Buddenbaum, H., Schlerf, M., Hill, J., 2005. Classification of coniferous tree species and age classes using hyperspectral data and geostatistical methods. Int. J. Remote Sens. 26, 5453–5465.

Buddenbaum, H., Seeling, S., Hill, J., 2013. Fusion of full-waveform lidar and imaging spectroscopy remote sensing data for the characterization of forest stands. Int. J. Remote Sens. 34, 4511–4524. https://doi.org/10.1080/01431161.2013.776721

Budkewitsch, P., Staenz, K., Secker, J., Rencz, A., Sangster, D., 2000. Spectral signatures of carbonate rocks surrounding the Nanisivik MVT Zn-Pb mine and implications of hyperspectral imaging for exploration in arctic environments. geogratis.gc.ca.

Canters, F., Cooper, S., Degerickx, J., Heiden, U., Jilge, M., Okujeni, A., Priem, F., Somers, B., Linden, S., 2021. Use of Image Endmember Libraries for Multi-Sensor, Multi-Scale, and Multi-Site Mapping of Urban Areas, in: Urban Remote Sensing. Wiley, pp. 189–215. https://doi.org/10.1002/9781119625865.ch10

Caras, T., Hedley, J., Karnieli, A., 2017. Implications of sensor design for coral reef detection: Upscaling ground hyperspectral imagery in spatial and spectral scales. Int. J. Appl. Earth Obs. Geoinf. 63, 68–77. https://doi.org/10.1016/j.jag.2017.07.009

Carder, K.L., Reinersman, P., Chen, R.F., Muller-Karger, F., Davis, C.O., Hamilton, M., 1993. AVIRIS calibration and application in coastal oceanic environments. Remote Sens. Environ. 44, 205–216. https://doi.org/10.1016/0034-4257(93)90016-Q

Cardoso-Fernandes, J., Silva, J., Lima, A., Teodoro, A.C., Perrotta, M., Cauzid, J., Roda-Robles, E., Ribeiro, M. dos A., 2020. Reflectance spectroscopy to validate remote sensing data/algorithms for satellite-based lithium (Li) exploration (Central East Portugal), in: Schulz, K., Nikolakopoulos, K.G., Michel, U. (Eds.), Earth Resources and Environmental Remote Sensing/GIS Applications XI. SPIE, p. 19. https://doi.org/10.1117/12.2573929

Casey, K.A., Kääb, A., Benn, D.I., 2012. Geochemical characterization of supraglacial debris via in situ and optical remote sensing methods: A case study in Khumbu Himalaya, Nepal. Cryosphere 6, 85–100. https://doi.org/10.5194/tc-6-85-2012

Cavalli, R., Fusilli, L., Pascucci, S., Pignatti, S., Santini, F., 2008. Hyperspectral Sensor Data Capability for Retrieving Complex Urban Land Cover in Comparison with Multispectral Data: Venice City Case Study (Italy). Sensors 8, 3299–3320. https://doi.org/10.3390/s8053299

Chabrillat, S., 2006. Land degradation indicators: Spectral indices. Ann. Arid Zone.

Chabrillat, S., Ben-Dor, E., Cierniewski, J., Gomez, C., Schmid, T., van Wesemael, B., 2019. Imaging Spectroscopy for Soil Mapping and Monitoring. Surv. Geophys. https://doi.org/10.1007/s10712-019-09524-0

Chabrillat, S., Eisele, A., Guillaso, S., Rogaß, C., Ben-Dor, E., Kaufmann, H., 2011. HYSOMA: An easy-to-use software interface for soil mapping applications of hyperspectral imagery. Proc. 7th EARSeL SIG Imaging Spectrosc. Work. 1–7.

Chabrillat, S., Foerster, S., Steinberg, A., Segl, K., 2014. Prediction of common surface soil properties using airborne and simulated EnMAP hyperspectral images: Impact of soil algorithm and sensor

characteristic. Int. Geosci. Remote Sens. Symp. 2914–2917. https://doi.org/10.1109/IGARSS.2014.6947086

Chabrillat, S., Goetz, A.F.H., Krosley, L., Olsen, H.W., 2002. Use of hyperspectral images in the identification and mapping of expansive clay soils and the role of spatial resolution. Remote Sens. Environ. 82, 431–445. https://doi.org/10.1016/S0034-4257(02)00060-3

Chen, F.H., 1988. Foundations on Expansive Soils, 2nd ed. ed. Elsevier Amsterdam.

Chen, J.M., Leblanc, S.G., 1997. Four-scale bidirectional reflectance model based on canopy architecture. IEEE Trans. Geosci. Remote Sens. 35, 1316–1337. https://doi.org/10.1109/36.628798

Cherlet, M., Hutchinson, C., Reynolds, J., Hill, J., 2018. World atlas of desertification. Brussels, Luxembourg.

Cheshire, A., 2009. UNEP/IOC guidelines on survey and monitoring of marine litter, IOC Technical Series No. 83. UNEP Regional Seas Reports and Studies.

Cho, M.A., Skidmore, A., Corsi, F., van Wieren, S.E., Sobhan, I., 2007. Estimation of green grass/herb biomass from airborne hyperspectral imagery using spectral indices and partial least squares regression. Int. J. Appl. Earth Obs. Geoinf. 9, 414–424. https://doi.org/10.1016/j.jag.2007.02.001

Choe, E., Kim, K.W., Bang, S., Yoon, I.H., Lee, K.Y., 2009. Qualitative analysis and mapping of heavy metals in an abandoned Au-Ag mine area using NIR spectroscopy. Environ. Geol. 58, 477–482. https://doi.org/10.1007/S00254-008-1520-9

Chudnovsky, A., Ben-Dor, E., Kostinski, A.B., Koren, I., 2009. Mineral content analysis of atmospheric dust using hyperspectral information from space. Geophys. Res. Lett. 36. https://doi.org/10.1029/2009GL037922

Ciais, P., Reichstein, M., Viovy, N., Granier, A., Ogée, J., Allard, V., Aubinet, M., Buchmann, N., Bernhofer, C., Carrara, A., Chevallier, F., De Noblet, N., Friend, A.D., Friedlingstein, P., Grünwald, T., Heinesch, B., Keronen, P., Knohl, A., Krinner, G., Loustau, D., Manca, G., Matteucci, G., Miglietta, F., Ourcival, J.M., Papale, D., Pilegaard, K., Rambal, S., Seufert, G., Soussana, J.F., Sanz, M.J., Schulze, E.D., Vesala, T., Valentini, R., 2005. Europe-wide reduction in primary productivity caused by the heat and drought in 2003. Nature 437, 529–533. https://doi.org/10.1038/nature03972

Cipar, J.J., Dunn, R., Cooley, T., 2011. Active volcano monitoring using a space-based hyperspectral imager [abs.]. Am. Geophys. Union, Fall Meet. Abstr. abstract no. NH51C-1238.

Clark, M.L., Roberts, D.A., Ewel, J.J., Clark, D.B., 2011. Estimation of tropical rain forest aboveground biomass with small-footprint lidar and hyperspectral sensors. Remote Sens. Environ. 115, 2931–2942. https://doi.org/10.1016/j.rse.2010.08.029

Clark, R.N., Swayze, G.A., Livo, K.E., Kokaly, R.F., Sutley, S.J., Dalton, J.B., McDougal, R.R., Gent, C.A., 2003. Imaging spectroscopy: Earth and planetary remote sensing with the USGS Tetracorder and expert systems. J. Geophys. Res. Planets 108. https://doi.org/10.1029/2002je001847

Cocks, T., Jenssen, R., Stewart, A., Wilson, I., Shields, T., 1998. The HyMap Airboarne Hyperspectral Sensor: The system, calibration and performance. EARSEL Work. Imaging Spectrosc. 1–6.

Cole, J.J., Prairie, Y.T., Caraco, N.F., McDowell, W.H., Tranvik, L.J., Striegl, R.G., Duarte, C.M., Kortelainen, P., Downing, J.A., Middelburg, J.J., Melack, J., 2007. Plumbing the global carbon cycle: Integrating inland waters into the terrestrial carbon budget. Ecosystems 10, 171–184. https://doi.org/10.1007/s10021-006-9013-8

Collins, W.E., Chang, S.-H., 1990. Geophysical Environmental Research Corporation 63-channel airborne imaging spectrometer and 12-band thermal scanner, in: Imaging Spectroscopy of the Terrestrial Environment. SPIE, pp. 62–71. https://doi.org/10.1117/12.21336

Combal, B., Baret, F., Weiss, M., Trubuil, A., Macé, D., Pragnère, A., Myneni, R., Knyazikhin, Y., Wang, L., 2003. Retrieval of canopy biophysical variables from bidirectional reflectance using prior information to solve the ill-posed inverse problem. Remote Sens. Environ. 84, 1–15. https://doi.org/10.1016/S0034-4257(02)00035-4

Conesa, J.A., 2022. Adsorption of PAHs and PCDD/Fs in Microplastics: A Review. Microplastics 2022,

Vol. 1, Pages 346-358 1, 346–358. https://doi.org/10.3390/MICROPLASTICS1030026

Conkin, J., Alisauskas, R.T., 2017. Conversion of tundra to exposed peat habitat by snow geese (Chen caerulescens caerulescens) and Ross's geese (C. rossii) in the central Canadian Arctic. Polar Biol. 40, 563–576. https://doi.org/10.1007/s00300-016-1979-x

Cooper, S., Okujeni, A., Pflugmacher, D., van der Linden, S., Hostert, P., 2021. Combining simulated hyperspectral EnMAP and Landsat time series for forest aboveground biomass mapping. Int. J. Appl. Earth Obs. Geoinf. 98, 102307. https://doi.org/10.1016/j.jag.2021.102307

Corson, M.R., Korwan, D.R., Lucke, R.L., Snyder, W.A., Davis, C.O., 2008. The hyperspectral imager for the coastal ocean (HICO) on the international space station, in: International Geoscience and Remote Sensing Symposium (IGARSS). https://doi.org/10.1109/IGARSS.2008.4779666

Crowley, J.K., 1993. Mapping playa evaporite minerals with AVIRIS data: A first report from death valley, California. Remote Sens. Environ. 44, 337–356. https://doi.org/10.1016/0034-4257(93)90025-S

Crowley, J.K., Hubbard, B.E., Mars, J.C., 2003. Analysis of potential debris flow source areas on Mount Shasta, California, by using airborne and satellite remote sensing data. Remote Sens. Environ. 87, 345–358. https://doi.org/10.1016/j.rse.2003.08.003

Cudahy, T., 2016. Mineral Mapping for Exploration: An Australian Journey of Evolving Spectral Sensing Technologies and Industry Collaboration. Geosciences 6, 52. https://doi.org/10.3390/geosciences6040052

Cudahy, T., Jones, M., Thomas, M., Laukamp, C., Caccetta, M., Hewson, R., Rodger, A., Verrall, M., 2008. Next Generation Mineral Mapping : Queensland Airborne HyMap and Satellite ASTER Surveys 2006-2008. CSIRO Explor. Min. Rep. P2007 / 364 152. https://doi.org/10.13140/RG.2.1.2828.1844

Cusworth, D.H., Duren, R.M., Thorpe, A.K., Pandey, S., Maasakkers, J.D., Aben, I., Jervis, D., Varon, D.J., Jacob, D.J., Randles, C.A., Gautam, R., Omara, M., Schade, G.W., Dennison, P.E., Frankenberg, C., Gordon, D., Lopinto, E., Miller, C.E., 2021. Multisatellite Imaging of a Gas Well Blowout Enables Quantification of Total Methane Emissions. Geophys. Res. Lett. https://doi.org/10.1029/2020GL090864

Cusworth, D.H., Jacob, D.J., Varon, D.J., Chan Miller, C., Liu, X., Chance, K., Thorpe, A.K., Duren, R.M., Miller, C.E., Thompson, D.R., Frankenberg, C., Guanter, L., Randles, C.A., 2019. Potential of next-generation imaging spectrometers to detect and quantify methane point sources from space. Atmos. Meas. Tech. 12, 5655–5668. https://doi.org/10.5194/AMT-12-5655-2019

Dadon, A., Karnieli, A., Ben-Dor, E., Beyth, M., 2012. Examination of spaceborne imaging spectroscopy data utility for stratigraphic and lithologic mapping, in: EAGE/GRSG Remote Sensing Workshop. p. 053507. https://doi.org/10.1117/1.3553234

Dalponte, M., Bruzzone, L., Gianelle, D., 2008. Fusion of hyperspectral and LIDAR remote sensing data for classification of complex forest areas. IEEE Trans. Geosci. Remote Sens. 46, 1416–1427. https://doi.org/10.1109/TGRS.2008.916480

Damm, A., Guanter, L., Laurent, V.C.E., Schaepman, M.E., Schickling, A., Rascher, U., 2014. FLD-based retrieval of sun-induced chlorophyll fluorescence from medium spectral resolution airborne spectroscopy data. Remote Sens. Environ. 147, 256–266. https://doi.org/10.1016/j.rse.2014.03.009

Danner, M., Berger, K., Wocher, M., Mauser, W., Hank, T., 2019. Fitted PROSAIL parameterization of leaf inclinations,water content and brown pigment content for winter wheat and maize canopies. Remote Sens. 11. https://doi.org/10.3390/rs11101150

Danner, M., Berger, K., Wocher, M., Mauser, W., Hank, T., 2017. Retrieval of Biophysical Crop Variables from Multi-Angular Canopy Spectroscopy. Remote Sens. 9, 726. https://doi.org/10.3390/rs9070726

De Foy, B., Molina, L.T., Molina, M.J., 2006. Satellite-derived land surface parameters for mesoscale modelling of the Mexico City basin. Atmos. Chem. Phys. 6, 1315–1330. https://doi.org/10.5194/acp-6-1315-2006

DeFries, R., Pagiola, S., Adamowicz, W.L., Akcakaya, H.R., Arcenas, A., Babu, S., Balk, D., Cramer, W., Falconı, F., Fritz, S., Green, R., Gutie, E., Hamilton, K., Kane, R., Latham, J., Matthews, E., Ricketts, T., Yue, T.X., Ash, N., Tho, J., Editors, R., Ceballos, G., Lavorel, S., Orians, G., Pacala, S., Supriatna, J., 2005. Analytical Approaches for Assessing Ecosystem Condition and Human Well-being, in: Ecosystems and Human Well-Being: Current State and Trends. pp. 36–71.

Degerickx, J., Okujeni, A., Iordache, M.D., Hermy, M., van der Linden, S., Somers, B., 2017. A novel spectral library pruning technique for spectral unmixing of Urban land cover. Remote Sens. 9, 565. https://doi.org/10.3390/rs9060565

Demattê, J.A.M., Huete, A.R., Ferreira Junior, L.G., Alves, M.C., Nanni, M.R., Cerri, C.E., 2000. Evaluation of tropical soils through ground and orbital sensors, in: International Conference on Geospatial Information in Agriculture and Forestry.

Dennison, P.E., Roberts, D.A., 2003. The effects of vegetation phenology on endmember selection and species mapping in southern California chaparral. Remote Sens. Environ. 87, 295–309. https://doi.org/10.1016/j.rse.2003.07.001

Di Mauro, B., Garzonio, R., Bramati, G., Cogliati, S., Cremonese, E., Julitta, T., Panigada, C., Rossini, M., Colombo, R., 2020. PRISMA hyperspectral satellite mission : first data on snow in the Alps. Eur. Geosci. Union 2020 19825. https://doi.org/10.5194/EGUSPHERE-EGU2020-19825

Dian, R., Li, S., Sun, B., Guo, A., 2021. Recent advances and new guidelines on hyperspectral and multispectral image fusion. Inf. Fusion 69, 40–51. https://doi.org/10.1016/j.inffus.2020.11.001

Diek, S., Chabrillat, S., Nocita, M., Schaepman, M.E., de Jong, R., 2019. Minimizing soil moisture variations in multi-temporal airborne imaging spectrometer data for digital soil mapping. Geoderma 337, 607–621. https://doi.org/10.1016/j.geoderma.2018.09.052

Dieke, G.H., Crosswhite, H.M., 1963. The Spectra of the Doubly and Triply Ionized Rare Earths. Appl. Opt. 2, 675. https://doi.org/10.1364/ao.2.000675

Dierssen, H.M., Zimmerman, R.C., Drake, L.A., Burdige, D., 2010. Benthic ecology from space: Optics and net primary production in seagrass and benthic algae across the Great Bahama Bank. Mar. Ecol. Prog. Ser. 411, 1–15. https://doi.org/10.3354/meps08665

Dinter, T., Rozanov, V. V., Burrows, J.P., Bracher, A., 2015. Retrieving the availability of light in the ocean utilising spectral signatures of vibrational Raman scattering in hyper-spectral satellite measurements. Ocean Sci. 11, 373–389. https://doi.org/10.5194/OS-11-373-2015

Donlon, C., Berruti, B., Buongiorno, A., Ferreira, M.H., Féménias, P., Frerick, J., Goryl, P., Klein, U., Laur, H., Mavrocordatos, C., Nieke, J., Rebhan, H., Seitz, B., Stroede, J., Sciarra, R., 2012. The Global Monitoring for Environment and Security (GMES) Sentinel-3 mission. Remote Sens. Environ. 120, 37–57. https://doi.org/10.1016/j.rse.2011.07.024

Dozier, J., Green, R.O., Nolin, A.W., Painter, T.H., 2009. Interpretation of snow properties from imaging spectrometry. Remote Sens. Environ. 113, S25–S37. https://doi.org/10.1016/j.rse.2007.07.029

Dozier, J., Painter, T.H., 2004. Multispectral and hyperspectral remote sensing of alpine snow properties. Annu. Rev. Earth Planet. Sci. 32, 465–494. https://doi.org/10.1146/annurev.earth.32.101802.120404

Dronova, I., Taddeo, S., 2022. Remote sensing of phenology: Towards the comprehensive indicators of plant community dynamics from species to regional scales. J. Ecol. 00, 1–25. https://doi.org/10.1111/1365-2745.13897

Drusch, M., Del Bello, U., Carlier, S., Colin, O., Fernandez, V., Gascon, F., Hoersch, B., Isola, C., Laberinti, P., Martimort, P., Meygret, A., Spoto, F., Sy, O., Marchese, F., Bargellini, P., 2012. Sentinel-2: ESA's Optical High-Resolution Mission for GMES Operational Services. Remote Sens. Environ. 120, 25–36. https://doi.org/10.1016/j.rse.2011.11.026

Dupiau, A., Jacquemoud, S., Briottet, X., Fabre, S., Viallefont-Robinet, F., Philpot, W., Di Biagio, C., Hébert, M., Formenti, P., 2022. MARMIT-2: An improved version of the MARMIT model to predict soil reflectance as a function of surface water content in the solar domain. Remote Sens. Environ. 272, 112951. https://doi.org/10.1016/J.RSE.2022.112951

Duren, R.M., Thorpe, A.K., Foster, K.T., Rafiq, T., Hopkins, F.M., Yadav, V., Bue, B.D., Thompson, D.R., Conley, S., Colombi, N.K., Frankenberg, C., McCubbin, I.B., Eastwood, M.L., Falk, M., Herner, J.D., Croes, B.E., Green, R.O., Miller, C.E., 2019. California's methane super-emitters. Nature 575, 180–184. https://doi.org/10.1038/s41586-019-1720-3

Eicken, H., Gradinger, R., Gaylord, A., Mahoney, A., Rigor, I., Melling, H., 2005. Sediment transport by sea ice in the Chukchi and Beaufort Seas: Increasing importance due to changing ice conditions? Deep. Res. Part II Top. Stud. Oceanogr. 52, 3281–3302. https://doi.org/10.1016/j.dsr2.2005.10.006

Eicken, H., Grenfell, T.C., Perovich, D.K., Richter-Menge, J.A., Frey, K., 2004. Hydraulic controls of summer Arctic pack ice albedo. J. Geophys. Res. Ocean. 109. https://doi.org/10.1029/2003JC001989

Elder, C.D., Thompson, D.R., Thorpe, A.K., Hanke, P., Walter Anthony, K.M., Miller, C.E., 2020. Airborne Mapping Reveals Emergent Power Law of Arctic Methane Emissions. Geophys. Res. Lett. 47, e2019GL085707. https://doi.org/10.1029/2019GL085707

EPA, 1998. Advanced measurement initiative workshop report: advanced measurement and sitecharacterization of mining impacts on public health and the environment, Tech. Rep. EPA-235-R-98-002. Colorado School of Mines, Golden, Colorado.

Eriksson, C., Burton, H., 2003. Origins and biological accumulation of small plastic particles infur seals from Macquarie Island. Ambio 32, 380–384.

European Commission, 2021. New EU Forest Strategy for 2030. Brussles.

European Commission, 2018. Communication From The Commission To The European Parliament, The Council, The European Economic And Social Committee And The Committee Of The Regions: EU actions to improve environmental compliance and governance.

European Commission, 2015. Copernicus: Europe's eyes on Earth. Brussels. https://doi.org/doi/10.2873/70140

FAO, 2010. Guidelines on sustainable forest management in drylands of sub-Saharan Africa, Arid Zone Forests and Forestry. The Food and Agriculture Organization of the United Nations and Earthscan, Rome.

Fassnacht, F.E., Latifi, H., Koch, B., 2012. An angular vegetation index for imaging spectroscopy data-Preliminary results: On forest damage detection in the Bavarian National Park, Germany. Int. J. Appl. Earth Obs. Geoinf. 19, 308–321. https://doi.org/10.1016/j.jag.2012.05.018

Feilhauer, H., Faude, U., Schmidtlein, S., 2011. Combining Isomap ordination and imaging spectroscopy to map continuous floristic gradients in a heterogeneous landscape. Remote Sens. Environ. 115, 2513–2524. https://doi.org/10.1016/j.rse.2011.05.011

Feilhauer, H., Somers, B., van der Linden, S., 2017. Optical trait indicators for remote sensing of plant species composition: Predictive power and seasonal variability. Ecol. Indic. 73, 825–833. https://doi.org/10.1016/j.ecolind.2016.11.003

Feilhauer, H., Zlinszky, A., Kania, A., Foody, G.M., Doktor, D., Lausch, A., Schmidtlein, S., 2021. Let your maps be fuzzy!—Class probabilities and floristic gradients as alternatives to crisp mapping for remote sensing of vegetation. Remote Sens. Ecol. Conserv. 7, 292–305. https://doi.org/10.1002/rse2.188

Féret, J.B., Berger, K., de Boissieu, F., Malenovský, Z., 2021. PROSPECT-PRO for estimating content of nitrogen-containing leaf proteins and other carbon-based constituents. Remote Sens. Environ. 252, 112173. https://doi.org/10.1016/J.RSE.2020.112173

Féret, J.B., le Maire, G., Jay, S., Berveiller, D., Bendoula, R., Hmimina, G., Cheraiet, A., Oliveira, J.C., Ponzoni, F.J., Solanki, T., de Boissieu, F., Chave, J., Nouvellon, Y., Porcar-Castell, A., Proisy, C., Soudani, K., Gastellu-Etchegorry, J.P., Lefèvre-Fonollosa, M.J., 2019. Estimating leaf mass per area and equivalent water thickness based on leaf optical properties: Potential and limitations of physical modeling and machine learning. Remote Sens. Environ. 231, 110959. https://doi.org/10.1016/j.rse.2018.11.002

Flanner, M.G., Zender, C.S., Randerson, J.T., Rasch, P.J., 2007. Present-day climate forcing and

response from black carbon in snow. J. Geophys. Res. 112, D11202. https://doi.org/10.1029/2006JD008003

Foerster, S., Carrère, V., Rast, M., Staenz, K., 2016. Preface: The environmental mapping and analysis program (EnMAP) mission: Preparing for Its scientific exploitation. Remote Sens. https://doi.org/10.3390/rs8110957

Forbes, B.C., Ebersole, J.J., Strandberg, B., 2001. Anthropogenic disturbance and patch dynamics in circumpolar arctic ecosystems. Conserv. Biol. https://doi.org/10.1046/j.1523-1739.2001.015004954.x

Forrest, A.L., Wittmann, M.E., Schmidt, V., Raineault, N.A., Hamilton, A., Pike, W., Schladow, S.G., Reuter, J.E., Laval, B.E., Trembanis, A.C., 2012. Quantitative assessment of invasive species in lacustrine environments through benthic imagery analysis. Limnol. Oceanogr. Methods 10, 65–74. https://doi.org/10.4319/lom.2012.10.65

Förster, M., Spengler, D., Buddenbaum, H., Hill, J., Kleinschmit, B., 2010. Ein überblick über die kombination spektraler und geometrischer modellierung zur anwendung in der forstlichen fernerkundung. Photogramm. Fernerkundung, Geoinf. https://doi.org/10.1127/1432-8364/2010/0053

Francos, N., Ben-Dor, E., 2022. A transfer function to predict soil surface reflectance from laboratory soil spectral libraries. Geoderma 405, 115432. https://doi.org/10.1016/J.GEODERMA.2021.115432

Franke, J., Roberts, D.A., Halligan, K., Menz, G., 2009. Hierarchical Multiple Endmember Spectral Mixture Analysis (MESMA) of hyperspectral imagery for urban environments. Remote Sens. Environ. 113, 1712–1723. https://doi.org/10.1016/j.rse.2009.03.018

Franke, J.A., Müller, C., Minoli, S., Elliott, J., Folberth, C., Gardner, C., Hank, T., Izaurralde, R.C., Jägermeyr, J., Jones, C.D., Liu, W., Olin, S., Pugh, T.A.M., Ruane, A.C., Stephens, H., Zabel, F., Moyer, E.J., 2022. Agricultural breadbaskets shift poleward given adaptive farmer behavior under climate change. Glob. Chang. Biol. 28, 167–181. https://doi.org/10.1111/GCB.15868

Frankenberg, C., Kulawik, S.S., Wofsy, S.C., Chevallier, F., Daube, B., Kort, E.A., O'Dell, C., Olsen, E.T., Osterman, G., 2016. Using airborne HIAPER pole-to-pole observations (HIPPO) to evaluate model and remote sensing estimates of atmospheric carbon dioxide. Atmos. Chem. Phys. 16, 7867–7878. https://doi.org/10.5194/ACP-16-7867-2016

Franklin, S.E., 2001. Remote sensing for sustainable forest management, Remote Sensing for Sustainable Forest Management. CRC Press. https://doi.org/10.1201/9781420032857

Fraser, R., McLennan, D., Ponomarenko, S., Olthof, I., 2012. Image-based predictive ecosystem mapping in Canadian arctic parks. Int. J. Appl. Earth Obs. Geoinf. 14, 129–138. https://doi.org/10.1016/j.jag.2011.08.013

Fraser, R., Olthof, I., Kokelj, S., Lantz, T., Lacelle, D., Brooker, A., Wolfe, S., Schwarz, S., 2014. Detecting Landscape Changes in High Latitude Environments Using Landsat Trend Analysis: 1. Visualization. Remote Sens. 6, 11533–11557. https://doi.org/10.3390/rs61111533

Fuentes, D.A., Gamon, J.A., Cheng, Y., Claudio, H.C., Qiu, H. lie, Mao, Z., Sims, D.A., Rahman, A.F., Oechel, W., Luo, H., 2006. Mapping carbon and water vapor fluxes in a chaparral ecosystem using vegetation indices derived from AVIRIS. Remote Sens. Environ. 103, 312–323. https://doi.org/10.1016/j.rse.2005.10.028

Gabrieli, A., Wright, R., Porter, J.N., Lucey, P.G., Honnibal, C., 2019. Applications of quantitative thermal infrared hyperspectral imaging (8–14 μm): measuring volcanic SO2 mass flux and determining plume transport velocity using a single sensor. Bull. Volcanol. 81, 47. https://doi.org/10.1007/s00445-019-1305-x

Galgani, F., Oosterbaan, L., Poitou, I., Hanke, G., Thompson, R., Amato, E., Janssen, C., Galgani, F., Fleet, D., Franeker, J. Van, Katsanevakis, S., Maes, T., 2010. Marine Litter, Marine Strategy Framework Directive Group 10 Report. https://doi.org/10.2788/86941

Gamon, J.A., Kovalchuck, O., Wong, C.Y.S., Harris, A., Garrity, S.R., 2015. Monitoring seasonal and diurnal changes in photosynthetic pigments with automated PRI and NDVI sensors.

Biogeosciences 12, 4149–4159. https://doi.org/10.5194/BG-12-4149-2015

Gamon, J.A., Somers, B., Malenovský, Z., Middleton, E.M., Rascher, U., Schaepman, M.E., 2019. Assessing Vegetation Function with Imaging Spectroscopy. Surv. Geophys. 40, 489–513. https://doi.org/10.1007/S10712-019-09511-5/FIGURES/3

Gascueña, A.B., 2020. Mineral exploration of rock wastes from sulfide mining using airborne hyperspectral imaging. Universidad de Granada. https://doi.org/10.30827/Digibug.65495

Gasela, M., Kganyago, M., De Jager, G., 2022. Testing the utility of the resampled nSight-2 spectral configurations in discriminating wetland plant species using Random Forest classifier. Geocarto Int. 1–16. https://doi.org/10.1080/10106049.2022.2060326

Ge, Y., Thomasson, J.A., Sui, R., 2011. Remote sensing of soil properties in precision agriculture: A review. Front. Earth Sci. 5, 229–238. https://doi.org/10.1007/s11707-011-0175-0

Gege, P., 2021. Radiometric Measurement Requirements to Derive Information on Phytoplankton Community Composition from Satellite, in: 2021 IEEE International Geoscience and Remote Sensing Symposium IGARSS. IEEE, pp. 1241–1244. https://doi.org/10.1109/IGARSS47720.2021.9554844

GEO, 2015. GEO Strategic Plan 2016-2025: Implementing GEOSS. Group on Earth Observation.

Gerard, F.F., North, P.R.J., 1997. Analyzing the effect of structural variability and canopy gaps on forest BRDF using a geometric-optical model. Remote Sens. Environ. 62, 46–62. https://doi.org/10.1016/S0034-4257(97)00070-9

Gholizadeh, A., Žižala, D., Saberioon, M., Borůvka, L., 2018. Soil organic carbon and texture retrieving and mapping using proximal, airborne and Sentinel-2 spectral imaging. Remote Sens. Environ. 218, 89–103. https://doi.org/10.1016/J.RSE.2018.09.015

Gholizadeh, H., Gamon, J.A., Helzer, C.J., Cavender-Bares, J., 2020. Multi-temporal assessment of grassland α- and β-diversity using hyperspectral imaging. Ecol. Appl. 30, e02145. https://doi.org/10.1002/eap.2145

Giardino, C., Brando, V.E., Dekker, A.G., Strömbeck, N., Candiani, G., 2007. Assessment of water quality in Lake Garda (Italy) using Hyperion. Remote Sens. Environ. 109, 183–195. https://doi.org/10.1016/j.rse.2006.12.017

Giardino, C., Brando, V.E., Gege, P., Pinnel, N., Hochberg, E., Knaeps, E., Reusen, I., Doerffer, R., Bresciani, M., Braga, F., Foerster, S., Champollion, N., Dekker, A., 2019. Imaging Spectrometry of Inland and Coastal Waters: State of the Art, Achievements and Perspectives. Surv. Geophys. 40, 401–429. https://doi.org/10.1007/S10712-018-9476-0/TABLES/1

Gläßer, C., Groth, D., Frauendorf, J., 2011. Monitoring of hydrochemical parameters of lignite mining lakes in Central Germany using airborne hyperspectral casi-scanner data. Int. J. Coal Geol. 86, 40–53. https://doi.org/10.1016/J.COAL.2011.01.007

Goetz, A.F.H., 2011. Measuring the earth from above: 30 years (and Counting) of hyperspectral imaging. Photonics Spectra 45, 42.

Goetz, A.F.H., Chabrillat, S., Lu, Z., 2001. Field Reflectance Spectrometry for Detection of Swelling Clays at Construction Sites. F. Anal. Chem. Technol. 5, 143–155. https://doi.org/10.1002/fact.1015

Goetz, A.F.H., Vane, G., Solomon, J.E., Rock, B.N., 1985. Imaging spectrometry for earth remote sensing. Science (80-.). 228, 1147–1153. https://doi.org/10.1126/science.228.4704.1147

Goodenough, D.G., Charlebois, D., Bhogal, A.S., Daley, N., 1998. Improved planner for intelligent monitoring of sustainable development of forests, in: International Geoscience and Remote Sensing Symposium (IGARSS). IEEE, pp. 397–399. https://doi.org/10.1109/igarss.1998.702917

Goodenough, D.G., Chen, H., Dyk, A., Han, T., McDonald, S., Murdoch, M., Olaf Niemann, K., Pearlman, J., West, C., 2003. EVEOSD Forest Information Products from AVIRIS and Hyperion, in: International Geoscience and Remote Sensing Symposium (IGARSS). IEEE, pp. 284–287. https://doi.org/10.1109/igarss.2003.1293751

Goodenough, D.G., Chen, H., Gordon, P., Niemann, K.O., Quinn, G., 2012. Forest applications with

hyperspectral imaging, in: International Geoscience and Remote Sensing Symposium (IGARSS). IEEE, pp. 7309–7312. https://doi.org/10.1109/IGARSS.2012.6351973

Goodenough, D.G., Dyk, A., Hobart, G., Chen, H., 2007. Forest information products from hyperspectral data Victoria and Hoquiam test sites, in: International Geoscience and Remote Sensing Symposium (IGARSS). IEEE, pp. 1532–1536. https://doi.org/10.1109/IGARSS.2007.4423101

Götze, C., Jung, A., Merbach, I., Wennrich, R., Gläßer, C., 2010. Spectrometric analyses in comparison to the physiological condition of heavy metal stressed floodplain vegetation in a standardised experiment. Open Geosci. 2, 132–137. https://doi.org/10.2478/v10085-010-0002-y

Gower, J.F.R., Borstad, G.A., Anger, C.D., Edel, H.R., 1992. CCD-Based Imaging Spectroscopy for Remote Sensing: The FLI and CASI Programs. Can. J. Remote Sens. 18, 199–208. https://doi.org/10.1080/07038992.1992.10855325

Graham, E.R., Thompson, J.T., 2009. Deposit- and suspension-feeding sea cucumbers (Echinodermata) ingest plastic fragments. J. Exp. Mar. Bio. Ecol. 368, 22–29. https://doi.org/10.1016/j.jembe.2008.09.007

Graham, G.E., Kokaly, R.F., Kelley, K.D., Hoefen, T.M., Johnson, M.R., Hubbard, B.E., 2018. Application of imaging spectroscopy for mineral exploration in Alaska: A study over porphyry Cu deposits in the eastern Alaska Range. Econ. Geol. 113, 489–510. https://doi.org/10.5382/econgeo.2018.4559

Gray, A., Krolikowski, M., Fretwell, P., Convey, P., Peck, L.S., Mendelova, M., Smith, A.G., Davey, M.P., 2020. Remote sensing reveals Antarctic green snow algae as important terrestrial carbon sink. Nat. Commun. 11, 1–9. https://doi.org/10.1038/s41467-020-16018-w

Green, R.O., Eastwood, M.L., Sarture, C.M., Chrien, T.G., Aronsson, M., Chippendale, B.J., Faust, J.A., Pavri, B.E., Chovit, C.J., Solis, M., Olah, M.R., Williams, O., 1998. Imaging Spectroscopy and the Airborne Visible/Infrared Imaging Spectrometer (AVIRIS). Remote Sens. Environ. 65, 227–248. https://doi.org/10.1016/S0034-4257(98)00064-9

Gregory, M.R., 2009. Environmental implications of plastic debris in marine settings- entanglement, ingestion, smothering, hangers-on, hitch-hiking and alien invasions. Philos. Trans. R. Soc. B Biol. Sci. 364, 2013–2025. https://doi.org/10.1098/rstb.2008.0265

Guanter, L., Irakulis-Loitxate, I., Gorroño, J., Sánchez-García, E., Cusworth, D.H., Varon, D.J., Cogliati, S., Colombo, R., 2021. Mapping methane point emissions with the PRISMA spaceborne imaging spectrometer. Remote Sens. Environ. 265, 112671. https://doi.org/10.1016/j.rse.2021.112671

Guanter, L., Kaufmann, H., Segl, K., Foerster, S., Rogass, C., Chabrillat, S., Kuester, T., Hollstein, A., Rossner, G., Chlebek, C., Straif, C., Fischer, S., Schrader, S., Storch, T., Heiden, U., Mueller, A., Bachmann, M., Mühle, H., Müller, R., Habermeyer, M., Ohndorf, A., Hill, J., Buddenbaum, H., Hostert, P., van der Linden, S., Leitão, P.J., Rabe, A., Doerffer, R., Krasemann, H., Xi, H., Mauser, W., Hank, T., Locherer, M., Rast, M., Staenz, K., Sang, B., 2015. The EnMAP Spaceborne Imaging Spectroscopy Mission for Earth Observation. Remote Sens 7, 8830–8857. https://doi.org/10.3390/rs70708830

Guanter, L., Richter, R., Moreno, J., 2006. Spectral calibration of hyperspectral imagery using atmospheric absorption features. Appl. Opt. 45, 2360–2370. https://doi.org/10.1364/AO.45.002360

Guanter, L., Zhang, Y., Jung, M., Joiner, J., Voigt, M., Berry, J.A., Frankenberg, C., Huete, A.R., Zarco-Tejada, P., Lee, J.E., Moran, M.S., Ponce-Campos, G., Beer, C., Camps-Valls, G., Buchmann, N., Gianelle, D., Klumpp, K., Cescatti, A., Baker, J.M., Griffis, T.J., 2014. Global and time-resolved monitoring of crop photosynthesis with chlorophyll fluorescence. Proc. Natl. Acad. Sci. U. S. A. 111. https://doi.org/10.1073/pnas.1320008111

Guzzetti, F., Mondini, A.C., Cardinali, M., Fiorucci, F., Santangelo, M., Chang, K.T., 2012. Landslide inventory maps: New tools for an old problem. Earth-Science Rev. https://doi.org/10.1016/j.earscirev.2012.02.001

Guzzetti, F., Reichenbach, P., Cardinali, M., Galli, M., Ardizzone, F., 2005. Probabilistic landslide hazard assessment at the basin scale. Geomorphology 72, 272–299. https://doi.org/10.1016/j.geomorph.2005.06.002

Haberl, H., Erb, K.H., Krausmann, F., Gaube, V., Bondeau, A., Plutzar, C., Gingrich, S., Lucht, W., Fischer-Kowalski, M., 2007. Quantifying and mapping the human appropriation of net primary production in earth's terrestrial ecosystems. Proc. Natl. Acad. Sci. U. S. A. 104, 12942–12947. https://doi.org/10.1073/pnas.0704243104

Haboudane, D., Miller, J.R., Tremblay, N., Zarco-Tejada, P.J., Dextraze, L., 2002. Integrated narrow-band vegetation indices for prediction of crop chlorophyll content for application to precision agriculture. Remote Sens. Environ. 81, 416–426. https://doi.org/10.1016/S0034-4257(02)00018-4

Halme, E., Pellikka, P., Mõttus, M., 2019. Utility of hyperspectral compared to multispectral remote sensing data in estimating forest biomass and structure variables in Finnish boreal forest. Int. J. Appl. Earth Obs. Geoinf. 83, 101942. https://doi.org/10.1016/j.jag.2019.101942

Hank, T., 2008. A Biophysically Based Coupled Model Approach for the Assessment of Canopy Processes Under Climate Change Conditions. Diss. der Fak. für Geowissenschaften, Digit. Hochschulschriften der LMU München, München. Ludwig-Maximilians-Universität München. https://doi.org/10.5282/EDOC.8725

Hank, T., Bach, H., Spannraft, K., Friese, M., Frank, T., Mauser, W., 2012. Improving the process-based simulation of growth heterogeneities in agricultural stands through assimilation of earth observation data, in: International Geoscience and Remote Sensing Symposium (IGARSS). IEEE, pp. 1006–1009. https://doi.org/10.1109/IGARSS.2012.6351232

Hank, T., Marzahn, P., Schlenz, F., Mauser, W., 2010. Assessing Moisture Conditions of Heterogeneous Land Surfaces Through Hyperspectral Analysis of Water Absorption Features, in: Methods. pp. 17–19.

Hank, T.B., Bach, H., Mauser, W., 2015. Using a remote sensing-supported hydro-agroecological model for field-scale simulation of heterogeneous crop growth and yield: Application for wheat in central europe. Remote Sens. 7, 3934–3965. https://doi.org/10.3390/rs70403934

Hank, T.B., Berger, K., Bach, H., Clevers, J.G.P.W., Gitelson, A., Zarco-Tejada, P., Mauser, W., 2019. Spaceborne Imaging Spectroscopy for Sustainable Agriculture: Contributions and Challenges. Surv. Geophys. https://doi.org/10.1007/s10712-018-9492-0

Hansen, M.C., Roy, D.P., Lindquist, E., Adusei, B., Justice, C.O., Altstatt, A., 2008. A method for integrating MODIS and Landsat data for systematic monitoring of forest cover and change in the Congo Basin. Remote Sens. Environ. 112, 2495–2513. https://doi.org/10.1016/j.rse.2007.11.012

Harris, J.R., Rogge, D., Hitchcock, R., Ijewliw, O., Wright, D., 2005. Mapping lithology in Canada's Arctic: application of hyperspectral data using the minimum noise fraction transformation and matched filtering. Can. J. Earth Sci. 42, 2173–2193. https://doi.org/10.1139/e05-064

Haubrock, S., Chabrillat, S., Kaufmann, H., 2005. Application of Hyperspectral Imaging for the Quantification of Surface Soil Moisture, in: Proceedings of 4th EARSeL Workshop on Imaging Spectroscopy. New Quality in Environmental Studies. pp. 163–171.

Haubrock, S.N., Chabrillat, S., Lemmnitz, C., Kaufmann, H., 2008. Surface soil moisture quantification models from reflectance data under field conditions. Int. J. Remote Sens. 29, 3–29. https://doi.org/10.1080/01431160701294695

Hedley, J.D., 2013. Hyperspectral Applications, in: Coral Reef Remote Sensing. Springer Netherlands, Dordrecht, pp. 79–112. https://doi.org/10.1007/978-90-481-9292-2_4

Heiden, U., Heldens, W., Roessner, S., Segl, K., Esch, T., Mueller, A., 2012. Urban structure type characterization using hyperspectral remote sensing and height information. Landsc. Urban Plan. 105, 361–375. https://doi.org/10.1016/j.landurbplan.2012.01.001

Heiden, U., Segl, K., Roessner, S., Kaufmann, H., 2007. Determination of robust spectral features for identification of urban surface materials in hyperspectral remote sensing data. Remote Sens. Environ. 111, 537–552. https://doi.org/10.1016/j.rse.2007.04.008

Heldens, W., Heiden, U., Esch, T., Stein, E., Müller, A., 2011. Can the Future EnMAP mission contribute to urban applications? A literature survey. Remote Sens. https://doi.org/10.3390/rs3091817

Heldens, W., Maronga, B., Zeidler, J., Kanani-Suhring, F., Hanke, W., Esch, T., 2019. Remote sensing-supported generation of surface descriptors for a highly detailed urban climate model, in: 2019 Joint Urban Remote Sensing Event, JURSE 2019. Institute of Electrical and Electronics Engineers Inc. https://doi.org/10.1109/JURSE.2019.8809010

Helland, I.S., 1990. PLS regression and statistical models. Scandivian J. Stat. 17, 97–114.

Herold, M., Roberts, D.A., Gardner, M.E., Dennison, P.E., 2004. Spectrometry for urban area remote sensing - Development and analysis of a spectral library from 350 to 2400 nm. Remote Sens. Environ. 91, 304–319. https://doi.org/10.1016/j.rse.2004.02.013

Hochberg, E.J., 2011. Remote sensing of coral reef processes. Coral Reefs An Ecosyst. Transit. 25–35. https://doi.org/10.1007/978-94-007-0114-4_3/COVER

Hoogenboom, G., Porter, C.H., Boote, K.J., Shelia, V., Wilkens, P.W., Singh, U., White, J.W., Asseng, S., Lizaso, J.I., Moreno, L.P., Pavan, W., Ogoshi, R., Hunt, L.A., Tsuji, G.Y., Jones, J.W., 2019. The DSSAT crop modeling ecosystem, in: Advances in Crop Modelling for a Sustainable Agriculture. Burleigh Dodds Science Publishing, pp. 173–216. https://doi.org/10.19103/as.2019.0061.10

Huang, C. ying, Anderegg, W.R.L., Asner, G.P., 2019. Remote sensing of forest die-off in the Anthropocene: From plant ecophysiology to canopy structure. Remote Sens. Environ. 231, 111233. https://doi.org/10.1016/J.RSE.2019.111233

Huang, S., Potter, C., Crabtree, R.L., Hager, S., Gross, P., 2010. Fusing optical and radar data to estimate sagebrush, herbaceous, and bare ground cover in Yellowstone. Remote Sens. Environ. 114, 251–264. https://doi.org/10.1016/j.rse.2009.09.013

Hubbard, S.S., Williams, K.H., Agarwal, D., Banfield, J., Beller, H., Bouskill, N., Brodie, E., Carroll, R., Dafflon, B., Dwivedi, D., Falco, N., Faybishenko, B., Maxwell, R., Nico, P., Steefel, C., Steltzer, H., Tokunaga, T., Tran, P.A., Wainwright, H., Varadharajan, C., 2018. The East River, Colorado, Watershed: A Mountainous Community Testbed for Improving Predictive Understanding of Multiscale Hydrological–Biogeochemical Dynamics. Vadose Zo. J. 17, 1–25. https://doi.org/10.2136/vzj2018.03.0061

Huck, P., Light, B., Eicken, H., Haller, M., 2007. Mapping sediment-laden sea ice in the Arctic using AVHRR remote-sensing data: Atmospheric correction and determination of reflectances as a function of ice type and sediment load. Remote Sens. Environ. 107, 484–495. https://doi.org/10.1016/j.rse.2006.10.002

Huemmrich, K.F., Gamon, J.A., Tweedie, C.E., Campbell, P.K.E., Landis, D.R., Middleton, E.M., 2013. Arctic tundra vegetation functional types based on photosynthetic physiology and optical properties. IEEE J. Sel. Top. Appl. Earth Obs. Remote Sens. 6, 265–275. https://doi.org/10.1109/JSTARS.2013.2253446

Hueni, A., Nieke, J., Schopfer, J., Kneubühler, M., Itten, K.I., 2009. The spectral database SPECCHIO for improved long-term usability and data sharing. Comput. Geosci. 35, 557–565. https://doi.org/10.1016/j.cageo.2008.03.015

Hunt, G.R., 1977. Spectral Signatures of Particulate Minerals in the Visible and Near Infrared. Geophysics 42, 501–513. https://doi.org/10.1190/1.1440721

Hunt, G.R., Ashley, R.P., 1979. Spectra of altered rocks in the visible and near infrared. Econ. Geol. 74, 1613–1629. https://doi.org/10.2113/GSECONGEO.74.7.1613

Hunt, G.R., Salisbury, J.W., 1970. Visible and near-infrared spectra of minerals and rocks: 1. Silicate minerals. Mod. Geol. 1, 283–300.

Ip, F., Dohm, J.M., Baker, V.R., Doggett, T., Davies, A.G., Castaño, R., Chien, S., Cichy, B., Greeley, R., Sherwood, R., Tran, D., Rabideau, G., 2006. Flood detection and monitoring with the Autonomous Sciencecraft Experiment onboard EO-1. Remote Sens. Environ. 101, 463–481. https://doi.org/10.1016/j.rse.2005.12.018

IPCC, 2022. Climate Change 2022: Impacts, Adaptation, and Vulnerability. Contribution of Working Group II to the Sixth Assessment Report of the Intergovernmental Panel on Climate Change, IPCC. Geneva, Switzerland. https://doi.org/10.1017/9781009325844

Irakulis-Loitxate, I., Guanter, L., Liu, Y.N., Varon, D.J., Maasakkers, J.D., Zhang, Yuzhong, Chulakadabba, A., Wofsy, S.C., Thorpe, A.K., Duren, R.M., Frankenberg, C., Lyon, D.R., Hmiel, B., Cusworth, D.H., Zhang, Yongguang, Segl, K., Gorroño, J., Sánchez-García, E., Sulprizio, M.P., Cao, K., Zhu, H., Liang, J., Li, X., Aben, I., Jacob, D.J., 2021. Satellite-based survey of extreme methane emissions in the Permian basin. Sci. Adv. 7. https://doi.org/10.1126/sciadv.abf4507

Istomina, L., Heygster, G., Huntemann, M., Schwarz, P., Birnbaum, G., Scharien, R., Polashenski, C., Perovich, D., Zege, E., Malinka, A., Prikhach, A., Katsev, I., 2015. Melt pond fraction and spectral sea ice albedo retrieval from MERIS data – Part 1: Validation against in situ, aerial, and ship cruise data. Cryosph. 9, 1551–1566. https://doi.org/10.5194/tc-9-1551-2015

Itten, K., Dell'Endice, F., Hueni, A., Kneubühler, M., Schläpfer, D., Odermatt, D., Seidel, F., Huber, S., Schopfer, J., Kellenberger, T., Bühler, Y., D'Odorico, P., Nieke, J., Alberti, E., Meuleman, K., 2008. APEX - the Hyperspectral ESA Airborne Prism Experiment. Sensors 8, 6235–6259. https://doi.org/10.3390/s8106235

Iwasaki, A., Ohgi, N., Tanii, J., Kawashima, T., Inada, H., 2011. Hyperspectral Imager Suite (HISUI)-Japanese hyper-multi spectral radiometer, in: International Geoscience and Remote Sensing Symposium (IGARSS). IEEE, pp. 1025–1028. https://doi.org/10.1109/IGARSS.2011.6049308

Jacquemoud, S., Verhoef, W., Baret, F., Bacour, C., Zarco-Tejada, P.J., Asner, G.P., François, C., Ustin, S.L., 2009. PROSPECT + SAIL models: A review of use for vegetation characterization. Remote Sens. Environ. 113, S56–S66. https://doi.org/10.1016/j.rse.2008.01.026

Jänicke, C., Okujeni, A., Cooper, S., Clark, M., Hostert, P., van der Linden, S., 2020. Brightness gradient-corrected hyperspectral image mosaics for fractional vegetation cover mapping in northern California. Remote Sens. Lett. 11, 1–10. https://doi.org/10.1080/2150704X.2019.1670518

Jędrych, M., Zagajewski, B., Marcinkowska-Ochtyra, A., 2017. Application of Sentinel-2 and EnMAP new satellite data to the mapping of alpine vegetation of the Karkonosze Mountains. Polish Cartogr. Rev. 49, 107–119. https://doi.org/10.1515/pcr-2017-0011

Ji, C., Heiden, U., Lakes, T., Feilhauer, H., 2021. Are urban material gradients transferable between areas? Int. J. Appl. Earth Obs. Geoinf. 100, 102332. https://doi.org/10.1016/j.jag.2021.102332

Ji, C., Jilge, M., Heiden, U., Stellmes, M., Feilhauer, H., 2022. Sampling Robustness in Gradient Analysis of Urban Material Mixtures. IEEE Trans. Geosci. Remote Sens. 60. https://doi.org/10.1109/TGRS.2020.3040342

Jiang, X., Zhen, J., Miao, J., Zhao, D., Shen, Z., Jiang, J., Gao, C., Wu, G., Wang, J., 2022. Newly-developed three-band hyperspectral vegetation index for estimating leaf relative chlorophyll content of mangrove under different severities of pest and disease. Ecol. Indic. 140, 108978. https://doi.org/10.1016/j.ecolind.2022.108978

Jilge, M., Habermeyer, M., Jürgens, C., 2015. Global Learning Spectral Archive - Anew Way to deal with Unknown Urban Spectra, in: AGU Fall Meeting, 14 – 18 December 2015,San Francisco, USA. San Francisco, USA.

Jin, M., Shepherd, J.M., Peters-Lidard, C., 2007. Development of a parameterization for simulating the urban temperature hazard using satellite observations in climate model. Nat. Hazards 43, 257–271. https://doi.org/10.1007/s11069-007-9117-2

Jones, B.M., Breen, A.L., Gaglioti, B. V., Mann, D.H., Rocha, A. V., Grosse, G., Arp, C.D., Kunz, M.L., Walker, D.A., 2013. Identification of unrecognized tundra fire events on the north slope of Alaska. J. Geophys. Res. Biogeosciences. https://doi.org/10.1002/jgrg.20113

Jordan, Y.C., Ghulam, A., Chu, M.L., 2014. Assessing the impacts of future urban development patterns and climate changes on total suspended sediment loading in surface waters using geoinformatics. J. Environ. Informatics 24, 65–79. https://doi.org/10.3808/jei.201400283

Jorgenson, J.C., Raynolds, M.K., Reynolds, J.H., Benson, A.-M., 2015. Twenty-Five Year Record of Changes in Plant Cover on Tundra of Northeastern Alaska. Arctic, Antarct. Alp. Res. 47, 785–806. https://doi.org/10.1657/aaar0014-097

Jorgenson, M.T., Grosse, G., 2016. Remote Sensing of Landscape Change in Permafrost Regions, in: Permafrost and Periglacial Processes. John Wiley and Sons Ltd, pp. 324–338. https://doi.org/10.1002/ppp.1914

JRC, 2013. Guidance on Monitoring of Marine Litter in European Seas. Ispra. https://doi.org/10.2788/99475

Kallio, K., Kutser, T., Hannonen, T., Koponen, S., Pulliainen, J., Vepsäläinen, J., Pyhälahti, T., 2001. Retrieval of water quality from airborne imaging spectrometry of various lake types in different seasons. Sci. Total Environ. 268, 59–77. https://doi.org/10.1016/S0048-9697(00)00685-9

Kamarainen, A.M., Penczykowski, R.M., Van De Bogert, M.C., Hanson, P.C., Carpenter, S.R., 2009. Phosphorus sources and demand during summer in a eutrophic lake. Aquat. Sci. 71, 214–227. https://doi.org/10.1007/s00027-009-9165-7

Kareiva, P., Watts, S., McDonald, R., Boucher, T., 2007. Domesticated nature: Shaping landscapes and ecosystems for human welfare. Science (80-.). 316, 1866–1869. https://doi.org/10.1126/SCIENCE.1140170/ASSET/B4F7EC62-C713-4820-B694-8F6B3BA4F0B0/ASSETS/GRAPHIC/316_1866_F3.JPEG

Kariuki, P.C., Woldai, T., van der Meer, F., 2004. Effectiveness of spectroscopy in identification of swelling indicator clay minerals. Int. J. Remote Sens. 25, 455–469. https://doi.org/10.1080/0143116031000084314

Kasmaeeyazdi, S., Mandanici, E., Balomenos, E., Tinti, F., Bonduà, S., Bruno, R., 2021. Mapping of Aluminum Concentration in Bauxite Mining Residues Using Sentinel-2 Imagery. Remote Sens. 2021, Vol. 13, Page 1517 13, 1517. https://doi.org/10.3390/RS13081517

Kattenborn, T., Fassnacht, F.E., Pierce, S., Lopatin, J., Grime, J.P., Schmidtlein, S., 2017. Linking plant strategies and plant traits derived by radiative transfer modelling. J. Veg. Sci. 28, 717–727. https://doi.org/10.1111/jvs.12525

Kaufmann, H., Sang, B., Storch, T., Segl, K., Foerster, S., Guanter, L., Erhard, M., Heider, B., Hofer, S., Honold, H.P., Penné, B., Bachmann, M., Habermeyer, M., Müller, A., Müller, R., Rast, M., Staenz, K., Straif, C., Chlebek, C., 2015. Environmental mapping and analysis program - A German hyperspectral mission, in: Qian, S. (Ed.), Optical Payloads for Space Missions. John Wiley & Sons, Ltd, pp. 161–181. https://doi.org/10.1002/9781118945179.ch7

Keeling, J., Mauger, A., … C.H.-, Sydney, U., 1998, U., 1998, U., 1998. Defining South Australian magnesite resources using high-resolution airborne spectrometry and survey-grade GPS, in: 5 Th Annual Airborne Geoscience Workshop. Pasadena, California.

Kemper, T., Sommer, S., 2004. Use of airborne hyperspectral data to estimate residual heavy metal contamination and acidification potential in the Guadiamar floodplain Andalusia, Spain after the Aznacollar mining accident. Proc. SPIE Remote Sens. Environ. Monit. GIS Appl. Geol. IV 5574, 224–234.

Kennedy, B.E., King, D.J., Duffe, J., 2021. Retrieval of Arctic Vegetation Biophysical and Biochemical Properties from CHRIS/PROBA Multi-Angle Imagery Using Empirical and Physical Modelling. Remote Sens. 13, 1830. https://doi.org/10.3390/rs13091830

Kennedy, B.E., King, D.J., Duffe, J., 2020. Comparison of Empirical and Physical Modelling for Estimation of Biochemical and Biophysical Vegetation Properties: Field Scale Analysis across an Arctic Bioclimatic Gradient. Remote Sens. 12, 3073. https://doi.org/10.3390/rs12183073

Kereszturi, G., Pullanagari, R.R., Mead, S., Schaefer, L.N., Procter, J., Schleiffarth, W.K., Kennedy, B., 2018. Geological Mapping of Hydrothermal Alteration on Volcanoes from Multi-Sensor Platforms, in: IGARSS 2018 - 2018 IEEE International Geoscience and Remote Sensing Symposium. IEEE, pp. 220–223. https://doi.org/10.1109/IGARSS.2018.8518818

Kereszturi, G., Schaefer, L.N., Miller, C., Mead, S., 2020. Hydrothermal Alteration on Composite Volcanoes: Mineralogy, Hyperspectral Imaging, and Aeromagnetic Study of Mt Ruapehu, New

Zealand. Geochemistry, Geophys. Geosystems 21. https://doi.org/10.1029/2020GC009270

Kijne, J., Barron, J., Hoff, H., Rockström, J., 2009. Opportunities to increase water productivity in agriculture with special reference to Africa and South Asia. A Rep. Prep. by Stock. Environ. Institute, Swedish Minist. Environ. Present. CSD 16, 48.

King, T., Kokaly, R., Eos, T.H.-, Transactions, undefined, 2012, undefined, 2012. Hyperspectral remote sensing data maps minerals in Afghanistan. Wiley Online Libr. 93, 325–326. https://doi.org/10.1029/2012EO340002

Kirk, J.T.O., 1994. Light and photosynthesis in aquatic ecosystems. Cambridge University Press, Cambridge. https://doi.org/10.1017/CBO9780511623370

Klein, A.G., Isacks, B.L., 1999. Spectral mixture analysis of Landsat thematic mapper images applied to the detection of the transient snowline on tropical Andean glaciers. Glob. Planet. Change 22, 139–154. https://doi.org/10.1016/S0921-8181(99)00032-6

Knipling, E.B., 1970. Physical and physiological basis for the reflectance of visible and near-infrared radiation from vegetation. Remote Sens. Environ. 1, 155–159. https://doi.org/10.1016/S0034-4257(70)80021-9

Knyazikhin, Y., Schull, M.A., Stenberg, P., Mõttus, M., Rautiainen, M., Yang, Y., Marshak, A., Carmona, P.L., Kaufmann, R.K., Lewis, P., Disney, M.I., Vanderbilt, V., Davis, A.B., Baret, F., Jacquemoud, S., Lyapustin, A., Myneni, R.B., 2013. Hyperspectral remote sensing of foliar nitrogen content. Proc. Natl. Acad. Sci. U. S. A. 110. https://doi.org/10.1073/pnas.1210196109

Kodikara, G.R.L., Woldai, T., van Ruitenbeek, F.J.A., Kuria, Z., van der Meer, F., Shepherd, K.D., van Hummel, G.J., 2012. Hyperspectral remote sensing of evaporate minerals and associated sediments in Lake Magadi area, Kenya. Int. J. Appl. Earth Obs. Geoinf. 14, 22–32. https://doi.org/10.1016/j.jag.2011.08.009

Koetz, B., Morsdorf, F., van der Linden, S., Curt, T., Allgöwer, B., 2008. Multi-source land cover classification for forest fire management based on imaging spectrometry and LiDAR data. For. Ecol. Manage. 256, 263–271. https://doi.org/10.1016/j.foreco.2008.04.025

Kokaly, R.F., Couvillion, B.R., Holloway, J.A.M., Roberts, D.A., Ustin, S.L., Peterson, S.H., Khanna, S., Piazza, S.C., 2013a. Spectroscopic remote sensing of the distribution and persistence of oil from the Deepwater Horizon spill in Barataria Bay marshes. Remote Sens. Environ. 129, 210–230. https://doi.org/10.1016/j.rse.2012.10.028

Kokaly, R.F., Couvillion, B.R., Holloway, J.A.M., Roberts, D.A., Ustin, S.L., Peterson, S.H., Khanna, S., Piazza, S.C., 2013b. Spectroscopic remote sensing of the distribution and persistence of oil from the Deepwater Horizon spill in Barataria Bay marshes. Remote Sens. Environ. 129, 210–230. https://doi.org/10.1016/J.RSE.2012.10.028

Konrad, C., 2016. U.S. Geological Survey Fact Sheet 076-03.

Kopeć, D., Zakrzewska, A., Halladin-Dąbrowska, A., Wylazłowska, J., Kania, A., Niedzielko, J., 2019. Using airborne hyperspectral imaging spectroscopy to accurately monitor invasive and expansive herb plants: Limitations and requirements of the method. Sensors 19, 2871. https://doi.org/10.3390/s19132871

Kötz, B., Schaepman, M., Morsdorf, F., Bowyer, P., Itten, K., Allgöwer, B., 2004. Radiative transfer modeling within a heterogeneous canopy for estimation of forest fire fuel properties, in: Remote Sensing of Environment. Elsevier BV, pp. 332–344. https://doi.org/10.1016/j.rse.2004.05.015

Kozak, P.K., Duke, E.F., Roselle, G.T., 2004. Mineral distribution in contact-metamorphosed siliceous dolomite at Ubehebe Peak, California, based on airborne imaging spectrometer data. Am. Mineral. 89, 701–713. https://doi.org/10.2138/am-2004-5-604

Krueger, G., Erzinger, J., Kaufmann, H., 1998. Laboratory and airborne reflectance spectroscopic analyses of lignite overburden dumps. J. Geochemical Explor. 64, 47–65. https://doi.org/10.1016/s0375-6742(98)00020-x

Kruse, F.A., Boardman, J.W., 2000. Characterization and mapping of kimberlites and related diatremes using hyperspectral remote sensing, in: IEEE Aerospace Conference Proceedings. IEEE, pp. 299–304. https://doi.org/10.1109/aero.2000.879859

Kuester, T., Chabrillat, S., 2017. Assessing the influence of variable fractional vegetation cover on soil spectral features using simulated canopy reflectance modeling T Kuester , S Chabrillat , S Foerster , D Spengler , L Guanter We do not inherit the earth from our ancestors , we borrow, in: EARSeL SIG Imaging Spectroscopy Workshop.

Kuriyama, Y., Konishi, K., Kanehiro, H., Otake, C., Kaminuma, T., Mato, Y., Takada, H., Kojima, A., 2002. Plastic pellets in the marine environment of Tokyo Bay and SagamiBay. Nippon Suisan Gakkaishi 68, 164–171.

Kusuma, K.N., Ramakrishnan, D., Pandalai, H.S., 2012. Spectral pathways for effective delineation of high-grade bauxites: A case study from the Savitri River Basin, Maharashtra, India, using EO-1 Hyperion data. Int. J. Remote Sens. 33, 7273–7290. https://doi.org/10.1080/01431161.2012.700131

Kuusk, A., Nilson, T., 2002. Forest reflectance and transmittance FRT user guide. Tartu Obs. 38.

Laidler, G.J., Treitz, P., 2003. Biophysical remote sensing of arctic environments. Prog. Phys. Geogr. 27, 44–68. https://doi.org/10.1191/0309133303pp358ra

Lammoglia, T., Filho, C.R. de S., 2011. Spectroscopic characterization of oils yielded from Brazilian offshore basins: Potential applications of remote sensing. Remote Sens. Environ. 115, 2525–2535. https://doi.org/https://doi.org/10.1016/j.rse.2011.04.038

Landmann, T., Piiroinen, R., Makori, D.M., Abdel-Rahman, E.M., Makau, S., Pellikka, P., Raina, S.K., 2015. Application of hyperspectral remote sensing for flower mapping in African savannas. Remote Sens. Environ. 166, 50–60. https://doi.org/10.1016/J.RSE.2015.06.006

Larsolle, A., Hamid Muhammed, H., 2007. Measuring crop status using multivariate analysis of hyperspectral field reflectance with application to disease severity and plant density. Precis. Agric. 8, 37–47. https://doi.org/10.1007/s11119-006-9027-4

Lassalle, G., 2021. Monitoring natural and anthropogenic plant stressors by hyperspectral remote sensing: Recommendations and guidelines based on a meta-review. Sci. Total Environ. 788, 147758. https://doi.org/10.1016/j.scitotenv.2021.147758

Laukamp, C., Cudahy, T., Thomas, M., Jones, M., Cleverley, J.S., Oliver, N.H.S., 2011. Hydrothermal mineral alteration patterns in the Mount Isa Inlier revealed by airborne hyperspectral data. Aust. J. Earth Sci. 58, 917–936. https://doi.org/10.1080/08120099.2011.571287

Launeau, P., Sotin, C., Girardeau, J., 2002. Cartography of the Ronda peridotite (Spain) by hyperspectral remote sensing. Bull. la Société Géologique Fr. 173, 491–508. https://doi.org/10.2113/173.6.491

Lausch, A., Bannehr, L., Beckmann, M., Boehm, C., Feilhauer, H., Hacker, J.M., Heurich, M., Jung, A., Klenke, R., Neumann, C., Pause, M., Rocchini, D., Schaepman, M.E., Schmidtlein, S., Schulz, K., Selsam, P., Settele, J., Skidmore, A.K., Cord, A.F., 2016. Linking Earth Observation and taxonomic, structural and functional biodiversity: Local to ecosystem perspectives. Ecol. Indic. 70, 317–339. https://doi.org/10.1016/j.ecolind.2016.06.022

Lausch, A., Erasmi, S., King, D.J., Magdon, P., Heurich, M., 2017. Understanding forest health with Remote sensing-Part II-A review of approaches and data models. Remote Sens. 9, 129. https://doi.org/10.3390/rs9020129

Lavorel, S., Grigulis, K., Lamarque, P., Colace, M.P., Garden, D., Girel, J., Pellet, G., Douzet, R., 2011. Using plant functional traits to understand the landscape distribution of multiple ecosystem services. J. Ecol. 99, 135–147. https://doi.org/10.1111/j.1365-2745.2010.01753.x

Le Maire, G., Davi, H., Soudani, K., François, C., Le Dantec, V., Dufrêne, E., 2005. Modeling annual production and carbon fluxes of a large managed temperate forest using forest inventories, satellite data and field measurements. Tree Physiol. 25, 859–872. https://doi.org/10.1093/treephys/25.7.859

le Maire, G., François, C., Soudani, K., Berveiller, D., Pontailler, J.Y., Bréda, N., Genet, H., Davi, H., Dufrêne, E., 2008. Calibration and validation of hyperspectral indices for the estimation of broadleaved forest leaf chlorophyll content, leaf mass per area, leaf area index and leaf canopy biomass. Remote Sens. Environ. 112, 3846–3864. https://doi.org/10.1016/j.rse.2008.06.005

Lee, K.-S., Cohen, W.B., Kennedy, R.E., Maiersperger, T.K., Gower, S.T., 2004. Hyperspectral versus multispectral data for estimating leaf area index in four different biomes 91, 508–520. https://doi.org/10.1016/j.rse.2004.04.010

Lee, Z., Carder, K.L., Mobley, C.D., Steward, R.G., Patch, J.S., 1999. Hyperspectral remote sensing for shallow waters: 2 Deriving bottom depths and water properties by optimization. Appl. Opt. 38, 3831. https://doi.org/10.1364/ao.38.003831

Leifer, I., Lehr, W.J., Simecek-Beatty, D., Bradley, E., Clark, R., Dennison, P., Hu, Y., Matheson, S., Jones, C.E., Holt, B., Reif, M., Roberts, D.A., Svejkovsky, J., Swayze, G., Wozencraft, J., 2012. State of the art satellite and airborne marine oil spill remote sensing: Application to the BP Deepwater Horizon oil spill. Remote Sens. Environ. 124, 185–209. https://doi.org/10.1016/J.RSE.2012.03.024

Leitão, P.J., Schwieder, M., Suess, S., Okujeni, A., Galvão, L.S., van der Linden, S., Hostert, P., 2015. Monitoring natural ecosystem and ecological gradients: Perspectives with EnMAP. Remote Sens. 7, 13098–13119. https://doi.org/10.3390/rs71013098

Li, Y., Liu, Y., Wu, S., Wang, C., Xu, A., Pan, X., 2017. Hyper-spectral estimation of wheat biomass after alleviating of soil effects on spectra by non-negative matrix factorization. Eur. J. Agron. 84, 58–66. https://doi.org/10.1016/J.EJA.2016.12.003

Lisitzin, A.P., 2002. Iceberg and Sea-Ice Sedimentation in the North Atlantic — Recent and Past, in: Sea-Ice and Iceberg Sedimentation in the Ocean. pp. 337–385. https://doi.org/10.1007/978-3-642-55905-1_12

Liu, N., Treitz, P., 2018. Remote sensing of Arctic percent vegetation cover and fAPAR on Baffin Island, Nunavut, Canada. Int. J. Appl. Earth Obs. Geoinf. 71, 159–169. https://doi.org/10.1016/j.jag.2018.05.011

Locherer, M., Hank, T., Danner, M., Mauser, W., 2015a. Retrieval of seasonal leaf area index from simulated EnMAP data through optimized LUT-based inversion of the PROSAIL model. Remote Sens. 7, 10321–10346. https://doi.org/10.3390/rs70810321

Locherer, M., Hank, T., Danner, M., Mauser, W., Rast, M., Staenz, K., Thenkabail, P.S., 2015b. Retrieval of Seasonal Leaf Area Index from Simulated EnMAP Data through Optimized LUT-Based Inversion of the PROSAIL Model. Remote Sens. 2015, Vol. 7, Pages 10321-10346 7, 10321–10346. https://doi.org/10.3390/RS70810321

Lu, B., Dao, P.D., Liu, J., He, Y., Shang, J., 2020. Recent Advances of Hyperspectral Imaging Technology and Applications in Agriculture. Remote Sens. 2020, Vol. 12, Page 2659 12, 2659. https://doi.org/10.3390/RS12162659

Lu, D., Weng, Q., 2006. Use of impervious surface in urban land-use classification. Remote Sens. Environ. 102, 146–160. https://doi.org/10.1016/j.rse.2006.02.010

Lucke, R.L., Corson, M., McGlothlin, N.R., Butcher, S.D., Wood, D.L., Korwan, D.R., Li, R.R., Snyder, W.A., Davis, C.O., Chen, D.T., 2011. Hyperspectral Imager for the Coastal Ocean: instrument description and first images. Appl. Opt. 50, 1501. https://doi.org/10.1364/ao.50.001501

Macander, M.J., Frost, G. V., Nelson, P.R., Swingley, C.S., 2017. Regional quantitative cover mapping of tundra plant functional types in Arctic Alaska. Remote Sens. 9, 1024. https://doi.org/10.3390/rs9101024

Machwitz, M., Giustarini, L., Bossung, C., Frantz, D., Schlerf, M., Lilienthal, H., Wandera, L., Matgen, P., Hoffmann, L., Udelhoven, T., 2014. Enhanced biomass prediction by assimilating satellite data into a crop growth model. Environ. Model. Softw. 62, 437–453. https://doi.org/10.1016/j.envsoft.2014.08.010

Malenovský, Z., Homolová, L., Lukeš, P., Buddenbaum, H., Verrelst, J., Alonso, L., Schaepman, M.E., Lauret, N., Gastellu-Etchegorry, J.P., 2019. Variability and Uncertainty Challenges in Scaling Imaging Spectroscopy Retrievals and Validations from Leaves Up to Vegetation Canopies. Surv. Geophys. 40, 631–656. https://doi.org/10.1007/S10712-019-09534-Y/FIGURES/5

Marcinkowska-Ochtyra, A., Zagajewski, B., Ochtyra, A., Jarocińska, A., Wojtuń, B., Rogass, C.,

Mielke, C., Lavender, S., 2017. Subalpine and alpine vegetation classification based on hyperspectral APEX and simulated EnMAP images. Int. J. Remote Sens. 38, 1839–1864. https://doi.org/10.1080/01431161.2016.1274447

Mars, J.C., Crowley, J.K., 2003. Mapping mine wastes and analyzing areas affected by selenium-rich water runoff in southeast Idaho using AVIRIS imagery and digital elevation data. Remote Sens. Environ. 84, 422–436. https://doi.org/10.1016/S0034-4257(02)00132-3

Martin, M.E., Newman, S.D., Aber, J.D., Congalton, R.G., 1998. Determining forest species composition using high spectral resolution remote sensing data. Remote Sens. Environ. 65, 249–254. https://doi.org/10.1016/S0034-4257(98)00035-2

Mato, Y., Isobe, T., Takada, H., Kanehiro, H., Ohtake, C., Kaminuma, T., 2001. Plastic resin pellets as a transport medium for toxic chemicals inthe marine environment. Environ. Sci. Technol. 35, 318–324.

Matson, P., Johnson, L., Billow, C., Miller, J., Pu, R., 1994. Seasonal patterns and remote spectral estimation of canopy chemistry across the Oregon transect. Ecol. Appl. 4, 280–298. https://doi.org/10.2307/1941934

Mattila, T.J., Hagelberg, E., Söderlund, S., Joona, J., 2022a. How farmers approach soil carbon sequestration? Lessons learned from 105 carbon-farming plans. Soil Tillage Res. 215, 105204. https://doi.org/10.1016/J.STILL.2021.105204

Mattila, T.J., Hagelberg, E., Söderlund, S., Joona, J., 2022b. How farmers approach soil carbon sequestration? Lessons learned from 105 carbon-farming plans. Soil Tillage Res. 215, 5147–5155. https://doi.org/10.1016/j.still.2021.105204

Mauser, W., Klepper, G., Zabel, F., Delzeit, R., Hank, T., Putzenlechner, B., Calzadilla, A., 2015. Global biomass production potentials exceed expected future demand without the need for cropland expansion. Nat. Commun. 6. https://doi.org/10.1038/ncomms9946

McCarthy, T.S., Arnold, V., Venter, J., Ellery, W.N., 2007. The collapse of Johannesburg's Klip River wetland. S. Afr. J. Sci. 103, 391–397. https://doi.org/10.10520/EJC96717

McCormick, C.A., Corlett, H., Stacey, J., Hollis, C., Feng, J., Rivard, B., Omma, J.E., 2021. Shortwave infrared hyperspectral imaging as a novel method to elucidate multi-phase dolomitization, recrystallization, and cementation in carbonate sedimentary rocks. Sci. Rep. 11, 21732. https://doi.org/10.1038/s41598-021-01118-4

Meiforth, J.J., Buddenbaum, H., Hill, J., Shepherd, J., 2020. Article monitoring of canopy stress symptoms in New Zealand kauri trees analysed with Aisa hyperspectral data. Remote Sens. 12, 926. https://doi.org/10.3390/rs12060926

Meroni, M., Rossini, M., Guanter, L., Alonso, L., Rascher, U., Colombo, R., Moreno, J., 2009. Remote sensing of solar-induced chlorophyll fluorescence: Review of methods and applications. Remote Sens. Environ. 113, 2037–2051. https://doi.org/10.1016/j.rse.2009.05.003

Metternicht, G., Hurni, L., Gogu, R., 2005. Remote sensing of landslides: An analysis of the potential contribution to geo-spatial systems for hazard assessment in mountainous environments. Remote Sens. Environ. 98, 284–303. https://doi.org/10.1016/j.rse.2005.08.004

Meyerson, F.A.B., Merino, L., Durand, J., 2007. Migration and environment in the context of globalization. Front. Ecol. Environ. 5, 182–190. https://doi.org/https://doi.org/10.1890/1540-9295(2007)5[182:MAEITC]2.0.CO;2

Michel, S., Gamet, P., Lefevre-Fonollosa, M.J., 2011. HYPXIM A hyperspectral satellite defined for science, security and defence users. Work. Hyperspectral Image Signal Process. Evol. Remote Sens. 1–4. https://doi.org/10.1109/WHISPERS.2011.6080864

Milewski, R., Chabrillat, S., Brell, M., Schleicher, A.M., Guanter, L., 2019. Assessment of the 1.75 µm absorption feature for gypsum estimation using laboratory, air- and spaceborne hyperspectral sensors. Int. J. Appl. Earth Obs. Geoinf. 77, 69–83. https://doi.org/10.1016/j.jag.2018.12.012

Milewski, R., Schmid, T., Chabrillat, S., Jiménez, M., Escribano, P., Pelayo, M., Ben-Dor, E., 2022. Analyses of the Impact of Soil Conditions and Soil Degradation on Vegetation Vitality and Crop Productivity Based on Airborne Hyperspectral VNIR–SWIR–TIR Data in a Semi-Arid Rainfed

Agricultural Area (Camarena, Central Spain). Remote Sens. 14, 5131. https://doi.org/10.3390/rs14205131

Miner, K.R., Turetsky, M.R., Malina, E., Bartsch, A., Tamminen, J., McGuire, A.D., Fix, A., Sweeney, C., Elder, C.D., Miller, C.E., 2022. Permafrost carbon emissions in a changing Arctic. Nat. Rev. Earth Environ. 2022 31 3, 55–67. https://doi.org/10.1038/s43017-021-00230-3

Minh, N.H., Minh, T.B., Watanabe, M., Kunisue, T., Monirith, I., Tanabe, S., Sakai, S., Subramanian, A., Sasikumar, K., Viet, P.H., Tuyen, B.C., Tana, T.S., Prudente, M.S., 2003. Open dumping site in Asian developing countries: A potential source of polychlorinated dibenzo-p-dioxins and polychlorinated dibenzofurans. Environ. Sci. Technol. 37, 1493–1502. https://doi.org/10.1021/es026078s

MMSD, 2002. Breaking new ground: Mining, minerals and sustainable development. London.

Moran, S.S., Vidal, A., Troufleau, D., Qi, J., Clarke, T.R., Pinter, P.J., Mitchell, T.A., Inoue, Y., Neale, C.M.U., 1997. Combining multifrequency microwave and optical data for crop management. Remote Sens. Environ. 61, 96–109. https://doi.org/10.1016/S0034-4257(96)00243-X

Mumby, P.J., Skirving, W., Strong, A.E., Hardy, J.T., LeDrew, E.F., Hochberg, E.J., Stumpf, R.P., David, L.T., 2004. Remote sensing of coral reefs and their physical environment. Mar. Pollut. Bull. 48, 219–228. https://doi.org/10.1016/j.marpolbul.2003.10.031

Mutanga, O., Skidmore, A.K., 2004. Hyperspectral band depth analysis for a better estimation of grass biomass (Cenchrus ciliaris) measured under controlled laboratory conditions. Int. J. Appl. Earth Obs. Geoinf. 5, 87–96. https://doi.org/10.1016/j.jag.2004.01.001

Myers-Smith, I.H., Forbes, B.C., Wilmking, M., Hallinger, M., Lantz, T., Blok, D., Tape, K.D., Macias-Fauria, M., Sass-Klaassen, U., Lévesque, E., Boudreau, S., Ropars, P., Hermanutz, L., Trant, A., Collier, L.S., Weijers, S., Rozema, J., Rayback, S.A., Schmidt, N.M., Schaepman-Strub, G., Wipf, S., Rixen, C., Ménard, C.B., Venn, S., Goetz, S., Andreu-Hayles, L., Elmendorf, S., Ravolainen, V., Welker, J., Grogan, P., Epstein, H.E., Hik, D.S., 2011. Shrub expansion in tundra ecosystems: dynamics, impacts and research priorities. Environ. Res. Lett. 6, 045509. https://doi.org/10.1088/1748-9326/6/4/045509

Myers-Smith, I.H., Kerby, J.T., Phoenix, G.K., Bjerke, J.W., Epstein, H.E., Assmann, J.J., John, C., Andreu-Hayles, L., Angers-Blondin, S., Beck, P.S.A., Berner, L.T., Bhatt, U.S., Bjorkman, A.D., Blok, D., Bryn, A., Christiansen, C.T., Cornelissen, J.H.C., Cunliffe, A.M., Elmendorf, S.C., Forbes, B.C., Goetz, S.J., Hollister, R.D., de Jong, R., Loranty, M.M., Macias-Fauria, M., Maseyk, K., Normand, S., Olofsson, J., Parker, T.C., Parmentier, F.J.W., Post, E., Schaepman-Strub, G., Stordal, F., Sullivan, P.F., Thomas, H.J.D., Tømmervik, H., Treharne, R., Tweedie, C.E., Walker, D.A., Wilmking, M., Wipf, S., 2020. Complexity revealed in the greening of the Arctic. Nat. Clim. Chang. https://doi.org/10.1038/s41558-019-0688-1

Mzid, N., Castaldi, F., Tolomio, M., Pascucci, S., Casa, R., Pignatti, S., 2022. Evaluation of Agricultural Bare Soil Properties Retrieval from Landsat 8, Sentinel-2 and PRISMA Satellite Data. Remote Sens. 14. https://doi.org/10.3390/rs14030714

Nepstad, D.C., Veríssimo, A., Alencar, A., Nobre, C., Lima, E., Lefebvre, P., Schlesinger, P., Potter, C., Moutinho, P., Mendoza, E., Cochrane, M., Brooks, V., 1999. Large-scale impoverishment of amazonian forests by logging and fire. Nature 398, 505–508. https://doi.org/10.1038/19066

Neville, R.A., Powell, I., 1992. Design of sfsi: an imaging spectrometer in the swir. Can. J. Remote Sens. 18, 210–222. https://doi.org/10.1080/07038992.1992.10855326

Nieke, J., Rast, M., 2018. Towards the copernicus hyperspectral imaging mission for the environment (CHIME), in: International Geoscience and Remote Sensing Symposium (IGARSS). https://doi.org/10.1109/IGARSS.2018.8518384

Niemann, K.O., Quinn, G., Stephen, R., Visintini, F., Parton, D., 2015. Hyperspectral Remote Sensing of Mountain Pine Beetle with an Emphasis on Previsual Assessment. Can. J. Remote Sens. 41, 191–202. https://doi.org/10.1080/07038992.2015.1065707

Nitze, I., Grosse, G., Jones, B.M., Arp, C.D., Ulrich, M., Fedorov, A., Veremeeva, A., 2017. Landsat-based trend analysis of lake dynamics across Northern Permafrost Regions. Remote Sens. 9, 640.

https://doi.org/10.3390/rs9070640

Nocita, M., Stevens, A., van Wesemael, B., Aitkenhead, M., Bachmann, M., Barthès, B., Dor, E. Ben, Brown, D.J., Clairotte, M., Csorba, A., Dardenne, P., Demattê, J.A.M., Genot, V., Guerrero, C., Knadel, M., Montanarella, L., Noon, C., Ramirez-Lopez, L., Robertson, J., Sakai, H., Soriano-Disla, J.M., Shepherd, K.D., Stenberg, B., Towett, E.K., Vargas, R., Wetterlind, J., 2015. Soil Spectroscopy: An Alternative to Wet Chemistry for Soil Monitoring. Adv. Agron. 132, 139–159. https://doi.org/10.1016/bs.agron.2015.02.002

Nolin, A.W., Dozier, J., Mertes, L.A.K., 1993. Mapping alpine snow using a spectral mixture modeling technique. Ann. Glaciol. 17, 121–124.

Nuernberg, D., Wollenburg, I., Dethleff, D., Eicken, H., Kassens, H., Letzig, T., Reimnitz, E., Thiede, J., 1994. Sediments in Arctic sea ice: Implications for entrainment, transport and release. Mar. Geol. 119, 185–214. https://doi.org/10.1016/0025-3227(94)90181-3

Numata, I., Cochrane, M.A., Jr, C.M.S., Sales, M.H., 2011. Carbon emissions from deforestation and forest fragmentation in the Brazilian Amazon. Environ. Res. Lett. 6, 44003. https://doi.org/10.1088/1748-9326/6/4/044003

Nurda, N., Noguchi, R., Ahamed, T., 2020. Forest productivity and carbon stock analysis from vegetation phenological indices using satellite remote sensing in Indonesia. Asia-Pacific J. Reg. Sci. 4, 657–690. https://doi.org/10.1007/S41685-020-00163-7/TABLES/3

Oelker, J., Losa, S.N., Richter, A., Bracher, A., 2022. TROPOMI-Retrieved Underwater Light Attenuation in Three Spectral Regions in the Ultraviolet and Blue. Front. Mar. Sci. 9, 296. https://doi.org/10.3389/fmars.2022.787992

Ogata, Y., Takada, H., Mizukawa, K., Hirai, H., Iwasa, S., Endo, S., Mato, Y., Saha, M., Okuda, K., Nakashima, A., Murakami, M., Zurcher, N., Booyatumanondo, R., Zakaria, M.P., Dung, L.Q., Gordon, M., Miguez, C., Suzuki S.and Moore, C., Karapanagioti, H.K., Weerts, S., McClurg, T., Burres, E., Smith, W., Van Velkenburg, M., Lang, J.S., Lang, R.C., Laursen, D., Danner, B., Stewardson, N., Thompson, R.C., 2009. International Pellet Watch: Global monitoring of persistent organicpollutants (POPs) in coastal Waters. 1. Initial phase data on PCBs,DDTs, and HCHs. Mar. Pollut. Bull. 58, 1437–1446.

Okoronkwo, N., Odemelam, S., Ano, O., 2009. Levels of toxic elements in soils of abandoned waste dump site. African J. Biotechnol. 5, 1241–1244. https://doi.org/10.4314/ajb.v5i13.43089

Okujeni, A., Canters, F., Cooper, S.D., Degerickx, J., Heiden, U., Hostert, P., Priem, F., Roberts, D.A., Somers, B., van der Linden, S., 2018. Generalizing machine learning regression models using multi-site spectral libraries for mapping vegetation-impervious-soil fractions across multiple cities. Remote Sens. Environ. 216, 482–496. https://doi.org/10.1016/J.RSE.2018.07.011

Okujeni, A., Jänicke, C., Cooper, S., Frantz, D., Hostert, P., Clark, M., Segl, K., van der Linden, S., 2021. Multi-season unmixing of vegetation class fractions across diverse Californian ecoregions using simulated spaceborne imaging spectroscopy data. Remote Sens. Environ. 264, 112558. https://doi.org/10.1016/J.RSE.2021.112558

Okujeni, A., van der Linden, S., Hostert, P., 2015a. Extending the vegetation-impervious-soil model using simulated EnMAP data and machine learning. Remote Sens. Environ. 158, 69–80. https://doi.org/10.1016/j.rse.2014.11.009

Okujeni, A., van der Linden, S., Hostert, P., 2015b. On the use of extended vegetation impervious-soil maps from simulated EnMAP data for characterizing urban functional areas, in: ESA-ESRIN Conference on Mapping Urban Areas from Space (MUAS). Frascati, Rome,Italy.

Okujeni, A., van der Linden, S., Tits, L., Somers, B., Hostert, P., 2013. Support vector regression and synthetically mixed training data for quantifying urban land cover 137, 184–197. https://doi.org/10.1016/j.rse.2013.06.007

Oldeland, J., Dorigo, W., Wesuls, D., Jürgens, N., 2010. Mapping bush encroaching species by seasonal differences in hyperspectral imagery. Remote Sens. 2, 1416–1438. https://doi.org/10.3390/rs2061416

Ollinger, S. V, Smith, M.L., 2005. Net primary production and canopy nitrogen in a temperate forest

landscape: An analysis using imaging spectroscopy, modeling and field data. Ecosystems 8, 760–778. https://doi.org/10.1007/s10021-005-0079-5

Ong, C., Cudahy, T.J., Caccetta, M.S., Piggott, M.S., 2003a. Deriving quantitative dust measurements related to iron ore handling from airborne hyperspectral data. Inst. Min. Metall. Trans. Sect. A Min. Technol. 112, 158–163. https://doi.org/10.1179/037178403225003555

Ong, C., Cudahy, T.J., Swayze, G., 2003b. Predicting Acid Drainage Related Physicochemical Measurements Using Hyperspectral Data, in: 3rd EARSeL Workshop on Imaging Spectroscopy. pp. 363–373.

Oppelt, N., Mauser, W., 2007. Airborne visible / infrared imaging spectrometer AVIS: Design, characterization and calibration. Sensors 7, 1934–1953. https://doi.org/10.3390/s7091934

Oppelt, N., Mauser, W., 2003. Hyperspectral remote sensing - a tool for the derivation of plant nitrogen and its spatial variability within maize and wheat canopies, in: Stafford, J., Werner, A. (Eds.), 4th EuropeanConference on Precision Agriculture. Wageningen Academic Publishers, pp. 493–498.

Orgiazzi, A., Ballabio, C., Panagos, P., Jones, A., Fernández-Ugalde, O., 2018. LUCAS Soil, the largest expandable soil dataset for Europe: a review. Eur. J. Soil Sci. 69, 140–153. https://doi.org/10.1111/ejss.12499

Pacheco-Labrador, J., El-Madany, T., Martin, M.P., Gonzalez-Cascon, R., Carrara, A., Moreno, G., Perez-Priego, O., Hammer, T., Moossen, H., Henkel, K., Kolle, O., Martini, D., Burchard, V., van der Tol, C., Segl, K., Reichstein, M., Migliavacca, M., 2020. Combining hyperspectral remote sensing and eddy covariance data streams for estimation of vegetation functional traits. Biogeosciences Discuss. 1–38. https://doi.org/10.5194/bg-2019-501

Painter, T.H., Dozier, J., Roberts, D.A., Davis, R.E., Green, R.O., 2003. Retrieval of subpixel snow-covered area and grain size from imaging spectrometer data. Remote Sens. Environ. 85, 64–77. https://doi.org/10.1016/S0034-4257(02)00187-6

Painter, T.H., Duval, B., Thomas, W.H., Mendez, M., Heintzelman, S., Dozier, J., 2001. Detection and Quantification of Snow Algae with an Airborne Imaging Spectrometer. Appl. Environ. Microbiol. 67, 5267–5272. https://doi.org/10.1128/aem.67.11.5267-5272.2001

Pearlman, J.S., Barry, P.S., Segal, C.C., Shepanski, J., Beiso, D., Carman, S.L., 2003. Hyperion, a space-based imaging spectrometer. IEEE Trans. Geosci. Remote Sens. 41, 1160–1173. https://doi.org/10.1109/TGRS.2003.815018

Peng, C., Ma, Z., Lei, X., Zhu, Q., Chen, H., Wang, W., Liu, S., Li, W., Fang, X., Zhou, X., 2011. A drought-induced pervasive increase in tree mortality across Canada's boreal forests. Nat. Clim. Chang. 1, 467–471. https://doi.org/10.1038/nclimate1293

Pepe, M., Pompilio, L., Gioli, B., Busetto, L., Boschetti, M., 2020. Detection and classification of non-photosynthetic vegetation from prisma hyperspectral data in croplands. Remote Sens. 12, 1–12. https://doi.org/10.3390/rs12233903

Pereira, H.M., Ferrier, S., Walters, M., Geller, G.N., Jongman, R.H.G., Scholes, R.J., Bruford, M.W., Brummitt, N., Butchart, S.H.M., Cardoso, A.C., Coops, N.C., Dulloo, E., Faith, D.P., Freyhof, J., Gregory, R.D., Heip, C., Höft, R., Hurtt, G., Jetz, W., Karp, D.S., McGeoch, M.A., Obura, D., Onoda, Y., Pettorelli, N., Reyers, B., Sayre, R., Scharlemann, J.P.W., Stuart, S.N., Turak, E., Walpole, M., Wegmann, M., 2013. Essential biodiversity variables. Science (80-.). 339, 277–278. https://doi.org/10.1126/science.1229931

Perovich, D.K., Light, B., Eicken, H., Jones, K.F., Runciman, K., Nghiem, S. V., 2007. Increasing solar heating of the Arctic Ocean and adjacent seas, 1979-2005: Attribution and role in the ice-albedo feedback. Geophys. Res. Lett. 34. https://doi.org/10.1029/2007GL031480

Petrou, Z.I., Manakos, I., Stathaki, T., 2015. Remote sensing for biodiversity monitoring: a review of methods for biodiversity indicator extraction and assessment of progress towards international targets. Biodivers. Conserv. 24, 2333–2363. https://doi.org/10.1007/s10531-015-0947-z

Peyghambari, S., Zhang, Y., 2021. Hyperspectral remote sensing in lithological mapping, mineral exploration, and environmental geology: an updated review. J. Appl. Remote Sens. 15, 031501. https://doi.org/10.1117/1.jrs.15.031501

Pfitzner, K.S., Harford, A.J., Whiteside, T.G., Bartolo, R.E., 2018. Mapping magnesium sulfate salts from saline mine discharge with airborne hyperspectral data. Sci. Total Environ. 640–641, 1259–1271. https://doi.org/10.1016/J.SCITOTENV.2018.05.396

Philipp, M., Dietz, A., Buchelt, S., Kuenzer, C., 2021. Trends in satellite earth observation for permafrost related analyses-a review. Remote Sens. 13, 1217. https://doi.org/10.3390/rs13061217

Phinn, S.R., Dekker, A.G., Brando, V.E., Roelfsema, C.M., 2005. Mapping water quality and substrate cover in optically complex coastal and reef waters: An integrated approach. Mar. Pollut. Bull. 51, 459–469. https://doi.org/10.1016/j.marpolbul.2004.10.031

Pickup, G., 1989. New land degradation survey techniques for arid Australia. - Problems and prospects. Rangel. J. 11, 74. https://doi.org/10.1071/rj9890074

Pidgeon, E., 2009. Carbon Sequestration by Coastal Marine Habitats: Important Missing Sinks, in: The Management of Natural Coastal Carbon Sinks. pp. 47–51.

Pleskachevsky, A., Lehner, S., Heege, T., Mott, C., 2011. Synergy and fusion of optical and synthetic aperture radar satellite data for underwater topography estimation in coastal areas. Ocean Dyn. 61, 2099–2120. https://doi.org/10.1007/s10236-011-0460-1

Portela, N.A., Silva, S.R.C., de Jesus, L.F.R., Dalmaschio, G.P., Sad, C.M.S., Castro, E.V.R., Morigaki, M.K., Silva Filho, E.A., Filgueiras, P.R., 2018. Spectroscopic evaluation of commercial H2S scavengers. Fuel 216, 681–685. https://doi.org/10.1016/j.fuel.2017.12.021

Post, E., Forchhammer, M.C., Bret-Harte, M.S., Callaghan, T. V., Christensen, T.R., Elberling, B., Fox, A.D., Gilg, O., Hik, D.S., Høye, T.T., Ims, R.A., Jeppesen, E., Klein, D.R., Madsen, J., McGuire, A.D., Rysgaard, S., Schindler, D.E., Stirling, I., Tamstorf, M.P., Tyler, N.J.C., Van Der Wal, R., Welker, J., Wookey, P.A., Schmidt, N.M., Aastrup, P., 2009. Ecological dynamics across the arctic associated with recent climate change. Science (80-.). 325, 1355–1358. https://doi.org/10.1126/science.1173113

Prevéy, J., Vellend, M., Rüger, N., Hollister, R.D., Bjorkman, A.D., Myers-Smith, I.H., Elmendorf, S.C., Clark, K., Cooper, E.J., Elberling, B., Fosaa, A.M., Henry, G.H.R., Høye, T.T., Jónsdóttir, I.S., Klanderud, K., Lévesque, E., Mauritz, M., Molau, U., Natali, S.M., Oberbauer, S.F., Panchen, Z.A., Post, E., Rumpf, S.B., Schmidt, N.M., Schuur, E.A.G., Semenchuk, P.R., Troxler, T., Welker, J.M., Rixen, C., 2017. Greater temperature sensitivity of plant phenology at colder sites: implications for convergence across northern latitudes. Glob. Chang. Biol. 23, 2660–2671. https://doi.org/10.1111/gcb.13619

Priem, F., Canters, F., 2016. Synergistic use of LiDAR and APEX hyperspectral data for high-resolution urban land cover mapping. Remote Sens. 8, 787. https://doi.org/10.3390/rs8100787

Priem, F., Somers, B., Canters, F., 2021. Iterative Spectral Distancing: a Novel Approach for Extracting Endmembers in Complex Urban Image Scenes, in: International Geoscience and Remote Sensing Symposium (IGARSS). IEEE, pp. 4035–4038. https://doi.org/10.1109/IGARSS47720.2021.9555079

Purdy, R., 2018. The eye in the sky that can spot illegal rubbish dumps from space. Independent.

R.E., C., J., S., 1996. A Coordinator's Guide to Volunteer Lake Monitoring Methods. North Am. Lake Manag. Soc. 96.

Radiarta, I.N., Saitoh, S.I., Yasui, H., 2011. Aquaculture site selection for Japanese kelp (Laminaria japonica) in southern Hokkaido, Japan, using satellite remote sensing and GIS-based models. ICES J. Mar. Sci. 68, 773–780. https://doi.org/10.1093/icesjms/fsq163

Ramirez-Lopez, L., Behrens, T., Schmidt, K., Stevens, A., Demattê, J.A.M., Scholten, T., 2013. The spectrum-based learner: A new local approach for modeling soil vis-NIR spectra of complex datasets. Geoderma 195–196, 268–279. https://doi.org/10.1016/j.geoderma.2012.12.014

Rasaiah, B., Jones, S., Bellman, C., Malthus, T., 2011. Building Better Hyperspectral Datasets: The Fundamental Role of Metadata Protocols in Hyperspectral Field Campaigns. Proc. Surv. Spat. Sci. Bienn. Conf. 2011 21-25 Novemb. 2011, Wellington, New Zeal. 35–48.

Rascher, U., Agati, G., Alonso, L., Cecchi, G., Champagne, S., Colombo, R., Damm, A., Daumard, F., de Miguel, E., Fernandez, G., Franch, B., Franke, J., Gerbig, C., Gioli, B., Gómez, J.A., Goulas,

Y., Guanter, L., Gutiérrez-de-la-Cámara, Ó., Hamdi, K., Hostert, P., Jiménez, M., Kosvancova, M., Lognoli, D., Meroni, M., Miglietta, F., Moersch, A., Moreno, J., Moya, I., Neininger, B., Okujeni, A., Ounis, A., Palombi, L., Raimondi, V., Schickling, A., Sobrino, J.A., Stellmes, M., Toci, G., Toscano, P., Udelhoven, T., van der Linden, S., Zaldei, A., 2009. CEFLES2: the remote sensing component to quantify photosynthetic efficiency from the leaf to the region by measuring sun-induced fluorescence in the oxygen absorption bands. Biogeosciences 6, 1181–1198. https://doi.org/10.5194/bg-6-1181-2009

Rascher, U., Alonso, L., Burkart, A., Cilia, C., Cogliati, S., Colombo, R., Damm, A., Drusch, M., Guanter, L., Hanus, J., Hyvärinen, T., Julitta, T., Jussila, J., Kataja, K., Kokkalis, P., Kraft, S., Kraska, T., Matveeva, M., Moreno, J., Muller, O., Panigada, C., Pikl, M., Pinto, F., Prey, L., Pude, R., Rossini, M., Schickling, A., Schurr, U., Schüttemeyer, D., Verrelst, J., Zemek, F., 2015. Sun-induced fluorescence - a new probe of photosynthesis: First maps from the imaging spectrometer HyPlant. Glob. Chang. Biol. 21, 4673–4684. https://doi.org/10.1111/gcb.13017

Raynolds, M.K., Walker, D., Epstein, H.E., Pinzon, J.E., Tucker, C.J., 2012. A new estimate of tundra-biome phytomass from trans-Arctic field data and AVHRR NDVI. Remote Sens. Lett. 3, 403–411. https://doi.org/10.1080/01431161.2011.609188

Rickard, L.J., Basedow, R.W., Zalewski, E.F., Silverglate, P.R., Landers, M., 1993. HYDICE: an airborne system for hyperspectral imaging, in: Vane, G. (Ed.), SPIE Proceedings. SPIE, pp. 173–179. https://doi.org/10.1117/12.157055

Ridd, M.K., 1995. Exploring a V-I-S (vegetation-impervious surface-soil) model for urban ecosystem analysis through remote sensing: comparative anatomy for cities. Int. J. Remote Sens. 16, 2165–2185. https://doi.org/10.1080/01431169508954549

Rivard, B., Rogge, D.M., Feng, J., Zhang, J., 2009. Spatial constraints on endmember extraction and optimization of per-pixel endmember sets for spectral unmixing, in: WHISPERS '09 - 1st Workshop on Hyperspectral Image and Signal Processing: Evolution in Remote Sensing. IEEE, pp. 1–4. https://doi.org/10.1109/WHISPERS.2009.5289088

Rizaludin Mahmud, M., Numata, S., Hosaka, T., 2020. Mapping an invasive goldenrod of Solidago altissima in urban landscape of Japan using multi-scale remote sensing and knowledge-based classification. Ecol. Indic. 111, 105975. https://doi.org/10.1016/J.ECOLIND.2019.105975

Roberts, D.A., Quattrochi, D.A., Hulley, G.C., Hook, S.J., Green, R.O., 2012. Synergies between VSWIR and TIR data for the urban environment: An evaluation of the potential for the Hyperspectral Infrared Imager (HyspIRI) Decadal Survey mission. Remote Sens. Environ. 117, 83–101. https://doi.org/10.1016/j.rse.2011.07.021

Rocha, A.D., Groen, T.A., Skidmore, A.K., 2019. Spatially-explicit modelling with support of hyperspectral data can improve prediction of plant traits. Remote Sens. Environ. 231, 111200. https://doi.org/10.1016/J.RSE.2019.05.019

Rockwell, B.W., Hofstra, A.H., 2008. Identification of quartz and carbonate minerals across northern Nevada using aster thermal infrared emissivity data-implications for geologic mapping and mineral resource investigations in well-studied and frontier areas. Geosphere 4, 218–246. https://doi.org/10.1130/GES00126.1

Roessner, S., Segl, K., Heiden, U., Kaufmann, H., 2001. Automated differentiation of urban surfaces based on airborne hyperspectral imagery. IEEE Trans. Geosci. Remote Sens. 39, 1525–1532. https://doi.org/10.1109/36.934082

Rogers, A., Medlyn, B.E., Dukes, J.S., Bonan, G., von Caemmerer, S., Dietze, M.C., Kattge, J., Leakey, A.D.B., Mercado, L.M., Niinemets, Ü., Prentice, I.C., Serbin, S.P., Sitch, S., Way, D.A., Zaehle, S., 2017. A roadmap for improving the representation of photosynthesis in Earth system models. New Phytol. 213, 22–42. https://doi.org/10.1111/NPH.14283

Rogge, D., Bauer, A., Zeidler, J., Mueller, A., Esch, T., Heiden, U., 2018. Building an exposed soil composite processor (SCMaP) for mapping spatial and temporal characteristics of soils with Landsat imagery (1984–2014). Remote Sens. Environ. 205, 1–17. https://doi.org/10.1016/J.RSE.2017.11.004

Rogge, D., Rivard, B., Segl, K., Grant, B., Feng, J., 2014. Mapping of NiCu-PGE ore hosting ultramafic

rocks using airborne and simulated EnMAP hyperspectral imagery, Nunavik, Canada. Remote Sens. Environ. 152, 302–317. https://doi.org/10.1016/j.rse.2014.06.024

Rosenthal, W., Dozier, J., 1996. Automated Mapping of Montane Snow Cover at Subpixel Resolution from the Landsat Thematic Mapper. Water Resour. Res. 32, 115–130. https://doi.org/10.1029/95wr02718

Rowan, L.C., Mars, J.C., 2003. Lithologic mapping in the Mountain Pass, California area using Advanced Spaceborne Thermal Emission and Reflection Radiometer (ASTER) data. Remote Sens. Environ. 84, 350–366. https://doi.org/10.1016/S0034-4257(02)00127-X

Rowan, L.C., Simpson, C.J., Mars, J.C., 2004. Hyperspectral analysis of the ultramafic complex and adjacent lithologies at Mordor, NT, Australia. Remote Sens. Environ. 91, 419–431. https://doi.org/10.1016/j.rse.2004.04.007

Roy, R., Launeau, P., Carrère, V., Pinet, P., Ceuleneer, G., Clénet, H., Daydou, Y., Girardeau, J., Amri, I., 2009. Geological mapping strategy using visible near-infrared-shortwave infrared hyperspectral remote sensing: Application to the Oman ophiolite (Sumail Massif). Geochemistry, Geophys. Geosystems 10, n/a-n/a. https://doi.org/10.1029/2008GC002154

Rudy, A.C.A., Lamoureux, S.F., Treitz, P., Collingwood, A., 2013. Identifying permafrost slope disturbance using multi-temporal optical satellite images and change detection techniques. Cold Reg. Sci. Technol. 88, 37–49. https://doi.org/10.1016/j.coldregions.2012.12.008

Salles, R. dos R., de Souza Filho, C.R., Cudahy, T., Vicente, L.E., Monteiro, L.V.S., 2017. Hyperspectral remote sensing applied to uranium exploration: A case study at the Mary Kathleen metamorphic-hydrothermal U-REE deposit, NW, Queensland, Australia. J. Geochemical Explor. 179, 36–50. https://doi.org/10.1016/J.GEXPLO.2016.07.002

Sanchez-Rodriguez, R., Seto, K., Simon, D., Solecki, W., Kraas, F., Laumann, G., 2005. Science plan: urbanization and global environmental change, Science Plan - urbanization and global environmental change, IHDP Report 15. Bonn.

Scaioni, M., Longoni, L., Melillo, V., Papini, M., 2014. Correction to Remote sensing for landslide investigations: An overview of recent achievements and perspectives. [Remote Sens. 6, (2014), 9600-9652]. Remote Sens. 6, 12666. https://doi.org/10.3390/rs61212666

Schaefer, L.N., Kereszturi, G., Villeneuve, M., Kennedy, B., 2021. Determining physical and mechanical volcanic rock properties via reflectance spectroscopy. J. Volcanol. Geotherm. Res. 420, 107393. https://doi.org/10.1016/J.JVOLGEORES.2021.107393

Schaepman, M.E., 2007. Spectrodirectional remote sensing: From pixels to processes. Int. J. Appl. Earth Obs. Geoinf. 9, 204–223. https://doi.org/10.1016/j.jag.2006.09.003

Schaepman, M.E., Itten, K.I., Schlaepfer, D.R., Kaiser, J.W., Brazile, J., Debruyn, W., Neukom, A., Feusi, H., Adolph, P., Moser, R., Schilliger, T., Vos, L. De, Brandt, G.M., Kohler, P., Meng, M., Piesbergen, J., Strobl, P., Gavira, J., Ulbrich, G.J., Meynart, R., 2004. APEX: current status of the airborne dispersive pushbroom imaging spectrometer, in: Meynart, R., Neeck, S.P., Shimoda, H., Lurie, J.B., Aten, M.L. (Eds.), SPIE Proceedings. SPIE. https://doi.org/10.1117/12.513745

Schaepman, M.E., Jehle, M., Hueni, A., D'Odorico, P., Damma, A., Weyermann, J., Schneider, F.D., Laurent, V., Popp, C., Seidel, F.C., Lenhard, K., Gege, P., Küchler, C., Brazile, J., Kohler, P., De Vos, L., Meuleman, K., Meynart, R., Schläpfer, D., Kneubühler, M., Itten, K.I., 2015. Advanced radiometry measurements and Earth science applicationswith the Airborne Prism Experiment (APEX). Remote Sens. Environ. 158, 207–219. https://doi.org/10.1016/j.rse.2014.11.014

Schaepman, M.E., Ustin, S.L., Plaza, A.J., Painter, T.H., Verrelst, J., Liang, S., 2009. Earth system science related imaging spectroscopy—An assessment. Remote Sens. Environ. 113, S123–S137. https://doi.org/10.1016/j.rse.2009.03.001

Schäfer, E., Heiskanen, J., Heikinheimo, V., Pellikka, P., 2016. Mapping tree species diversity of a tropical montane forest by unsupervised clustering of airborne imaging spectroscopy data. Ecol. Indic. 64, 49–58. https://doi.org/10.1016/J.ECOLIND.2015.12.026

Scheffler, D., Hollstein, A., Diedrich, H., Segl, K., Hostert, P., 2017. AROSICS: An automated and robust open-source image co-registration software for multi-sensor satellite data. Remote Sens. 9.

https://doi.org/10.3390/rs9070676

Schiefer, F., Schmidtlein, S., Kattenborn, T., 2021. The retrieval of plant functional traits from canopy spectra through RTM-inversions and statistical models are both critically affected by plant phenology. Ecol. Indic. 121, 107062. https://doi.org/10.1016/J.ECOLIND.2020.107062

Schiller, H., Doerffer, R., 1999. Neural network for emulation of an inverse model operational derivation of Case II water properties from MERIS data. Int. J. Remote Sens. 20, 1735–1746. https://doi.org/10.1080/014311699212443

Schlerf, M., Atzberger, C., 2006. Inversion of a forest reflectance model to estimate structural canopy variables from hyperspectral remote sensing data. Remote Sens. Environ. 100, 281–294. https://doi.org/10.1016/j.rse.2005.10.006

Schlerf, M., Atzberger, C., Hill, J., 2005. Remote sensing of forest biophysical variables using HyMap imaging spectrometer data. Remote Sens. Environ. 95, 177–194. https://doi.org/10.1016/j.rse.2004.12.016

Schlerf, M., Atzberger, C., Hill, J., Buddenbaum, H., Werner, W., Schüler, G., 2010. Retrieval of chlorophyll and nitrogen in Norway spruce (Picea abies L. Karst.) using imaging spectroscopy. Int. J. Appl. Earth Obs. Geoinf. 12, 17–26. https://doi.org/10.1016/j.jag.2009.08.006

Schmid, T., Rodriguez-Rastrero, M., Escribano, P., Palacios-Orueta, A., Ben-Dor, E., Plaza, A., Milewski, R., Huesca, M., Bracken, A., Cicuendez, V., Pelayo, M., Chabrillat, S., 2016. Characterization of Soil Erosion Indicators Using Hyperspectral Data from a Mediterranean Rainfed Cultivated Region. IEEE J. Sel. Top. Appl. Earth Obs. Remote Sens. 9, 845–860. https://doi.org/10.1109/JSTARS.2015.2462125

Schmidtlein, S., Sassin, J., 2004. Mapping of continuous floristic gradients in grasslands using hyperspectral imagery. Remote Sens. Environ. 92, 126–138. https://doi.org/10.1016/j.rse.2004.05.004

Schuldt, B., Buras, A., Arend, M., Vitasse, Y., Beierkuhnlein, C., Damm, A., Gharun, M., Grams, T.E.E., Hauck, M., Hajek, P., Hartmann, H., Hiltbrunner, E., Hoch, G., Holloway-Phillips, M., Körner, C., Larysch, E., Lübbe, T., Nelson, D.B., Rammig, A., Rigling, A., Rose, L., Ruehr, N.K., Schumann, K., Weiser, F., Werner, C., Wohlgemuth, T., Zang, C.S., Kahmen, A., 2020. A first assessment of the impact of the extreme 2018 summer drought on Central European forests. Basic Appl. Ecol. 45, 86–103. https://doi.org/10.1016/j.baae.2020.04.003

Schweiger, A.K., Cavender-Bares, J., Townsend, P.A., Hobbie, S.E., Madritch, M.D., Wang, R., Tilman, D., Gamon, J.A., 2018. Plant spectral diversity integrates functional and phylogenetic components of biodiversity and predicts ecosystem function. Nat. Ecol. Evol. 2018 26 2, 976–982. https://doi.org/10.1038/s41559-018-0551-1

Seeley, M., Asner, G.P., 2021. Imaging spectroscopy for conservation applications. Remote Sens. 13, 1–17. https://doi.org/10.3390/rs13020292

Segl, K., Guanter, L., Rogass, C., Kuester, T., Roessner, S., Kaufmann, H., Sang, B., Mogulsky, V., Hofer, S., 2012. EeteSThe EnMAP end-to-end simulation tool. IEEE J. Sel. Top. Appl. Earth Obs. Remote Sens. 5, 522–530. https://doi.org/10.1109/JSTARS.2012.2188994

Shaver, G.R., Rastetter, E.B., Salmon, V., Street, L.E., van de Weg, M.J., Rocha, A., van Wijk, M.T., Williams, M., 2013. Pan-Arctic modelling of net ecosystem exchange of CO2. Philos. Trans. R. Soc. B Biol. Sci. 368, 20120485. https://doi.org/10.1098/rstb.2012.0485

Simelton, E., Fraser, E.D.G., Termansen, M., Benton, T.G., Gosling, S.N., South, A., Arnell, N.W., Challinor, A.J., Dougill, A.J., Forster, P.M., 2012. The socioeconomics of food crop production and climate change vulnerability: a global scale quantitative analysis of how grain crops are sensitive to drought. Food Secur. 4, 163–179. https://doi.org/10.1007/s12571-012-0173-4

Skidmore, A.K., Coops, N.C., Neinavaz, E., Ali, A., Schaepman, M.E., Paganini, M., Kissling, W.D., Vihervaara, P., Darvishzadeh, R., Feilhauer, H., Fernandez, M., Fernández, N., Gorelick, N., Geijzendorffer, I., Heiden, U., Heurich, M., Hobern, D., Holzwarth, S., Muller-Karger, F.E., Van De Kerchove, R., Lausch, A., Leitão, P.J., Lock, M.C., Mücher, C.A., O'Connor, B., Rocchini, D., Roeoesli, C., Turner, W., Vis, J.K., Wang, T., Wegmann, M., Wingate, V., 2021. Priority list

of biodiversity metrics to observe from space. Nat. Ecol. Evol. 5, 896–906. https://doi.org/10.1038/s41559-021-01451-x

Skidmore, A.K., Pettorelli, N., Coops, N.C., Geller, G.N., Hansen, M., Lucas, R., Mücher, C.A., O'Connor, B., Paganini, M., Pereira, H.M., Schaepman, M.E., Turner, W., Wang, T., Wegmann, M., 2015. Environmental science: Agree on biodiversity metrics to track from space. Nature 523, 403–405. https://doi.org/10.1038/523403a

Skiles, S.M., Flanner, M., Cook, J.M., Dumont, M., Painter, T.H., 2018. Radiative forcing by light-absorbing particles in snow. Nat. Clim. Chang. 8, 964–971. https://doi.org/10.1038/s41558-018-0296-5

Skowronek, S., Asner, G.P., Feilhauer, H., 2017. Performance of one-class classifiers for invasive species mapping using airborne imaging spectroscopy. Ecol. Inform. 37, 66–76. https://doi.org/10.1016/J.ECOINF.2016.11.005

Small, C., 2003. High spatial resolution spectral mixture analysis of urban reflectance. Remote Sens. Environ. 88, 170–186. https://doi.org/10.1016/j.rse.2003.04.008

Small, C., 2001. Spectral Dimensionality and Scale of Urban Radiance, in: AVIRIS Workshop Proceedings.

Smith, M.L., Ollinger, S. V., Martin, M.E., Aber, J.D., Hallett, R.A., Goodale, C.L., 2002. Direct estimation of aboveground forest productivity through hyperspectral remote sensing of canopy nitrogen. Ecol. Appl. 12, 1286–1302. https://doi.org/10.1890/1051-0761(2002)012[1286:DEOAFP]2.0.CO;2

Somers, B., Asner, G.P., 2013. Multi-temporal hyperspectral mixture analysis and feature selection for invasive species mapping in rainforests 136.

Stefano, P., Angelo, P., Simone, P., Filomena, R., Federico, S., Tiziana, S., Umberto, A., Vincenzo, C., Acito, N., Marco, D., Stefania, M., Giovanni, C., Raffaele, C., Roberto, D.B., Giovanni, L., Cristina, A., 2013. The PRISMA hyperspectral mission: Science activities and opportunities for agriculture and land monitoring, in: International Geoscience and Remote Sensing Symposium (IGARSS). pp. 4558–4561. https://doi.org/10.1109/IGARSS.2013.6723850

Steinberg, A., Chabrillat, S., Stevens, A., Segl, K., Foerster, S., 2016. Prediction of common surface soil properties based on Vis-NIR airborne and simulated EnMAP imaging spectroscopy data: Prediction accuracy and influence of spatial resolution. Remote Sens. 8, 613. https://doi.org/10.3390/rs8070613

Stevens, A., Nocita, M., Tóth, G., Montanarella, L., van Wesemael, B., 2013. Prediction of Soil Organic Carbon at the European Scale by Visible and Near InfraRed Reflectance Spectroscopy. PLoS One 8, e66409. https://doi.org/10.1371/journal.pone.0066409

Stewart, I.D., Oke, T.R., 2012. Local climate zones for urban temperature studies. Bull. Am. Meteorol. Soc. 93, 1879–1900. https://doi.org/10.1175/BAMS-D-11-00019.1

Stibal, M., Box, J.E., Cameron, K.A., Langen, P.L., Yallop, M.L., Mottram, R.H., Khan, A.L., Molotch, N.P., Chrismas, N.A.M., Calì Quaglia, F., Remias, D., Smeets, C.J.P.P., van den Broeke, M.R., Ryan, J.C., Hubbard, A., Tranter, M., van As, D., Ahlstrøm, A.P., 2017. Algae Drive Enhanced Darkening of Bare Ice on the Greenland Ice Sheet. Geophys. Res. Lett. 44, 11,463-11,471. https://doi.org/10.1002/2017GL075958

Stow, D.A., Hope, A., McGuire, D., Verbyla, D., Gamon, J., Huemmrich, F., Houston, S., Racine, C., Sturm, M., Tape, K., Hinzman, L., Yoshikawa, K., Tweedie, C., Noyle, B., Silapaswan, C., Douglas, D., Griffith, B., Jia, G.J., Epstein, H., Walker, D., Daeschner, S., Petersen, A., Zhou, L., Myneni, R., 2004. Remote sensing of vegetation and land-cover change in Arctic Tundra Ecosystems. Remote Sens. Environ. 89, 281–308. https://doi.org/10.1016/j.rse.2003.10.018

Suess, S., van der Linden, S., Okujeni, A., Leitão, P.J., Schwieder, M., Hostert, P., 2015. Using Class Probabilities to Map Gradual Transitions in Shrub Vegetation from Simulated {EnMAP} Data 7, 10668–10688. https://doi.org/10.3390/rs70810668

Swayze, G.A., Clark, R.N., Goetz, A.F.H., Livo, K.E., Breit, G.N., Kruse, F.A., Sutley, S.J., Snee, L.W., Lowers, H.A., Post, J.L., Stoffregen, R.E., Ashley, R.P., 2014. Mapping Advanced Argillic

Alteration at Cuprite, Nevada, Using Imaging Spectroscopy. Econ. Geol. 109, 1179–1221. https://doi.org/10.2113/econgeo.109.5.1179

Swayze, G.A., Kokaly, R.F., Higgins, C.T., Clinkenbeard, J.P., Clark, R.N., Lowers, H.A., Sutley, S.J., 2009. Mapping potentialy asbestos-bearing rocks using imaging spectroscopy. Geology 37, 763–766. https://doi.org/10.1130/G30114A.1

Swayze, G.A., Smith, K.S., Clark, R.N., Sutley, S.J., Pearson, R.M., Vance, J.S., Hageman, P.L., Briggs, P.H., Meier, A.L., Singleton, M.J., Roth, S., 2000. Using imaging spectroscopy to map acidic mine waste. Environ. Sci. Technol. 34, 47–54. https://doi.org/10.1021/es990046w

Takeuchi, N., 2002. Optical characteristics of cryoconite (surface dust) on glaciers: the relationship between light absorbency and the property of organic matter contained in the cryoconite. Ann. Glaciol. 34, 409–414. https://doi.org/10.3189/172756402781817743

Takeuchi, N., Dial, R., Kohshima, S., Segawa, T., Uetake, J., 2006. Spatial distribution and abundance of red snow algae on the Harding Icefield, Alaska derived from a satellite image. Geophys. Res. Lett. 33. https://doi.org/10.1029/2006GL027819

Taylor, G.R., 2004. Field and image spectrometry for soil mapping, in: 12th Australian RemoteSensing Conference. Fremantle, WA, Australia.

Tedesco, M., Doherty, S., Fettweis, X., Alexander, P., Jeyaratnam, J., Stroeve, J., 2016. The darkening of the Greenland ice sheet: Trends, drivers, and projections (1981-2100). Cryosphere 10, 477–496. https://doi.org/10.5194/TC-10-477-2016

Tenhunen, J., Valentini, R., Koestner, B., Zimmermann, R., Granier, A., 1998. Variation in forestgas exchange at landscape to continental scales. Ann. des Sci. For. 55, 1–11.

Thenkabail, P.S., Lyon, J.G., 2016. Hyperspectral remote sensing of vegetation. CRC press.

Thiemann, S., Kaufmann, H., 2002. Lake water quality monitoring using hyperspectral airborne data - A semiempirical multisensor and multitemporal approach for the Mecklenburg Lake District, Germany. Remote Sens. Environ. 81, 228–237. https://doi.org/10.1016/S0034-4257(01)00345-5

Thiemann, S., Kaufmann, H., 2000. Determination of chlorophyll content and trophic state of lakes using field spectrometer and IRS-1C satellite data in the Mecklenburg Lake District, Germany. Remote Sens. Environ. 73, 227–235. https://doi.org/10.1016/S0034-4257(00)00097-3

Thomas, M., Walter, M.R., 2002. Application of hyperspectral infrared analysis of hydrothermal alteration on Earth and Mars. Astrobiology 2, 335–351. https://doi.org/10.1089/153110702762027916

Thompson, D.R., Kahn, B.H., Green, R.O., Chien, S.A., Middleton, E.M., Tran, D.Q., 2018. Global spectroscopic survey of cloud thermodynamic phase at high spatial resolution, 2005-2015. Atmos. Meas. Tech. 11, 1019–1030. https://doi.org/10.5194/AMT-11-1019-2018

Thompson, D.R., Thorpe, A.K., Frankenberg, C., Green, R.O., Duren, R., Guanter, L., Hollstein, A., Middleton, E., Ong, L., Ungar, S., 2016. Space-based remote imaging spectroscopy of the Aliso Canyon CH4 superemitter. Geophys. Res. Lett. 43, 6571–6578. https://doi.org/10.1002/2016GL069079

Thompson, R.C., Olson, Y., Mitchell, R.P., Davis, A., Rowland, S.J., John, A.W.G., McGonigle, D., Russell, A.E., 2004. Lost at Sea: Where Is All the Plastic? Science (80-.). 304, 838. https://doi.org/10.1126/science.1094559

Thorpe, A.K., Frankenberg, C., Thompson, D.R., Duren, R.M., Aubrey, A.D., Bue, B.D., Green, R.O., Gerilowski, K., Krings, T., Borchardt, J., Kort, E.A., Sweeney, C., Conley, S., Roberts, D.A., Dennison, P.E., 2017. Airborne DOAS retrievals of methane, carbon dioxide, and water vapor concentrations at high spatial resolution: Application to AVIRIS-NG. Atmos. Meas. Tech. 10, 3833–3850. https://doi.org/10.5194/AMT-10-3833-2017

Torres, R., Snoeij, P., Geudtner, D., Bibby, D., Davidson, M., Attema, E., Potin, P., Rommen, B.Ö., Floury, N., Brown, M., Traver, I.N., Deghaye, P., Duesmann, B., Rosich, B., Miranda, N., Bruno, C., L'Abbate, M., Croci, R., Pietropaolo, A., Huchler, M., Rostan, F., 2012. GMES Sentinel-1 mission. Remote Sens. Environ. 120, 9–24. https://doi.org/10.1016/j.rse.2011.05.028

Tralli, D.M., Blom, R.G., Zlotnicki, V., Donnellan, A., Evans, D.L., 2005. Satellite remote sensing of

earthquake, volcano, flood, landslide and coastal inundation hazards. ISPRS J. Photogramm. Remote Sens. 59, 185–198. https://doi.org/10.1016/j.isprsjprs.2005.02.002

Tucker, C.J., Slayback, D.A., Pinzon, J.E., Los, S.O., Myneni, R.B., Taylor, M.G., 2001. Higher northern latitude normalized difference vegetation index and growing season trends from 1982 to 1999. Int. J. Biometeorol. 45, 184–190. https://doi.org/10.1007/s00484-001-0109-8

Tziolas, N., Tsakiridis, N., Ben-Dor, E., Theocharis, J., Zalidis, G., 2019. A memory-based learning approach utilizing combined spectral sources and geographical proximity for improved VIS-NIR-SWIR soil properties estimation. Geoderma 340, 11–24. https://doi.org/10.1016/j.geoderma.2018.12.044

Tziolas, N., Tsakiridis, N., Ogen, Y., Kalopesa, E., Ben-Dor, E., Theocharis, J., Zalidis, G., 2020. An integrated methodology using open soil spectral libraries and Earth Observation data for soil organic carbon estimations in support of soil-related SDGs. Remote Sens. Environ. 244, 111793. https://doi.org/10.1016/j.rse.2020.111793

Ubilava, D., 2012. El Niño, La Niña, and world coffee price dynamics. Agric. Econ. 43, 17–26. https://doi.org/10.1111/j.1574-0862.2011.00562.x

UN, 2022. World population prospects 2022: summary of Results. New York. https://doi.org/UN DESA/POP/2022/TR/NO. 3

UNCCD, 1994. United Nations convention to combat desertification.

UNEP, 2022. Emissions Gap Report 2022:The Closing Window — Climate crisis calls for rapid transformation of societies. Nairobi.

UNEP, 2012. Global Environment Outlook (GEO) 5: Environment for the Future We Want.

UNEP, 2009. Marine litter: A global challenge.

Ungar, S.G., Pearlman, J.S., Mendenhall, J.A., Reuter, D., 2003. Overview of the Earth Observing One (EO-1) mission. IEEE Trans. Geosci. Remote Sens. 41, 1149–1159. https://doi.org/10.1109/TGRS.2003.815999

Ustin, S.L., Gamon, J.A., 2010. Remote sensing of plant functional types. New Phytol. 186, 795–816. https://doi.org/10.1111/j.1469-8137.2010.03284.x

Ustin, S.L., Roberts, D.A., Gamon, J.A., Asner, G.P., Green, R.O., 2004. Using imaging spectroscopy to study ecosystem processes and properties. Bioscience 54, 523–534. https://doi.org/10.1641/0006-3568(2004)054[0523:UISTSE]2.0.CO;2

Vaglio Laurin, G., Puletti, N., Hawthorne, W., Liesenberg, V., Corona, P., Papale, D., Chen, Q., Valentini, R., 2016. Discrimination of tropical forest types, dominant species, and mapping of functional guilds by hyperspectral and simulated multispectral Sentinel-2 data. Remote Sens. Environ. 176, 163–176. https://doi.org/10.1016/j.rse.2016.01.017

Vahtmäe, E., 2011. Detecting patterns and changes in a complex benthic environment of the Baltic Sea. J. Appl. Remote Sens. 5, 053559. https://doi.org/10.1117/1.3653271

Vahtmäe, E., Kutser, T., Martin, G., Kotta, J., 2006. Feasibility of hyperspectral remote sensing for mapping benthic macroalgal cover in turbid coastal waters - A Baltic Sea case study. Remote Sens. Environ. 101, 342–351. https://doi.org/10.1016/j.rse.2006.01.009

Van Cleemput, E., Helsen, K., Feilhauer, H., Honnay, O., Somers, B., 2021. Spectrally defined plant functional types adequately capture multidimensional trait variation in herbaceous communities. Ecol. Indic. 120, 106970. https://doi.org/10.1016/j.ecolind.2020.106970

Van Cleemput, E., Roberts, D.A., Honnay, O., Somers, B., 2019. A novel procedure for measuring functional traits of herbaceous species through field spectroscopy. Methods Ecol. Evol. 10, 1332–1338. https://doi.org/10.1111/2041-210X.13237

Van der Linden, S., 2007. Classifying segmented hyperspectral data from a heterogeneous urban environment using support vector machines. J. Appl. Remote Sens. 1, 013543. https://doi.org/10.1117/1.2813466

van der Linden, S., Hostert, P., 2009. The influence of urban structures on impervious surface maps from airborne hyperspectral data. Remote Sens. Environ. 113, 2298–2305.

https://doi.org/10.1016/j.rse.2009.06.004

van der Linden, S., Okujeni, A., Canters, F., Degerickx, J., Heiden, U., Hostert, P., Priem, F., Somers, B., Thiel, F., 2019a. Imaging Spectroscopy of Urban Environments. Surv. Geophys. 40, 471–488. https://doi.org/10.1007/S10712-018-9486-Y/FIGURES/8

van der Linden, S., Okujeni, A., Canters, F., Degerickx, J., Heiden, U., Hostert, P., Priem, F., Somers, B., Thiel, F., 2019b. Imaging Spectroscopy of Urban Environments. Surv. Geophys. https://doi.org/10.1007/s10712-018-9486-y

van der Meer, F., 2004. Analysis of spectral absorption features in hyperspectral imagery. Int. J. Appl. Earth Obs. Geoinf. 5, 55–68. https://doi.org/10.1016/j.jag.2003.09.001

van der Meer, F.D., van der Werff, H.M.A., van Ruitenbeek, F.J.A., Hecker, C.A., Bakker, W.H., Noomen, M.F., van der Meijde, M., Carranza, E.J.M., de Smeth, J.B., Woldai, T., 2012. Multi- and hyperspectral geologic remote sensing: A review. Int. J. Appl. Earth Obs. Geoinf. 14, 112–128. https://doi.org/10.1016/j.jag.2011.08.002

Van Langevelde, F., Prins, H., 2007. Resilience and restoration of soft-bottom near-shore ecosystems. Hydrobiologia 591, 1–4. https://doi.org/10.1007/s10750-007-0779-2

Van Ruitenbeek, F.J.A., Cudahy, T.J., van der Meer, F.D., Hale, M., 2012. Characterization of the hydrothermal systems associated with Archean VMS-mineralization at Panorama, Western Australia, using hyperspectral, geochemical and geothermometric data. Ore Geol. Rev. 45, 33–46. https://doi.org/10.1016/j.oregeorev.2011.07.001

Van Wesemael, B., Chabrillat, S., Wilken, F., 2021. High-spectral resolution remote sensing of soil organic carbon dynamics. Remote Sens. 13, 1293. https://doi.org/10.3390/rs13071293

Vane, G., Goetz, A.F.H., Wellman, J.B., 1983. Airborne Imaging Spectrometer: a New Tool for Remote Sensing. IEEE Trans. Geosci. Remote Sens. GE-22, 546–549. https://doi.org/10.1109/tgrs.1984.6499168

Vane, G., Green, R.O., Chrien, T.G., Enmark, H.T., Hansen, E.G., Porter, W.M., 1993. The airborne visible/infrared imaging spectrometer (AVIRIS). Remote Sens. Environ. 44, 127–143. https://doi.org/10.1016/0034-4257(93)90012-M

Vapnik, V.N., 1998. Statistical learning theory. Wiley.

Veraverbeke, S., Dennison, P., Gitas, I., Hulley, G., Kalashnikova, O., Katagis, T., Kuai, L., Meng, R., Roberts, D., Stavros, N., 2018. Hyperspectral remote sensing of fire: State-of-the-art and future perspectives. Remote Sens. Environ. 216, 105–121. https://doi.org/10.1016/J.RSE.2018.06.020

Veraverbeke, S., Stavros, E.N., Hook, S.J., 2014. Assessing fire severity using imaging spectroscopy data from the Airborne Visible/Infrared Imaging Spectrometer (AVIRIS) and comparison with multispectral capabilities. Remote Sens. Environ. 154, 153–163. https://doi.org/10.1016/j.rse.2014.08.019

Verrelst, J., Camps-Valls, G., Muñoz-Marí, J., Rivera, J.P., Veroustraete, F., Clevers, J.G.P.W., Moreno, J., 2015. Optical remote sensing and the retrieval of terrestrial vegetation bio-geophysical properties - A review. ISPRS J. Photogramm. Remote Sens. 108, 273–290. https://doi.org/10.1016/j.isprsjprs.2015.05.005

Verrelst, J., Malenovský, Z., Van der Tol, C., Camps-Valls, G., Gastellu-Etchegorry, J.P., Lewis, P., North, P., Moreno, J., 2019. Quantifying Vegetation Biophysical Variables from Imaging Spectroscopy Data: A Review on Retrieval Methods. Surv. Geophys. 40, 589–629. https://doi.org/10.1007/S10712-018-9478-Y/FIGURES/9

Verrelst, J., Rivera-Caicedo, J.P., Reyes-Muñoz, P., Morata, M., Amin, E., Tagliabue, G., Panigada, C., Hank, T., Berger, K., 2021. Mapping landscape canopy nitrogen content from space using PRISMA data. ISPRS J. Photogramm. Remote Sens. 178, 382–395. https://doi.org/10.1016/j.isprsjprs.2021.06.017

Walker, D., Leibman, M.O., Epstein, H.E., Forbes, B.C., Bhatt, U.S., Raynolds, M.K., Comiso, J.C., Gubarkov, A.A., Khomutov, A. V, Jia, G.J., Kaarlejärvi, E., Kaplan, J.O., Kumpula, T., Kuss, P., Matyshak, G., Moskalenko, N.G., Orekhov, P., Romanovsky, V.E., Ukraientseva, N.G., Yu, Q., 2009. Spatial and temporal patterns of greenness on the Yamal Peninsula, Russia: Interactions of

ecological and social factors affecting the Arctic normalized difference vegetation index. Environ. Res. Lett. 4, 045004. https://doi.org/10.1088/1748-9326/4/4/045004

Wan, Y., Fan, Y., Jin, M., 2021. Application of hyperspectral remote sensing for supplementary investigation of polymetallic deposits in Huaniushan ore region, northwestern China. Sci. Rep. 11, 440. https://doi.org/10.1038/s41598-020-79864-0

Wang, X., Chen, S., Wang, J., 2020. An Adaptive Snow Identification Algorithm in the Forests of Northeast China. IEEE J. Sel. Top. Appl. Earth Obs. Remote Sens. 13, 5211–5222. https://doi.org/10.1109/JSTARS.2020.3020168

Wang, Y., Suarez, L., Poblete, T., Gonzalez-Dugo, V., Ryu, D., Zarco-Tejada, P.J., 2022. Evaluating the role of solar-induced fluorescence (SIF) and plant physiological traits for leaf nitrogen assessment in almond using airborne hyperspectral imagery. Remote Sens. Environ. 279, 113141. https://doi.org/10.1016/J.RSE.2022.113141

Ward, K.J., Chabrillat, S., Brell, M., Castaldi, F., Spengler, D., Foerster, S., 2020. Mapping soil organic carbon for airborne and simulated enmap imagery using the lucas soil database and a local plsr. Remote Sens. 12, 1–20. https://doi.org/10.3390/rs12203451

Warren, S.G., Wiscombe, W.J., 1980. A model for the spectral albedo of snow. II: snow containing atmospheric aerosols. J. Atmos. Sci. 37, 2734–2745. https://doi.org/10.1175/1520-0469(1980)037<2734:AMFTSA>2.0.CO;2

Watt, M.S., Buddenbaum, H., Leonardo, E.M.C., Estarija, H.J.C., Bown, H.E., Gomez-Gallego, M., Hartley, R., Massam, P., Wright, L., Zarco-Tejada, P.J., 2020. Using hyperspectral plant traits linked to photosynthetic efficiency to assess N and P partition. ISPRS J. Photogramm. Remote Sens. 169, 406–420. https://doi.org/10.1016/J.ISPRSJPRS.2020.09.006

Weiss, M., Baret, F., Eerens, H., Swinnen, E., 2010. FAPAR over Europe for the past 29 years: A temporally consistent product derived from AVHRR and VEGETATION Sensors, in: RAQRS III. Third International Symposium Recent Advances in Quantitative Remote Sensing. Torrent, Valencia, Spain, p. 6 p.

Weiss, M., Troufleau, D., Baret, F., Chauki, H., Prévot, L., Olioso, A., Bruguier, N., Brisson, N., 2001. Coupling canopy functioning and radiative transfer models for remote sensing data assimilation. Agric. For. Meteorol. 108, 113–128. https://doi.org/10.1016/S0168-1923(01)00234-9

Weng, Q., Hu, X., Lu, D., 2008. Extracting impervious surfaces from medium spatial resolution multispectral and hyperspectral imagery: A comparison. Int. J. Remote Sens. 29, 3209–3232. https://doi.org/10.1080/01431160701469024

Wepener, V., van Dyk, C., Bervoets, L., O'Brien, G., Covaci, A., Cloete, Y., 2011. An assessment of the influence of multiple stressors on the Vaal River, South Africa. Phys. Chem. Earth 36, 949–962. https://doi.org/10.1016/j.pce.2011.07.075

Wesemael, B. van, 2022. Spectral mapping of soil organic carbon, in: Advances in Measuring Soil Health. Burleigh Dodds Science Publishing, London, pp. 263–286. https://doi.org/10.1201/9781003048046-10

Wetherley, E.B., McFadden, J.P., Roberts, D.A., 2018. Megacity-scale analysis of urban vegetation temperatures. Remote Sens. Environ. 213, 18–33. https://doi.org/10.1016/J.RSE.2018.04.051

Wetherley, E.B., Roberts, D.A., McFadden, J.P., 2017. Mapping spectrally similar urban materials at sub-pixel scales. Remote Sens. Environ. 195, 170–183. https://doi.org/10.1016/J.RSE.2017.04.013

White, M.A., Thornton, P.E., Running, S.W., Nemani, R.R., 2000. Parameterization and Sensitivity Analysis of the BIOME–BGC Terrestrial Ecosystem Model: Net Primary Production Controls. Earth Interact. 4, 1–85. https://doi.org/10.1175/1087-3562(2000)004<0003:pasaot>2.0.co;2

Williams, M., Bell, R., Spadavecchia, L., Street, L.E., Van Wijk, M.T., 2008. Upscaling leaf area index in an Arctic landscape through multiscale observations. Glob. Chang. Biol. 14, 1517–1530. https://doi.org/10.1111/j.1365-2486.2008.01590.x

Williamson, G.B., Laurance, W.F., Oliveira, A.A., Delamônica, P., Gascon, C., Lovejoy, T.E., Pohl, L., 2000. Amazonian tree mortality during the 1997 El Nino drought. Conserv. Biol. 14, 1538–

1542. https://doi.org/10.1046/j.1523-1739.2000.99298.x

Windeler, D.S., Lyon, R.J.P., 1991. Discriminating dolomitization of marble in the Ludwig skarn near Yerington, Nevada using high-resolution airborne infrared imagery. Photogramm. Eng. Remote Sens. 57, 1171–1177.

Witten, D.M., Tibshirani, R., Hastie, T., 2009. A penalized matrix decomposition, with applications to sparse principal components and canonical correlation analysis. Biostatistics 10, 515–534. https://doi.org/10.1093/biostatistics/kxp008

Wocher, M., Berger, K., Danner, M., Mauser, W., Hank, T., 2020. RTM-based dynamic absorption integrals for the retrieval of biochemical vegetation traits. Int. J. Appl. Earth Obs. Geoinf. 93, 102219. https://doi.org/10.1016/j.jag.2020.102219

Wocher, M., Berger, K., Danner, M., Mauser, W., Hank, T., 2018. Physically-based retrieval of canopy equivalent water thickness using hyperspectral data. Remote Sens. 10, 1924. https://doi.org/10.3390/rs10121924

Wong, M.H., Wu, S.C., Deng, W.J., Yu, X.Z., Luo, Q., Leung, A.O.W., Wong, C.S.C., Luksemburg, W.J., Wong, A.S., 2007. Export of toxic chemicals - A review of the case of uncontrolled electronic-waste recycling. Environ. Pollut. 149, 131–140. https://doi.org/10.1016/j.envpol.2007.01.044

Wookey, P.A., Aerts, R., Bardgett, R.D., Baptist, F., Bråthen, K., Cornelissen, J.H.C., Gough, L., Hartley, I.P., Hopkins, D.W., Lavorel, S., Shaver, G.R., 2009. Ecosystem feedbacks and cascade processes: Understanding their role in the responses of Arctic and alpine ecosystems to environmental change. Glob. Chang. Biol. 15, 1153–1172. https://doi.org/10.1111/j.1365-2486.2008.01801.x

Wrona, F.J., Johansson, M., Culp, J.M., Jenkins, A., Mård, J., Myers-Smith, I.H., Prowse, T.D., Vincent, W.F., Wookey, P.A., 2016. Transitions in Arctic ecosystems: Ecological implications of a changing hydrological regime. J. Geophys. Res. Biogeosciences 121, 650–674. https://doi.org/10.1002/2015JG003133

Wu, C., Murray, A.T., 2003. Estimating impervious surface distribution by spectral mixture analysis. Remote Sens. Environ. 84, 493–505. https://doi.org/10.1016/S0034-4257(02)00136-0

Wulder, M.A., White, J.C., Carroll, A.L., Coops, N.C., 2009. Challenges for the operational detection of mountain pine beetle green attack with remote sensing. For. Chron. 85, 32–38. https://doi.org/10.5558/tfc85032-1

Wulf, H., Mulder, T., Schaepman, M.E., Keller, A., Jörg, P.C., Schaepman, M.E., 2015. Remote sensing of soils, Remote sensing of soils. University of Zurich, Remote Sensing Laboratories. https://doi.org/10.5167/UZH-109992

Xie, R., Darvishzadeh, R., Skidmore, A.K., Heurich, M., Holzwarth, S., Gara, T.W., Reusen, I., 2021. Mapping leaf area index in a mixed temperate forest using Fenix airborne hyperspectral data and Gaussian processes regression. Int. J. Appl. Earth Obs. Geoinf. 95, 102242. https://doi.org/10.1016/J.JAG.2020.102242

Xu, B., Gong, P., 2007. Land-use/land-cover classification with multispectral and hyperspectral EO-1 data. Photogramm. Eng. Remote Sensing 73, 955–965. https://doi.org/10.14358/PERS.73.8.955

Yang, C., Chai, F., Yang, F., Santosh, M., Xu, Q., Wang, W., 2018. Genesis of the Huangtupo Cu–Zn deposit, Eastern Tianshan, NW China: Constraints from geology, Rb–Sr and Re–Os geochronology, fluid inclusions, and H–O–S–Pb isotopes. Ore Geol. Rev. 101, 725–739. https://doi.org/10.1016/J.OREGEOREV.2018.08.021

Yang, J., Wan, J., Ma, Y., Zhang, J., Hu, Y., 2020. Characterization analysis and identification of common marine oil spill types using hyperspectral remote sensing. Int. J. Remote Sens. 41, 7163–7185. https://doi.org/10.1080/01431161.2020.1754496

Yang, L., 2000. Integration of a numerical model and remotely sensed data to study urban/rural land surface climate processes. Comput. Geosci. 26, 451–468. https://doi.org/10.1016/S0098-3004(99)00124-7

Yang, Y., 2009. Remote sensing and geospatial technologies for coastal ecosystem assessment and

management, in: Lecture Notes in Geoinformation and Cartography. Springer Berlin Heidelberg, Heidelberg, pp. 1–14.

Ye, C., Li, Y., Cui, P., Liang, L., Pirasteh, S., Marcato, J., Goncalves, W.N., Li, J., 2019. Landslide detection of hyperspectral remote sensing data based on deep learning with constrains. IEEE J. Sel. Top. Appl. Earth Obs. Remote Sens. 12, 5047–5060. https://doi.org/10.1109/JSTARS.2019.2951725

Zabcic, N., Rivard, B., Ong, C., Mueller, A., 2014. Using airborne hyperspectral data to characterize the surface pH and mineralogy of pyrite mine tailings. Int. J. Appl. Earth Obs. Geoinf. 32, 152–162. https://doi.org/10.1016/J.JAG.2014.04.008

Zabel, F., Putzenlechner, B., Mauser, W., 2014. Correction: Global agricultural land resources - A high resolution suitability evaluation and its perspectives until 2100 under climate change conditions. PLoS One 9, e107522. https://doi.org/10.1371/journal.pone.0114980

Zagajewski, B., Kycko, M., Tømmervik, H., Bochenek, Z., Wojtuń, B., Bjerke, J.W., Kłos, A., 2018. Feasibility of hyperspectral vegetation indices for the detection of chlorophyll concentration in three high Arctic plants: Salix polaris, Bistorta vivipara, and Dryas octopetala. Acta Soc. Bot. Pol. 87. https://doi.org/10.5586/asbp.3604

Zarfl, C., Fleet, D., Fries, E., Galgani, F., Gerdts, G., Hanke, G., Matthies, M., 2011. Microplastics in oceans. Mar. Pollut. Bull. 62, 1589–1591. https://doi.org/10.1016/j.marpolbul.2011.02.040

Zege, E., Malinka, A., Katsev, I., Prikhach, A., Heygster, G., Istomina, L., Birnbaum, G., Schwarz, P., 2015. Algorithm to retrieve the melt pond fraction and the spectral albedo of Arctic summer ice from satellite optical data. Remote Sens. Environ. 163, 153–164. https://doi.org/doi:10.1016/j.rse.2015.03.012

Zeng, H., Jia, G.J., Forbes, B.C., 2013. Shifts in Arctic phenology in response to climate and anthropogenic factors as detected from multiple satellite time series. Environ. Res. Lett. 8, 035036. https://doi.org/10.1088/1748-9326/8/3/035036

Zhang, C., Douglas, T.A., Anderson, J.E., 2021. Modeling and mapping permafrost active layer thickness using field measurements and remote sensing techniques. Int. J. Appl. Earth Obs. Geoinf. 102, 102455. https://doi.org/10.1016/j.jag.2021.102455

Zhang, C., Douglas, T.A., Anderson, J.E., 2020. Mapping Vegetation and Seasonal Thaw Depth in Central Alaska Using Airborne Hyperspectral and LiDAR Data. Int. Geosci. Remote Sens. Symp. 3070–3073. https://doi.org/10.1109/IGARSS39084.2020.9323660

Zhang, X., Han, X., Li, C., Tang, X., Zhou, H., Jiao, L., 2019. Aerial image road extraction based on an improved generative adversarial network. Remote Sens. 11, 953. https://doi.org/10.3390/rs11080953

Zhu, J., Hastie, T., 2002. Kernel logistic regression and the import vector machine. Adv. Neural Inf. Process. Syst. 14, 185–205.

List of abbreviations

The EnMAP mission team has built up a Glossary of Terms and Abbreviations that comprises contributions from many team members and is continuously updated and extended. The glossary is publicly available at http://www.enmap.org/mission.

Abbreviation	Full Name
AERONET	Aerosol Robotic Network
AHSI	Advanced Hyperspectral Imager
AHSI	Advanced Hyperspectral Imager
AI	Artificial Intelligence
AIS	Airborne Imaging Spectrometer
AISA	Airborne Imaging Spectrometer for Applications
ALI	Advanced Land Imager
ALT	Active Layer Thickness
APAR	Absorbed Photosynthetically Active Radiation
APEX	Airborne Prism Experiment
API	Application Programming Interface
ASI	Agenzia Spaziale Italiana
ASTER	Advanced Spaceborn Thermal Emission and Reflection Radiometer
ASTM	American Society for Testing and Materials'
ATBD	Algorithms Theoretical Baseline Documents
AVIRIS	Airborne Visible Infrared Imaging Spectrometer
AVIS	Airborn Visible/Infrared Imaging Spectrometer
BOA	Bottom Of Atmosphere
BRDF	Bidirectional Reflectance Distribution Function
CAL/VAL	Calibration/Validation
CARD4L	CEOS Analysis Ready Data for Land
CASI	Compact Airborn Spectropgraphic imager
CBD	Convention on Biolgical Diversity
CBD	Convention on Biological Diversity
CBERS	China–Brazil Earth Resources Satellite
CEOS	Committee on Earth Observation Satellites
CHIME	Copernicus Hyperspectral Imaging Mission for the Environment
CHRIS	Compact High Resolution Imaging Spectrometer
CNES	Centre National d'Études Spatiales
DDE	Dichlorodiphenyldichloroethylene
DDT	Dichlorodiphenyltrichloroethane

DEM	Digital elevation model
DESIS	DLR Earth Sensing Imaging Spectrometer
DG	Director General
DL	Deep Learning
DLR	German Aerospace Agency
DLR EOC	Earth Observation Center
DLR GSOC	German Space Observation Center
EARSeL	European Associatoin of Remote Sensing Laboratories
EBV	Essential Biodiversity Variables
EeteS	EnMAP end-to-end scene simulator
EIT	EnMAP Insturment Planning
EMIT	Earth Surface Mineral Dust Source Investigation
EnMAP	EnVironmental Mapping adn Analysis Program
EnSAG	EnMAP Science Advisory Group
EnSAG	EnMAP Science Advisory Group
ESA	European Space Agency
FAO	Food and Agricultural Organization of the United Nations
fAPAR	Fraction of Absorbed Photosynthetically Active Radiation
FEC	Future Earth Coasts
FLI	Forward Looking Interferometer
GBIF	Global Biodiversity Information Facility
GCOS	Global Climate Observing Systems
GEO	Group on Earth Observations
GEO	Global Environment Outlook
GEO	Group on Earth Observations
GEOSS	Global Earth Observation System of Systems
GER/DAIS	Geophysical and Environmental Research/Digital Airborne Imaging Spectrometer
GFZ	German Research Centre for Geosciences
GLP	Global Land Project
GOOS	Global Ocean Observing System
GS	Ground Segment
GTOS	Global Terrestrial Observing System
GUI	Graphical User Interface
HICO	Hyperspectral Imager for the Coastal Ocean
HISUI	Hyperspectral Imager Suite
HRS	Hyperspectral Remote Sensing
HUB	Humboldt-Universität zu Berlin
HYPXIM	HYPerspectral-X Imager
HZG	Helmholtz-Zentrum Geesthacht
IGBP	International Geosphere-Biosphere Program
IHDP	International Human Dimensions Program

IMEO	International Methane Emissions Observatory
IPBES	Intergovernmental Platform on Biodiversity & Ecosystem Services
IPCC	Intergovernmental Panel on Climate Change
IRS	Infrared Sounder
ISS	International Space Station
IUNC	International Union for the Conservation of Nature
JAXA	Japan Aerospace Exploration Agency
LAI	Leaf Area Index
LAP	Light-Absorbing Particles
LCZ	Local Climate Zone
LMA	Leaf Mass per Area
LMU	Ludwig-Maximilians-Universität München
LOICZ	Land Ocean Interaction in the Coastal Zone Program
LUCAS	Land Use/Cover Area frame statistical Survey
MERIS	MEdium Resolution Imaging Spectrometer
MIVIS	Multispectral Infrared Visible Imaging Spectromete
ML	Machine learning
MOOC	Massive Open Online Course
MSFD	Marine Strategy Framework Directive
NASA	National Aeronautics and Space Administration
NIR	Near Infrared
OGC	Open Geospatial Consortium
OHB SE	Otto Hydraulic Bremen Societas Europaea
PCB	Polychlorinated Biphenyl
PICS	Pseudo Invariant Calibration Sites
PRISMA	PRescursore IperSpettrale della Missione Operative
PVP	Product Validation Plant
RadCalNet	Radiometric Calibration Network
REDD	UN Collaborative Initiative on Reducing Emissions from Deforestation and Forest Degradation
SAR	Synthetic Aperture Radar
SBA	Societal Benefit Area
SBG PACE	Surface Biology and Geology - Plankton, Aerosol, Cloud, ocean Ecosystem
SDG	Sustainable Development Goals
SFSI	SWIR Full Spectrum Imager
SFTP	Secure File Transfer Protocol
SNR	Signal to Noise Ratio
SPOT HRV	Satellite Pour l'Observation de la Terre - High Resolution Visible
SSL	Soil Spectral Library
SWIR	Shortwave Infrared
SZA	Solar Zenith Angle

TIR	Thermal Infrared
UB	University of Bonn
UNCCD	United Nations Convention on Combating Desertification
UNEP	United Nations Environment Programme
UNESCO	United Nations Eductaional, Scientific and Cultural Organization
UNFCCC	United Nations Framework Convention on Climate Change
UT	University of Trier
VIIRS	Visible Infrared Imaging Radiometer Suite
VIS	Visible
V-I-S	Vegetation – Impervious surface - Soil
VNIR	Visibe-Near Infrared
VZA	Viewing Zenith Angle
WCRP	World Climate Research Programme
WMO	World Meteorlogical Organization

Acknowledgements

We are thankful to Alison Beamish, Ashley Bracken, Theodor Becker and Kathrin Ward for their thoughtful reviews and all authors for their valuable contributions to the document.

The core funding of the mission is provided by the German Space Agency at DLR with resources of the German Ministry for Economic Affairs and Climate Action and with contributions from the German Aerospace Center (DLR), OHB System AG and GFZ.